Electron cooling application for luminosity preservation in an experiment with internal targets at COSY.

Final report

JINR I.N.Meshkov, A.O.Sidorin, A.V.Smirnov, G.V.Trubnikov

COSY K.Fan, R. Maier, D. Prasuhn, H.J.Stein

Dubna, 2001

Contents

Abstract 3

Introduction 4

1. Target and beam parameters 5

2. ANKE experiment without cooling 6
2.1. Interaction with the target 7
2.2. Calculations in presence of intrabeam scattering 9

3. Beam parameter evolution with existing stochastic cooling system 13

4. 4. Electron cooling application 16
4.1. Beam parameter evolution with an electron cooling 16
4.2. Electron cooling in experiments with the pellet target 20
4.3. Possible development of the existing electron cooling system 30

5. Electron cooling system with circulating electron beam 32
5.1. Magnetic field limitations 32
5.2. Principles of electron cooling with circulating electron beam 33
5.3. Storage ring with longitudinal magnetic field 35
5.3.1. Particle dynamics in the ring with longitudinal magnetic field. 35
5.3.2. Current limitation due to microwave instability 38
5.3.3. Transverse-longitudinal relaxation of the electron beam 40
5.4. Electron cooling with circulating electron beam in experiments with internal target 41
5.4. Induction acceleration of the electron beam 44

6. Principles of the electron cooling system design 45

7. Program of experiments at LEPTA 47
7.1. General parameters of the LEPTA ring 47
7.2. Preliminary program of experiments 48
7.2.1. Tuning of injection system and helical quadrupole winding 48
7.2.2. Study of the circulating beam dynamics 51

Summary 53
1. Role of the cooling in experiments with internal targets 53
2. The possibility of the existing stochastic cooling system application 54
3. The possibility of an electron cooling application 55
4. Electron cooling system with circulating beam 55

Conclusion and recommendations 56

References 58

Abstract

This report is dedicated to investigation of the beam parameter evolution in the experiments with internal target. In calculations of the proton and deuteron beams we concentrated on cluster, atomic beam, storage cell and pellet targets at ANKE experiment mainly. In these calculations electron and stochastic cooling, intrabeam scattering, scattering on the target and residual gas atoms are taken into account. Beam parameter evolution is investigated in the long-term time scale, up to one hour, at different beam energies in the range from 1.0 to 2.7 GeV for proton beam and from 1 to 2.11 GeV for deuteron beam. The results of numerical simulations of the proton and deuteron beam parameters at different energies obtained using new version of BETACOOL program (elaborated at the first stage of this work [1]) are presented.

Optimum parameters of the electron cooling system are estimated. The COSY experiment requirements can be satisfied even when electron cooling time is rather long. That allows to apply an electron cooling system with circulating electron beam [2]. Such a system has potentially low cost in comparison with other possibilities. At the energy range from 500 keV to 1.5 MeV only longitudinal magnetic field can provide an effective focusing of an intensive electron beam. The electron beam acceleration can be produced both by induction acceleration of electrons or using an RF electron LINAC. Specific limitations of such a cooling system are discussed. Preliminary design of the electron cooling system with circulating electron beam is described in the report.

This report contains also preliminary program of experiments at LEPTA (Low Energy Particle Toroidal Accumulator), which are aimed to study the problems of electron cooling system with circulating electron beam. Presently the construction of LEPTA ring is in the final stage at JINR and experiments with circulating beam will be started the next year.

Introduction

The existing stochastic cooling system or an electron cooling system, which cover total energy range of the proton or deuteron beam at COSY, can be used for the following applications:
- at injection energy to increase the intensity of the polarized proton beam with a combined cooling/stacking injection,
- at energy range from about 1 GeV to top energy of 2.7 GeV (2.11 GeV for deuteron beam) for luminosity preservation in an experiment with internal targets,
- for preparation of the proton beam parameters for fast extraction in an experiment with external target.

The ultimate possible efficiency of the beam cooling application at ANKE experiments is investigated in the beginning of this report.

The existing COSY stochastic cooling system is successfully used now for luminosity preservation in the COSY-11 experiment with cluster beam apparatus at relatively low proton beam intensity. Expected target density in ANKE experiment is about one order of magnitude higher and one plans to increase the beam intensity by upgrade the COSY injection system. The investigation of the efficiency of the stochastic cooling system at these parameters is one of the goals of this report. Efficiency of an electron cooling system in difference with stochastic one does not depend on beam intensity but depends very strongly on beam energy. Comparison between two cooling methods is the next goal of this work.

The optimum choice of the electron cooling system parameters and preliminary design of the cooling system with circulating electron beam are also the topics of the report.

Further development of this work is experimental investigations of the electron cooling system with circulating electron beam. We plan to investigate its problems at LEPTA (Low Energy Particle Toroidal Accumulator) ring, which is under construction in JINR now. LEPTA parameters are closed to estimated parameters of COSY electron cooling system. This report contains preliminary program of experiments at LEPTA, which are aimed to study an electron cooling system with circulating electron beam. Electron beam parameters after injection and adjustment of the septum and kicker coils will be measured at special test bench using optic method of the electron beam diagnostics, developed in JINR [3]. Dynamics of circulating electron beam will be investigated when LEPTA assembling is finished. Resonance behaviour and beam stability at injection energy will be studied using RF acceleration of the electron beam. And final test of the cooling system will be performed after installation of the betatron yoke. It will include the injection of electron beam, its acceleration to maximum energy and extraction for diagnostic of the electron temperature.

Presently the construction of the general elements of LEPTA magnetic system is in the final stage and we plan to start assembling of the ring and first experiments with electron beam in the next year. Expected term of the experimental program completion is two years.

1. Target and beam parameters

The internal targets used in COSY are listed in the Table 1.1.

Table 1.1. Experiments with internal targets

Target	EDDA	COSY 11	ANKE
1. Strip or filament	filament		strip
2. Cluster		x	x
3. Pellet			x
4. Atomic beam	x		x
5. Storage cell	x		x

The beam life time in the experiments with solid targets is so short that luminosity preservation using the beam cooling seems to be unrealistic. All the other types of the target will be used in the ANKE experiment and the results of the calculations for them can be extended to other experiments with corresponding corrections the lattice functions in the target position. Therefore in this report general attention was directed to the ANKE experiment.

The cluster beam apparatus of ANKE experiment is very similar to COSY 11 one and maximum designed value of target areal density was equal to 5 x 10^{13} atoms/ cm^2. However, the value really achieved now is substantially higher and can be estimated from of the particle energy loss due to interaction with target using the experiment parameters (Table 1.2.). The formula for relation between relative energy loss of the proton beam and proton revolution frequency, one can calculate the ΔE value:

$$\frac{\Delta E}{E} = \frac{1+\gamma}{\gamma}\frac{1}{\eta}\frac{\Delta f}{f}, \qquad (1.1)$$

here η is off-momentum factor, γ is Lorenz factor.

Table 1.2. ANKE experiment with hydrogen cluster beam target at January/February 2001.

Proton beam kinetic energy, GeV	2.65
Revolution frequency, MHz	1.5
Off momentum factor, η	-0.13
Frequency shift during 300 seconds, Hz	192

Theoretical value of the mean energy loss during single cross the target is [4]:

$$\Delta E = 2\xi \, ln\left(\frac{E_{max}}{I} - \beta^2\right), \qquad (1.2)$$

here E_{max} is the maximum energy loss in a head-on collision of the projectile with a target electron:

$$E_{\max} = \frac{2m_e c^2 \beta^2 \gamma^2}{1 + 2\gamma \frac{m_e}{M} + \left(\frac{m_e}{M}\right)^2}, \tag{1.3}$$

m_e is the electron mass and M - the projectile mass, ξ is a quantity which is proportional to the areal density ρx of the target (ρ – target density in g/cm^3):

$$\xi = 0.1535 \frac{MeV\, cm^2}{g} \frac{Z_1^2}{\beta^2} \frac{Z_2}{A_2} \rho x, \tag{1.4}$$

where, Z_P and Z_T are the charge number of projectile and target atoms, I is ionisation potential: $I = Z_T^{0.9} \times 16\, eV$

Experimental value of the energy losses follows from Formula (1.1):

$$\Delta E_{str,\exp} = \frac{1+\gamma}{\gamma} \frac{E}{\eta} \frac{\Delta f}{f} \frac{T_0}{\tau_{\exp}}, \tag{1.5}$$

T_0 – revolution period, $\tau_{\exp}$ = 300 sec is the experiment duration.

Experimental value of the energy loss during one revolution in the ring is 7.3 meV, which gives the target areal density of $1.3 \cdot 10^{15}$ Atoms/cm^2.

The maximum designed areal density of the storage cell is expected to be of 10^{14} atoms/cm^2.

The frozen pellet target provides a total number of atoms per pellet of $1.8 \cdot 10^{14}$ – $1.1 \cdot 10^{16}$. Influence of the target on the beam parameters can be estimated by introducing the "effective areal density" which is proportional to ratio of the atom number per the pellet to the beam cross section. We assume that in each moment of time one pellet is inside the beam. At the beam emittance of 1π·mm·mrad the effective target density lies between $3 \cdot 10^{14}$ and $2 \cdot 10^{16}$ Atoms/cm^2.

Maximum achieved intensity of the proton beam is $7 \cdot 10^{10}$. In the future one can expect improvement of the intensity to 10^{11} or even more by upgrade of the injection system. Now the maximum beam energy is 2.65 GeV, but it is possible in the future to increase this value to 2.7 GeV. At the same magnetic rigidity the maximum deuteron beam energy is 2.11 GeV.

Thus, in this report the calculations of the beam parameters were fulfilled at target density from 10^{15} to 10^{16} Atoms/cm^2 (at lower value the experiment can be performed during long time duration without cooling), at the beam intensity up to 10^{11} particles and in the beam energy range from 1 GeV to 2.7 GeV for protons and to 2.11 GeV for deuterons. The ring acceptance was taken of 10^{-5} π·m·rad in the both planes, which is corresponds to expected aperture of the gas storage sell. The initial beam parameters were taken approximately corresponded to these ones after acceleration: emittances of 10^{-6} π·m·rad in the both planes and momentum spread of 10^{-4}.

2. ANKE experiment without cooling

Efficiency of the cooling application at experiment with internal target is determined by relation between different sources of the particle losses. Generals of them are the following:
- single scattering on the target atoms on a large angle,
- the same for residual gas atoms,
- emittance growth and aperture limitation,
- momentum spread growth and limitation of longitudinal acceptance.

The particle losses due to single scattering on the target atoms restricts the experiment duration and can not be effected by the beam cooling. Emittance and momentum growth can be compensated by stochastic or electron cooling. In this case luminosity life time is determined only by single scattering process. The sources of the beam phase volume growth are the multiple scattering on residual gas and the target atoms, intrabeam scattering.

First of all influence of residual gas on the beam life time was investigated under assumption that average pressure in COSY vacuum chamber is $5 \cdot 10^{-9}$ Torr and gas composition is 95% of hydrogen and 5% of nitrogen. At these conditions the particle life time is about 10^6 seconds and emittance growth rate at minimum beam energy of 1 GeV is about $3 \cdot 10^{-10}$ $\pi \cdot m \cdot rad/sec$. Thus the interaction with the residual gas does not restrict particle life time and slightly influences on the particle losses due to emittance growth.

2.1. Interaction with the target

Ultimate efficiency of the beam cooling can be estimated in the case of high target density and low intensity of the ion beam – in this case beam parameters are determined only by interaction with the target. Multiple scattering on the target atoms leads to the linear in time growth of the beam emittance and particle losses takes place when the beam emittance increases up to 0.3 of the ring acceptance [4]. The period of time when the emittance growth does not lead to the particle losses can be estimated by the following formula:

$$\tau = \frac{A\tau_\varepsilon}{3\varepsilon}, \qquad (2.1)$$

which gives the time of emittance growth from zero value to acceptance limit. Here A is the ring acceptance, τ_ε is the characteristic time of the emittance growth calculated at certain value of the beam emittance ε.

Fig. 2.1, 2.2 show the characteristic times of the single scattering process and emittance growth up to acceptance limit in both planes for proton and deuteron beam. The ring acceptance was taken of 10^{-5} $\pi \cdot m \cdot rad$ in the both planes. The beta functions of the ring at the target position were taken of 2 meters in the horizontal plane and of 3 meters in the vertical one. The presented values correspond to the hydrogen target at the areal density of 10^{16} Atoms/cm^2 and beam emittances of 10^{-6} $\pi \cdot m \cdot rad$ in the both planes. All the characteristic times are linearly scaled with the target density and can be simply recalculated to each required value. The difference in the energy dependence of the single and multiple scattering life times appears because of in the single scattering life time calculation the particle losses due to nuclear scattering are taken into account. The difference between horizontal and

vertical degrees of freedom is explained by the difference in the beta functions in the target position.

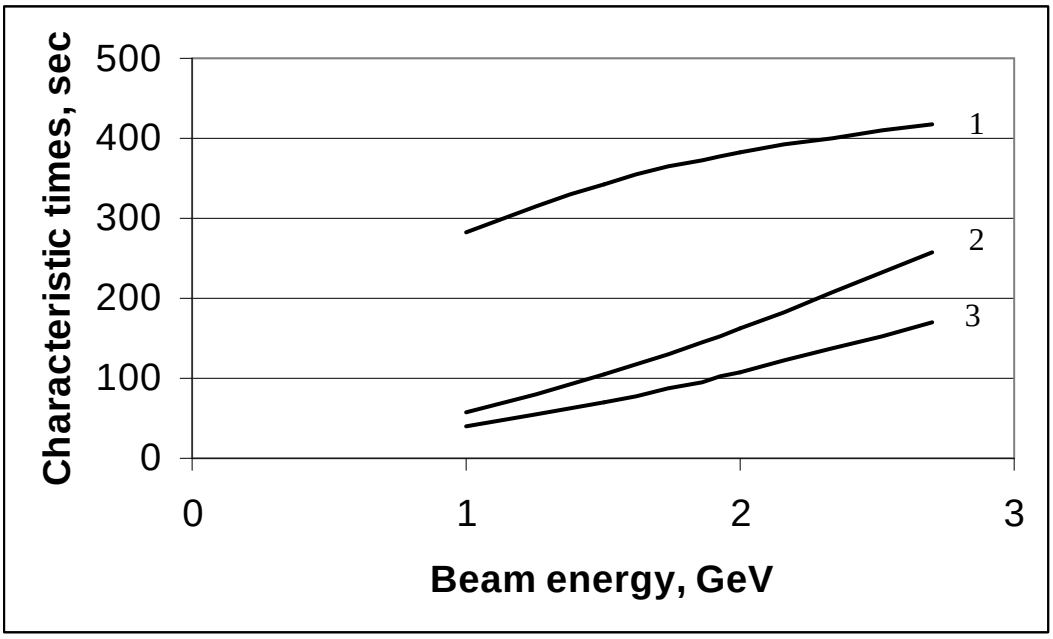

Fig. 2.1. The *proton beam* life time due to single scattering on the target atoms (1) and the times of emittance growth up to the acceptance limit in horizontal (2) and in vertical (3) planes.

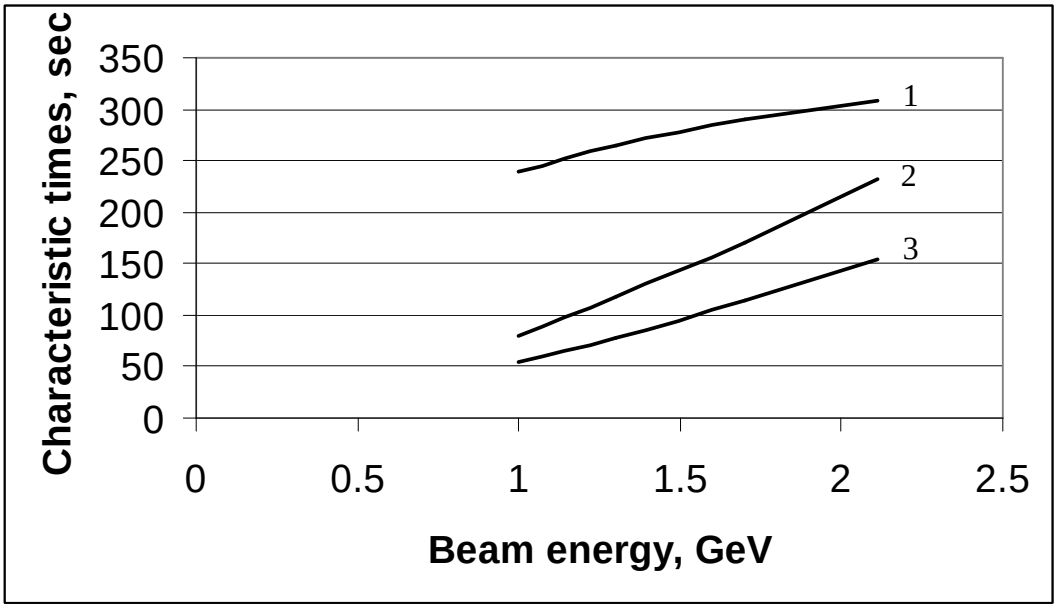

Fig. 2.2. The *deuteron beam* life time due to single scattering on the target atoms (1) and the times of emittance growth up to the acceptance limit in horizontal (2) and in vertical (3) planes.

For both kinds of particles (protons and deuterons) the experiment duration is limited by about 5 minutes at the target density of the order of a few 10^{16} Atoms/cm^2 and by about 1 hour at the target density of about 10^{15} Atoms/cm^2. Correspondingly in the following

calculations we will investigate two cases: short term beam parameter evolution at high target density and long term evolution at low target density.

For both beams in the total energy range the particle losses due to aperture limitation play a significant role and suppression of the emittance growth by the beam cooling can increase the integral luminosity of the experiment by several times. Ultimate possible efficiency of the cooling decreases with the increase of the beam energy, and for deuteron beam at maximum energy the maximum gain in the luminosity is less than two times.

More accurate estimations of the possible cooling efficiency at high beam intensity have to include consideration of the intrabeam scattering process.

2.2. Calculations in presence of intrabeam scattering

The intrabeam scattering calculations are performed for the lattice parameters given in Fig. 2.3. Initial beam parameters in the numerical investigations were chosen the following: beam emittance in the both planes is equal to 10^{-6} π·m·rad, momentum spread is equal to 10^{-4}.

Calculations were performed taking into account the beam interaction with residual gas and target atoms and intrabeam scattering in the ion beam. The initial beam intensity was chosen to be equal maximum expected value of 10^{11} particles. An example of the calculations of short term variation of the beam parameters at the target areal density of 10^{16} Atoms/cm^2 is presented in the Fig. 2.4 for proton beam at energy of 2.7 GeV.

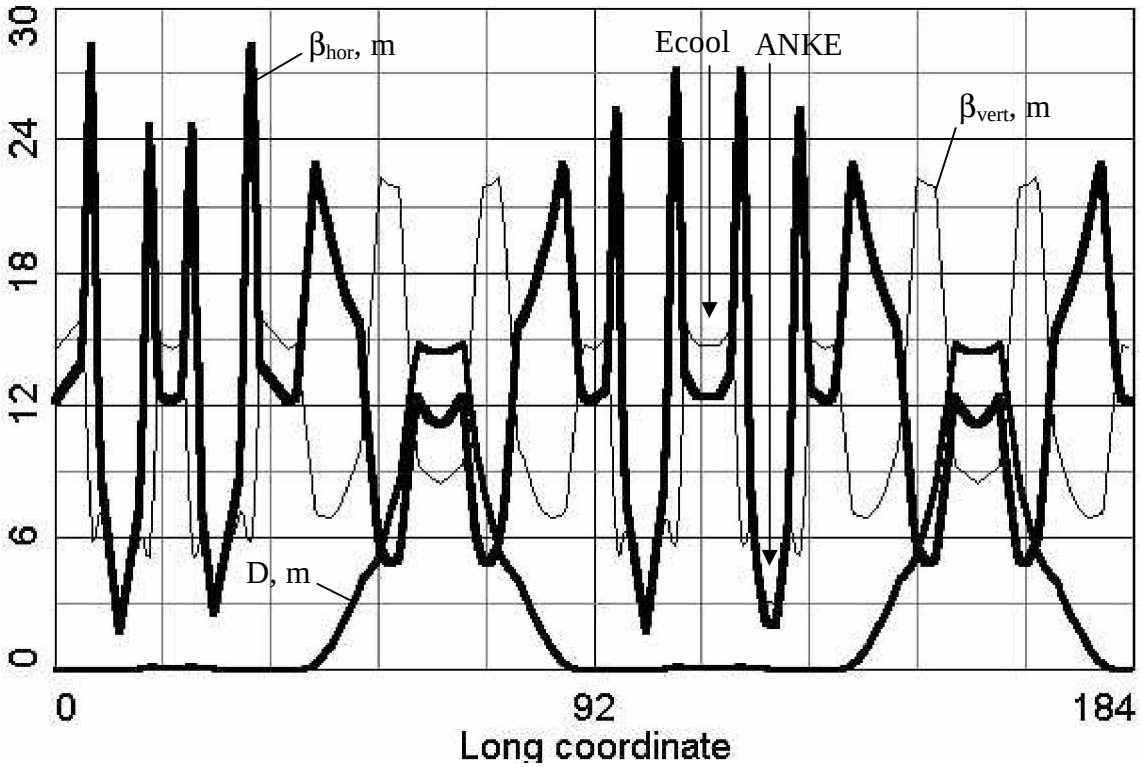

Fig 2.3. Lattice parameters at ANKE experiment, Q = 3.571, γ_{tr} = 2.243.
In the cooling section: Beta-functions = 13/15 m, Dispersion = 0,
in ANKE: Beta-functions = 2/3 m, Dispersion = 0

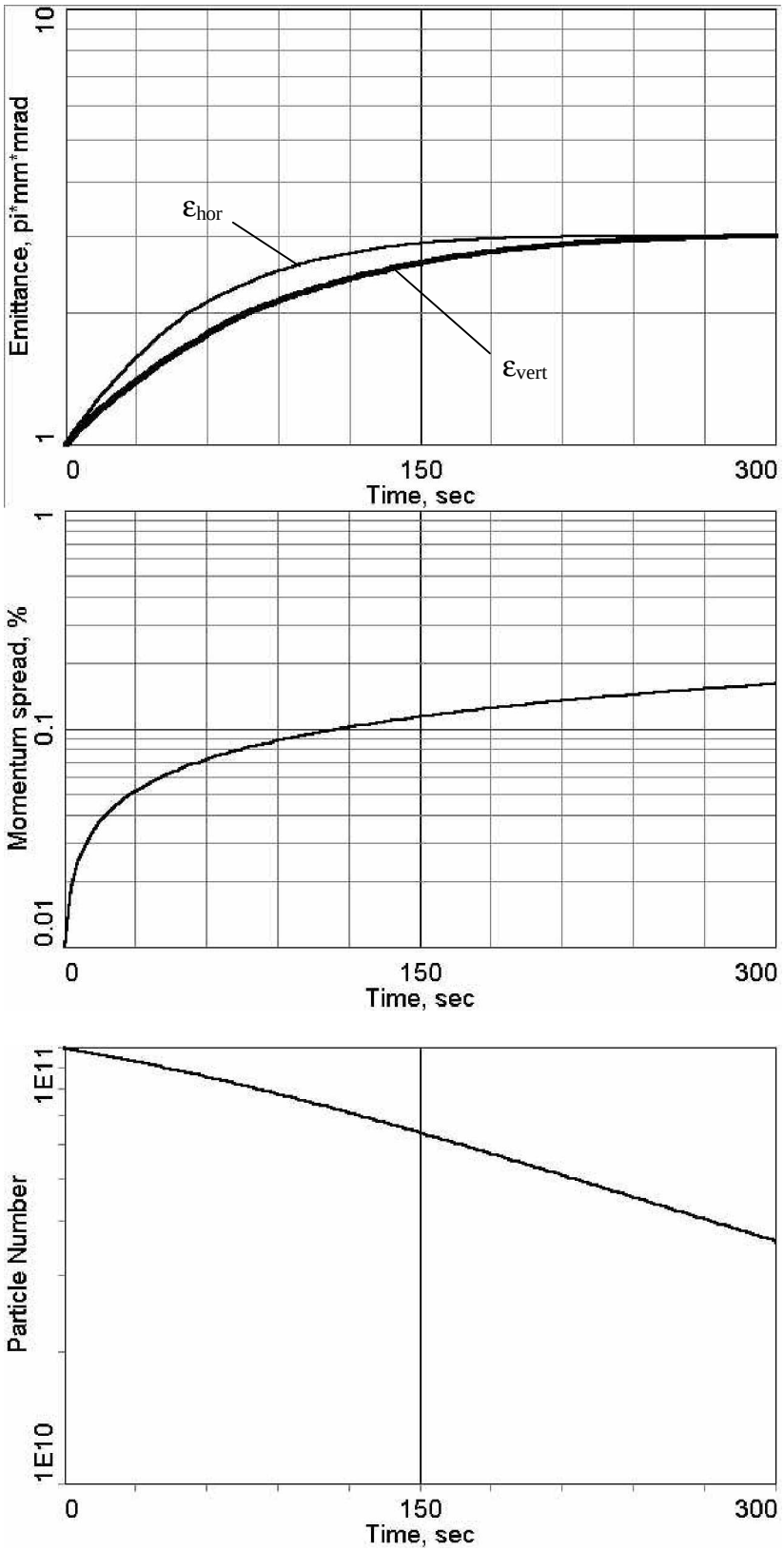

Fig. 2.4. The dependencies of the proton beam emittance (a), momentum spread (b) particle number (c) on time, target density is 10^{16} Atoms/cm^2.

One can see that after five minutes of experiment the beam emittance is limited by the ring acceptance, and the particle number decreases from 10^{11} to $3.6 \cdot 10^{10}$. The particle number after five minutes of experiment calculated without taking into account aperture limitation is equal

to $4.85 \cdot 10^{10}$. The ratio between final particle number calculated without and with the aperture limitation can be used as a parameter, which characterises the gain in the experiment luminosity when the cooling completely suppresses the emittance growth. The ultimate possible cooling effect on the experiment (ratio of the beam intensity with cooling to that one without cooling) at high target density is presented in the Fig. 2.5. The possible gain in the particle number after one hour of experiment at the target density of 10^{15} Atoms/cm^2 is presented in the Fig 2.6.

One can see that the beam cooling can provide maximum gain in the beam intensity at minimum beam energy and for the proton beam, where this value is up to ten times. The gain for deuteron beam is about two times less due to intrabeam scattering dependence on the particle mass. At maximum energy the gain decreases to the value of about 50%. It is explained by the strong dependence of the intrabeam scattering on energy (as $\beta^3\gamma^4$). As result at maximum beam energy the emittance growth due to this process does not play a significant role. The difference between hydrogen and deuterium targets is negligible because of the main processes are determined by the interaction of the beam with electrons of the target atoms.

In the presented version of the numerical program the particle losses due to longitudinal acceptance limitation are not taken into account, correspondingly presented calculations can underestimate the particle losses due to growth of the momentum spread.

The next chapters of the report are dedicated to calculations of the beam parameter evolution in the presence of stochastic or electron cooling.

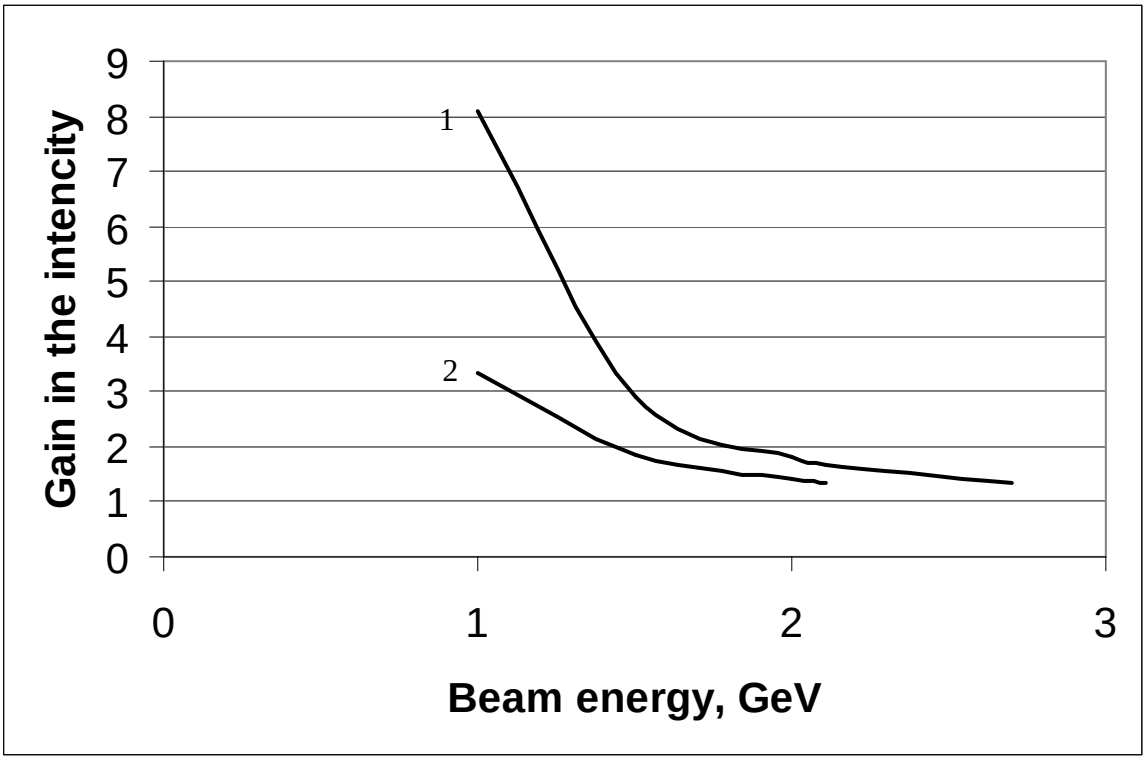

Fig. 2.5. Ultimate gain in the beam intensity which can be obtained using cooling at the experiment duration of *5 minutes*: 1 – proton beam, 2 – deuteron beam. The hydrogen target density is 10^{16} *Atoms/cm*^{2}, initial beam intensity is 10^{11} particles.

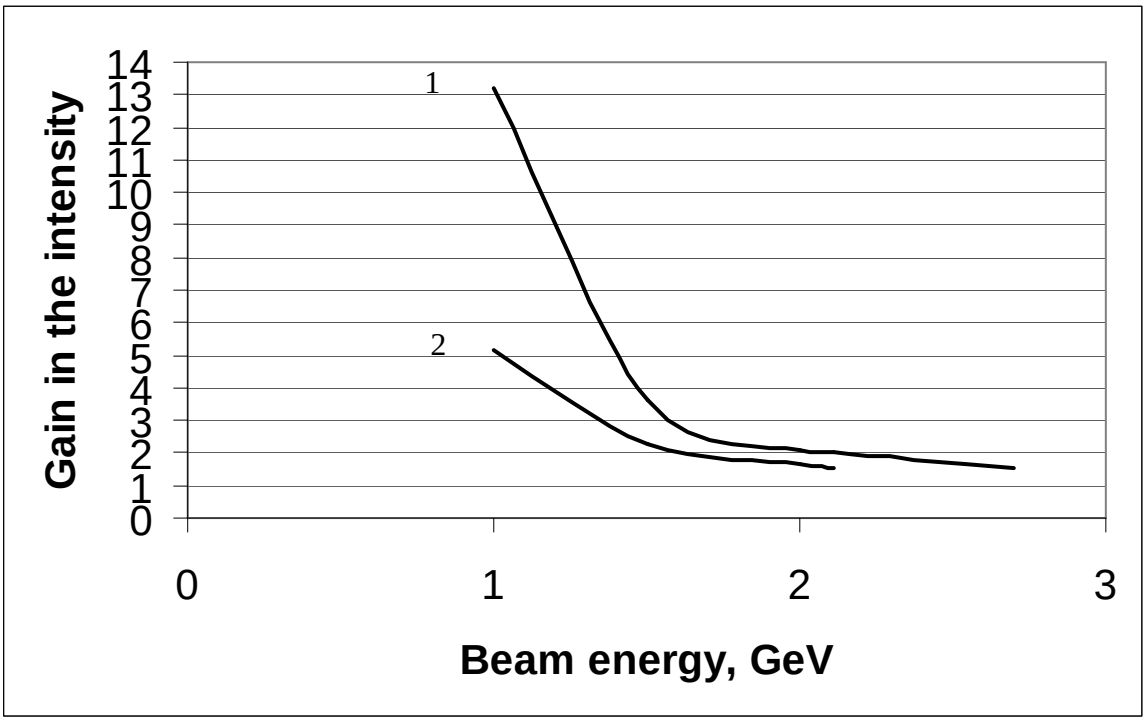

Fig. 2.6. Ultimate gain in the beam intensity which can be obtained using cooling at the experiment duration of *1 hour*: 1 – proton beam, 2 – deuteron beam. The hydrogen target density is 10^{15} *Atoms/cm*^{2}, initial beam intensity is 10^{11} particles.

3. Beam parameter evolution with existing stochastic cooling system

The parameters of the stochastic cooling system used in the following calculations are presented in the Table 3.1. The band I is used for horizontal cooling, the Band II for longitudinal one.

Table 3.1. Parameters of stochastic cooling system

	Band I	Band II
Lower frequency, GHz	1	1
Upper frequency, GHz	1.8	3
Bandwidth, GHz	0.8	2

Fig. 3.1. shows the emittance and momentum spread evolution of the proton beam at energy of 1 GeV and initial particle number of 10^{11} under common action of the hydrogen target of 10^{16} Atoms/cm^2 areal density, residual gas, intrabeam scattering and stochastic cooling. As one can see the emittances in both plane increase to acceptance limit during first 30 seconds and after that cooling does not influence on this value. Momentum spread increases during first part of the calculation period but after about 3 minutes cooling begins to prevail on the heating processes and momentum spread decreases. To this moment the particle number decreases to the value of about $2 \cdot 10^{10}$ and continues to decrease during last minutes. *Stochastic cooling does not influence on the particle losses at these experiment parameters.*

At target density of 10^{16} Atoms/cm^2 the similar situation takes a place at maximum proton beam energy of 2.7 GeV and initial beam intensity of 10^{11} particles: stochastic cooling does not compensate emittance growth, and the gain in the particle number after 5 minutes of experiment accompanied with cooling is less than 10%.

In order to estimate a range of the beam parameters in which the stochastic cooling can be effective in the experiment with internal target the particle number corresponding to an equilibrium between heating due to interaction with the target, residual gas, intrabeam scattering and stochastic cooling was calculated (Fig. 3.2, 3.3).

Maximum efficiency of the stochastic cooling corresponds to the maximum beam energy due to dependence of the mixing factor on off momentum factor. When the particle number is higher than about 10^{10} the intrabeam scattering (IBS) begins to play a significant role, that one can see from the change of the curve derivatives in the Fig. 3.2, 3.3. More attractive region of parameters for the existing stochastic cooling system application is the target density below 10^{15} Atoms/cm^2 and particle number of a few units of 10^{10}. This region corresponds to long term experiment and the Fig. 3.4 presents the emittance and momentum spread evolution during one hour under common action of IBS, target, residual gas and stochastic cooling. (Beam energy is 2.7 GeV, initial intensity is $2 \cdot 10^{10}$ particles, target density is 10^{15} Atoms/cm^2.) After the beam relaxation the stochastic cooling stabilises the horizontal emittance and the momentum spread, vertical emittance increases during the first 30 minutes to acceptance limit. The computer simulation shows that the particle number decreases during 1 hour of experiment to the value of $7.4 \cdot 10^9$. Without cooling the final particle number is about $5.6 \cdot 10^9$. Thus the stochastic cooling application gives the gain in the experiment luminosity of about 30%.

As a conclusion from this analysis one can expect effective application of existing stochastic cooling in the experiment with internal target when the beam intensity is about or below of $2 \cdot 10^{10}$ particles, and the target density does not exceed 10^{15} Atoms/cm^2.

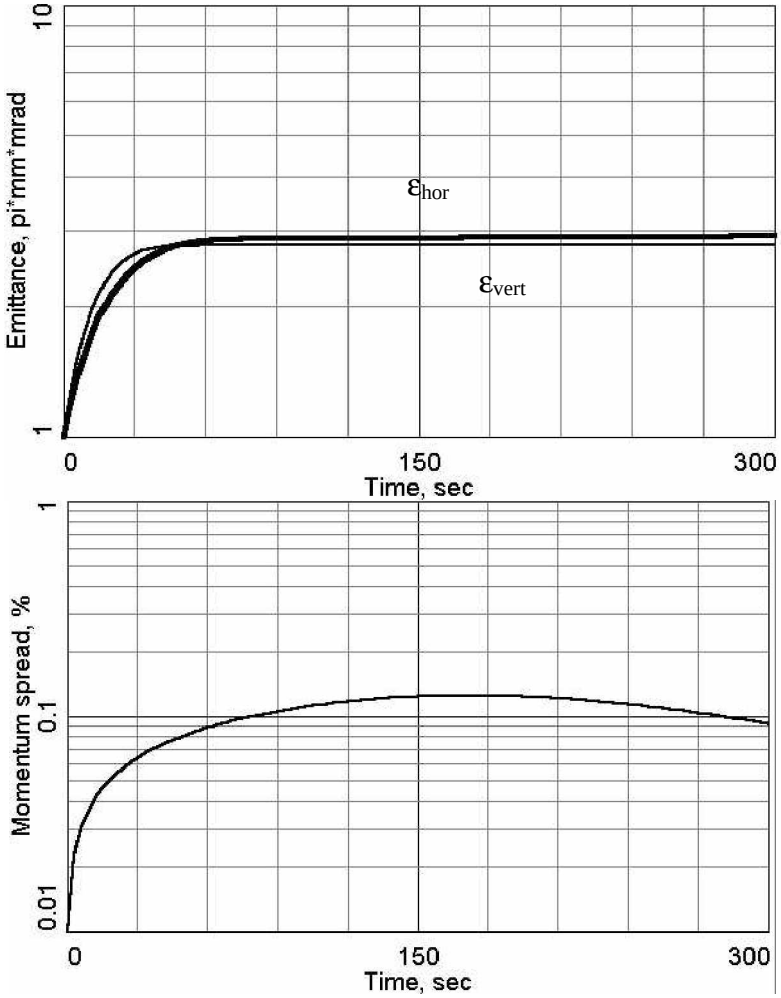

Fig. 3.1. Emittance and momentum spread evolution at stochastic cooling. Target density is 10^{16} Atoms/cm^2, beam energy 1 GeV, the beam intensity is 10^{11} protons.

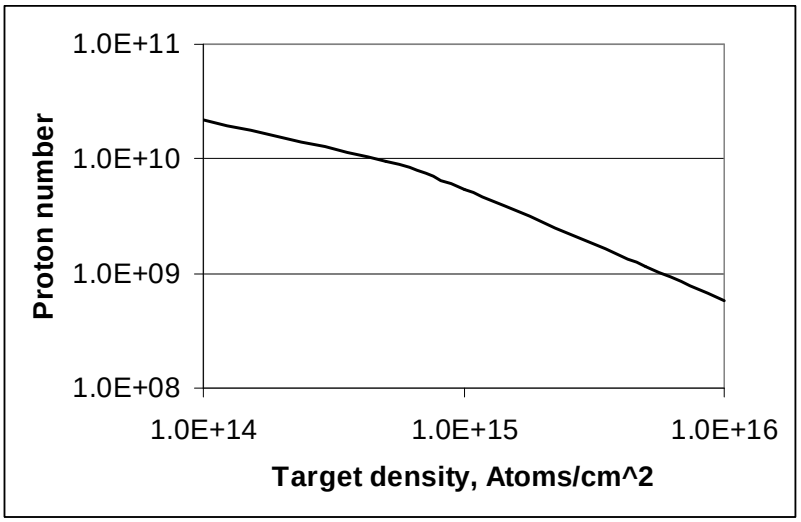

Fig. 3.2. Proton number corresponding to equilibrium between heating effects and stochastic cooling in the horizontal degree of freedom. Beam energy is 2.0 GeV.

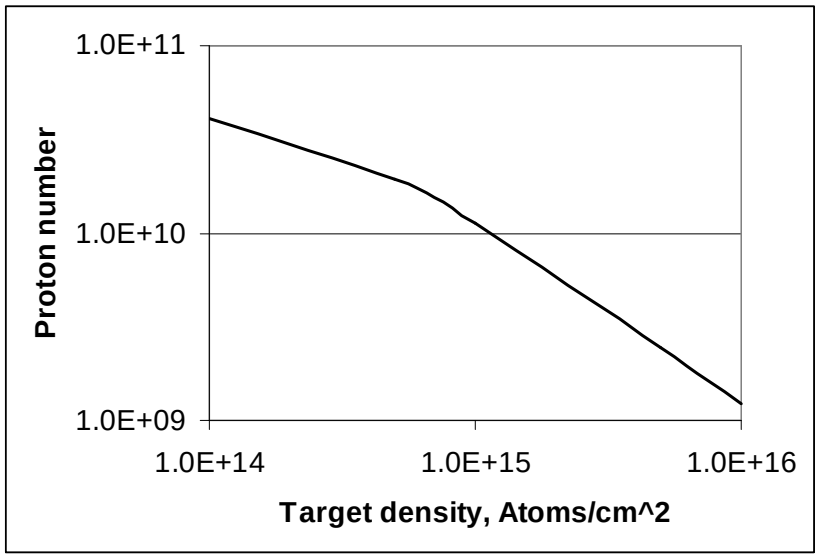

Fig. 3.3. Proton number corresponding to equilibrium between heating effects and stochastic cooling in the horizontal degree of freedom. Beam energy is 2.7 GeV.

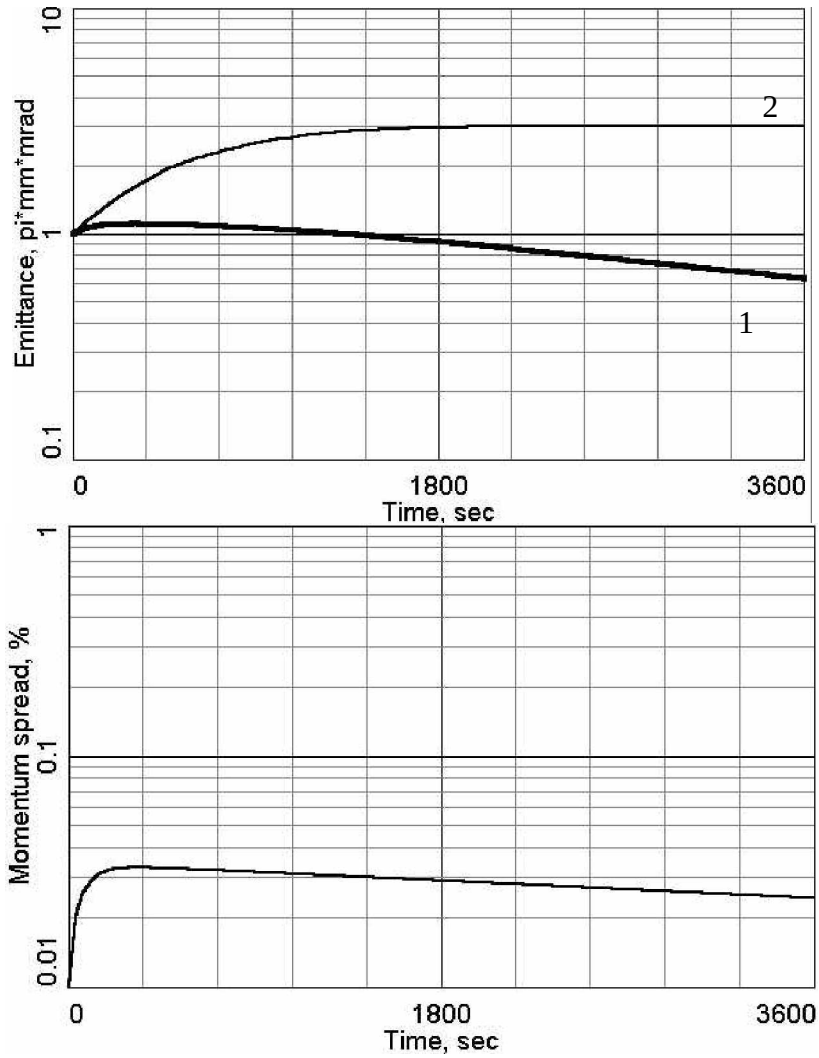

Fig. 3.4. Emittance (1 - horizontal, 2 - vertical) and momentum spread evolution. Target density is 10^{15} Atoms/cm^2, beam energy 2.7 GeV, initial beam intensity is $2 \cdot 10^{10}$ protons.

4. Electron cooling application

4.1. Beam parameter evolution with an electron cooling

The calculations in this chapter were performed at the electron beam and solenoid parameters corresponding to the existing COSY electron cooling system (Table 4.1). Longitudinal and transverse temperature were chosen using the results of the friction force measurements performed at COSY in May 2001. Only the maximum electron beam energy is varied in accordance with the proton energy.

Table 4.1. Electron cooling system parameters.

Effective length of the cooling section, m	1.4
Maximum magnetic field value, kG	1.2
Maximum value of electron beam current, A	3
Electron beam radius, cm	1.26
Transverse electron temperature, meV	300
Longitudinal electron temperature, meV	10
Neutralisation factor, %	30
Beta functions in the cooling section, m	13/15

The beam parameter evolution is calculated taking into account all general heating effects: interaction with residual gas, internal target and intrabeam scattering.

At minimum proton energy of 1 GeV and target density of 10^{16} Atoms/cm^2 the value of the electron beam current required for compensation of the beam heating in all degrees of freedom is of the order of a few Amperes. Fig. 4.1 presents the emittance and momentum spread evolution during 5 minutes of experiment at electron beam current of 1.5 A. After the relaxation of the beam parameters at initial stage the emittances and momentum spread keep to be the constant values during long time and the particle losses are determined only by the single scattering on the target atoms. In this range of parameters electron cooling application have a maximum efficiency and after five minutes of experiment it allows to have proton beam of 10 times higher intensity than without cooling.

At maximum proton energy (2.7 GeV) even maximum electron beam current can not provide the stabilisation of the emittance and momentum growth. However at electron beam current of 3 A (Fig. 4.2) the heating processes are substantially suppressed and gain in the particle number after five minutes of experiment is about 20% which is close to maximum achievable value (see Fig. 2.5). The experiment at high target density will be considered more detail in the next chapter.

At lower target density the electron cooling stabilises the proton beam parameters in the total energy range. In the Fig. 4.3 the equilibrium beam parameters as a function of beam energy are presented. The electron beam current was chosen to obtain equilibrium proton beam emittance of about 10^{-6} π·m·rad. The equilibrium is reached during about 10 minutes and after that emittance and momentum spread slowly decrease with decrease of the particle number due to losses in the target.

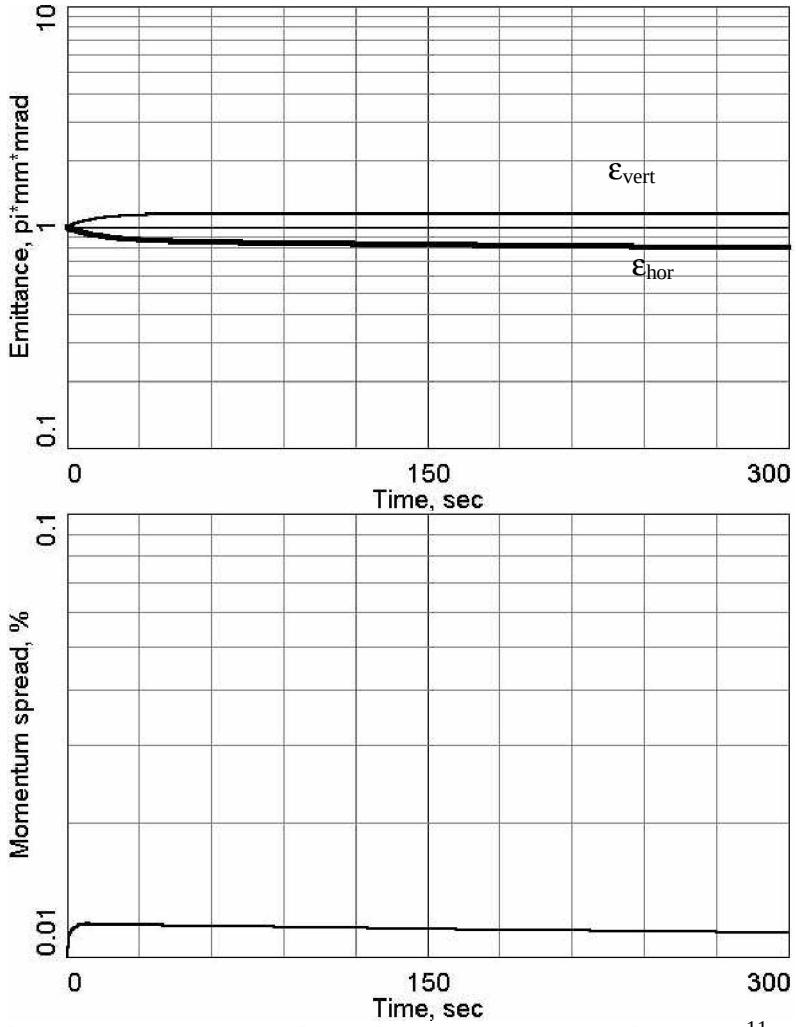

Fig. 4.1. Proton beam parameter time dependencies. Proton number is 10^{11}, energy is 1 GeV, target density is 10^{16} Atoms/cm^2. Electron beam current is 1.5 A.

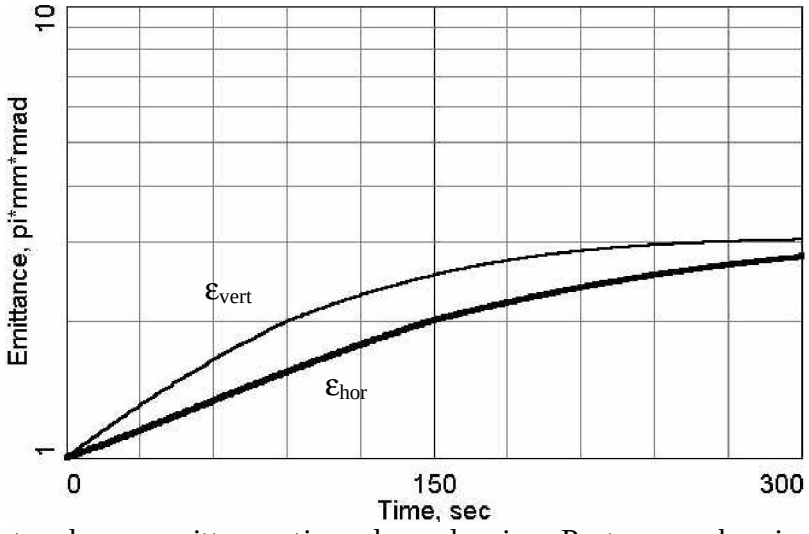

Fig. 4.2, a. Proton beam emittance time dependencies. Proton number is 10^{11}, energy is 2.7 GeV, target density is 10^{16} Atoms/cm^2. Electron beam current is 3 A.

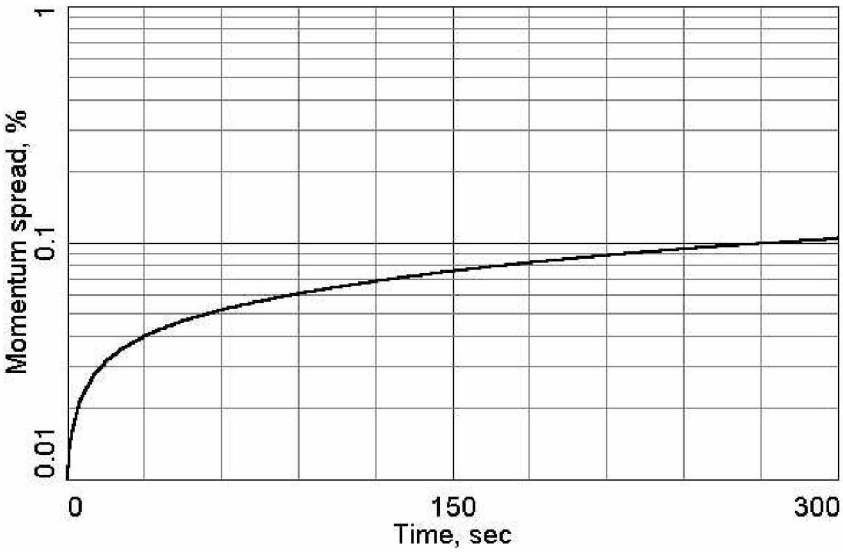

Fig. 4.2, b. Proton beam momentum spread time dependencies. Proton number is 10^{11}, energy is 2.7 GeV, target density is 10^{16} Atoms/cm^2. Electron beam current is 3 A.

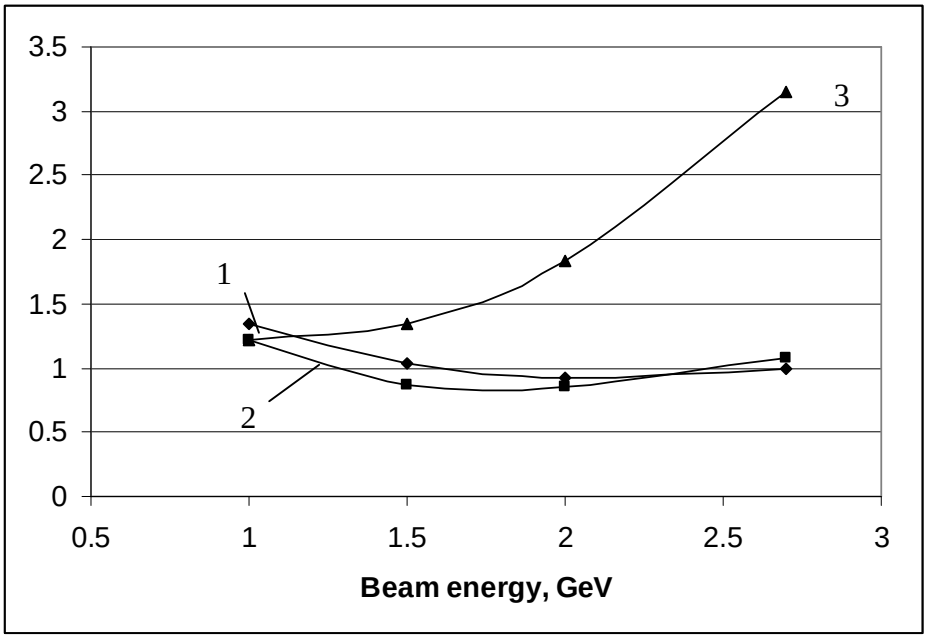

Fig 4.3. Equilibrium proton beam parameters as a function of the beam energy.
1 –horizontal emittance in 10^{-6} π·m·rad, 2 – vertical emittance in 10^{-6} π·m·rad, 3 – momentum spread in 10^{-4}. Proton number is 10^{11}, target density 10^{15} Atoms/cm^2.

Analogous dependencies for deuteron beam are presented in the Fig. 4.4. In the first approximation the cooling time for deuterons is two times longer than for protons, but charcteristic time of the emittance growth due to multiple scattering with the target atoms is longer by four times. As result the electron beam current required to obtain the equilibrium is about two times lower. The values of the electron beam current used in the calculations of the Fig 4.3 – 4.4 are presented in the Fig. 4.5. The equilibrium is reached in the case of deuteron beam during 20 – 30 minutes and this time is comparable with the particle life time due to single scattering on the target atoms.

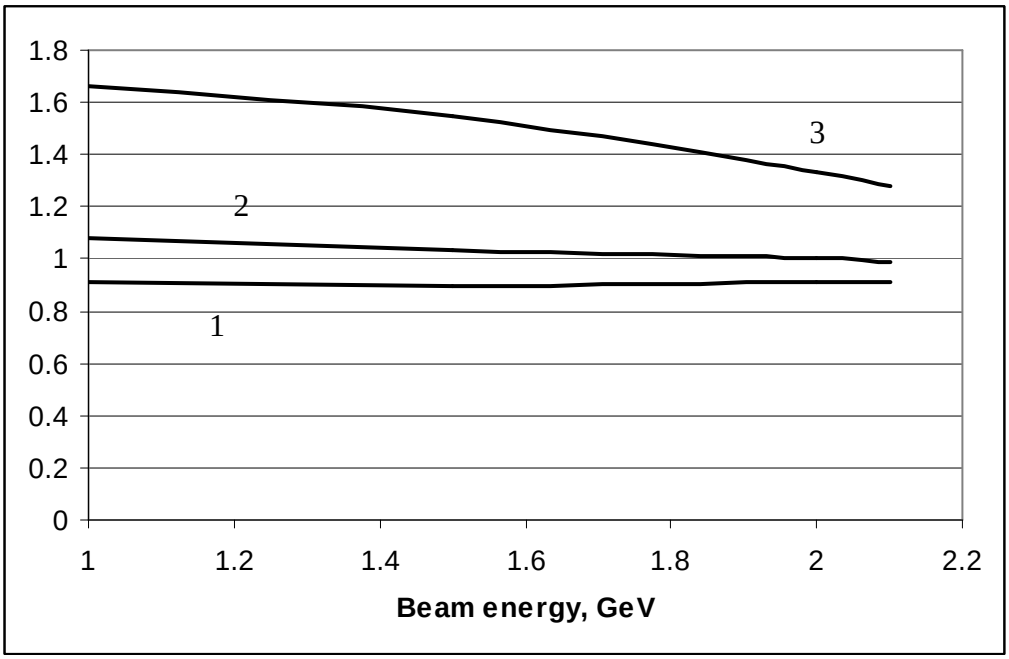

Fig 4.4. Equilibrium *deuteron beam* parameters as a function of the beam energy.
1 – horizontal emittance in 10^{-6} π·m·rad, 2 – vertical emittance in 10^{-6} π·m·rad, 3 – momentum spread in 10^{-4}. Deuteron number is 10^{11}, target density 10^{15} Atoms/cm^2.

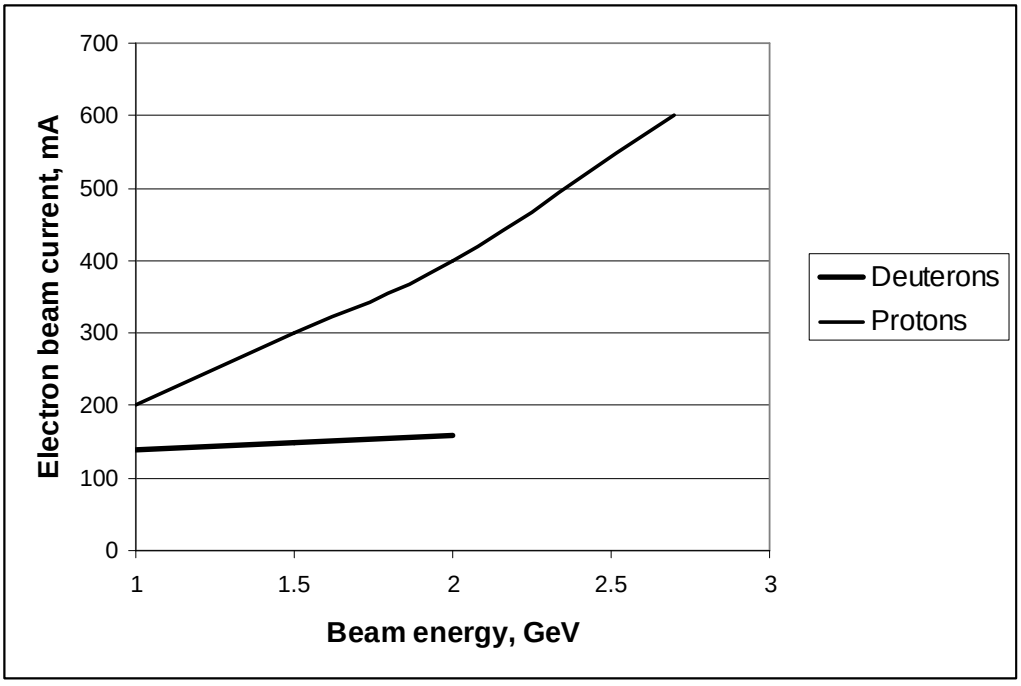

Fig. 4.5. The electron beam current required to reach the equilibrium emittance in both planes of about 10^{-6} π·m·rad.

The stabilization of the ion beam parameters is important in the experiment with cluster beam target. The target dimension in the horizontal plane is less than the ion beam dimension corresponding to the acceptance limit. The numerical model used in these calculations does not permit to solve the problem correctly in the case, when the horizontal emittance is varied during the experiment. However one can estimate possible gain in the experiment luminosity due to horizontal emittance stabilization as a ratio between maximum beam dimension and

target dimension. This ratio is about 1.5 – 2 and taking into account that the characteristic time of emittance growth without cooling is about 10 minutes the gain in the luminosity can be estimated by the value 1.5.

The electron beam radius of 1.26 cm required for electron cooling at injection energy is more than two times bigger than ion beam one at experiment with internal target. Decrease of the electron beam radius permits to decrease the beam current. In the experiments with gas jet and cluster targets this fact does not play a significant role due to small value of the electron beam current density required for effective cooling. In the experiment with higher target density and at maximum beam energy the electron beam current density has to be as high as possible and an accurate choice of the electron beam radius is necessary to minimize the electron beam current. The optimum electron beam parameters will be discussed below.

4.2. Electron cooling in experiments with the pellet target

In the experiment with the pellet target the effective target density depends on the beam cross section and as a result its value is changed when the beam emittance is varied. Correspondingly the efficiency of electron cooling system can be substantially higher in the case, when the cooling suppresses the heating effects. In the previous chapter the electron cooling efficiency in the experiment with high target density was considered only from the side of the suppression the particle losses due to acceptance limitation and effective target density was assumed to be constant. In this chapter we investigate the experiment with the pellet target taking into account variation of the effective target density.

In this chapter the parameters of the electron cooling system presented in the Table 5 (chapter 5) are used in the simulations. The proton beam intensity is 10^{11} particles, which corresponds to the expected value after installation of new injection system.

The luminosity of the experiment with pellet target is determined by the expression:

$$L = \frac{N_b N_t}{S_t T_{rev}} P, \tag{4.1}$$

where N_b is the particle number in the beam, T_{rev} – revolution period, N_t is particle number in the target, S_t – target cross-section, P – probability of the particle cross the target.

Assuming that the pellets cross the beam one by one with the period equal to the time duration of the beam crossing by a pellet, one can estimate the probability as the following:

$$P = \frac{S_t}{S_b} \approx \frac{S_t}{\pi \sqrt{\beta_x \varepsilon_x \beta_y \varepsilon_y}} \tag{4.2}$$

where $\beta_{x,y}$ –horizontal and vertical beta functions in the target position (dispersion in the target position is closed to zero), $\varepsilon_{x,y}$ – corresponding two-sigma emittances. As a result we have:

$$L = \frac{N_b N_t}{\pi T_{rev} \sqrt{\beta_x \varepsilon_x \beta_y \varepsilon_y}} \tag{4.3}$$

The pellet diameter lies in the range from 20 to 80 μm, the target density is about $1.4 \cdot 10^{22}$ Atoms/cm^3. Target parameters and luminosity of the experiment are presented in the Table 4.2. The luminosity is calculated under assumption that one pellet is in the beam, beam emittance is 1 π·mm·mrad in the both transverse planes, the proton beam intensity is 10^{11} particles and beam energy is 2.7 GeV.

The luminosity life time is equal to:

$$\frac{1}{L}\frac{dL}{dt} = \frac{1}{N_b}\frac{dN_b}{dt} - \frac{1}{\varepsilon_x}\frac{d\varepsilon_x}{dt} - \frac{1}{\varepsilon_y}\frac{d\varepsilon_y}{dt}. \qquad (4.4)$$

Thus, in difference with the case of gas storage cell target the luminosity life time depends not only on the particle life time, but also on the emittance variation. At optimum experiment conditions the electron cooling can provide practically constant luminosity during long period of time by corresponding choice of the electron beam current. In the Fig. 4.6 the luminosity of the experiment at maximum beam energy is presented for pellet diameter of 40 μm and 50 μm.

Table 4.2. The pellet target parameters

Pellet diameter, μm	Number of particles	Target cross-section, cm2	Target length, cm	Luminosyty, cm-2*sec-1
20	$1.8 \cdot 10^{14}$	$3.14 \cdot 10^{-6}$	0.00157	$3.66 \cdot 10^{32}$
30	$5.94 \cdot 10^{14}$	$7.07 \cdot 10^{-6}$	0.00236	$1.21 \cdot 10^{33}$
40	$1.43 \cdot 10^{15}$	$1.26 \cdot 10^{-5}$	0.00314	$2.91 \cdot 10^{33}$
50	$2.75 \cdot 10^{15}$	$1.96 \cdot 10^{-5}$	0.00393	$5.6 \cdot 10^{33}$
60	$4.84 \cdot 10^{15}$	$2.83 \cdot 10^{-5}$	0.00471	$9.85 \cdot 10^{33}$
70	$7.54 \cdot 10^{15}$	$3.85 \cdot 10^{-5}$	0.0055	$1.54 \cdot 10^{34}$
80	$1.1 \cdot 10^{16}$	$5.03 \cdot 10^{-5}$	0.00628	$2.32 \cdot 10^{34}$

At pellet diameter of 40 μm electron cooling compensate the particle losses by corresponding decrease of the beam emittance and the experiment luminosity variation during first five minutes is negligible. At the same conditions without electron cooling the luminosity decreases by about 3 times. At bigger pellet diameter the power of electron cooling is not high enough to suppress the beam heating due to interaction with target and the cooling application leads only to some increase of the luminosity life time.

The effectiveness of the cooling application can be estimated by comparison of an integral luminosity after certain period of experiment with and without of the cooling. The integral luminosity for some period of experiment can be calculated:

$$L_{\text{int}} = \frac{N_t}{\pi T_{rev}\sqrt{\beta_x \beta_y}} \int_0^{T_{\text{exp}}} \frac{N_b}{\sqrt{\varepsilon_x \varepsilon_y}} dt. \qquad (4.5)$$

Or in the case of numerical integration of the beam dynamics

$$L_{\text{int}} = \frac{N_t}{\pi\sqrt{\beta_x \beta_y}} \frac{\Delta t}{T_{rev}} \sum_{i=1}^{n} \frac{N_b}{\sqrt{\varepsilon_x \varepsilon_y}}, \tag{4.6}$$

where Δt is integration step over time, n is the number of the integration steps.

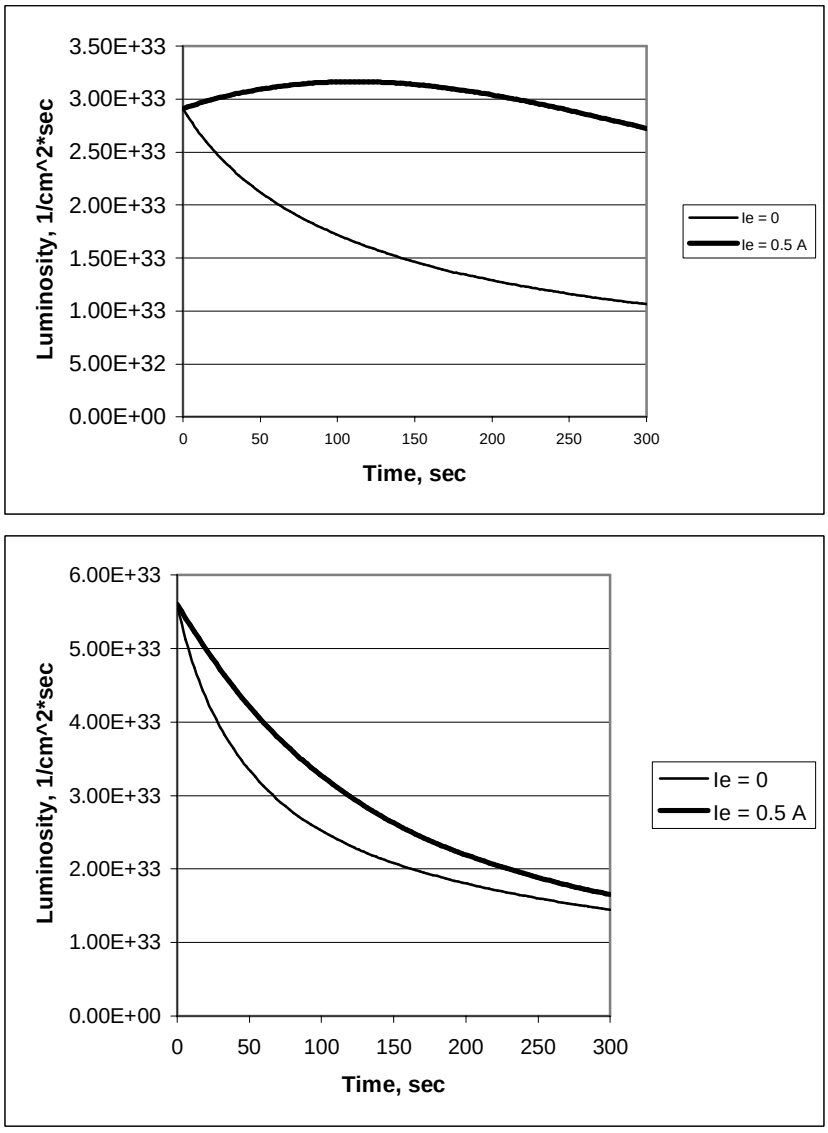

Fig. 4.6. Luminosity time dependence at pellet diameter of 40 μm (upper plot) and 50 μm (bottom plot), proton beam energy is 2.7 GeV.

The gain in the integral luminosity after five minutes of the experiment provided by the cooling application (Fig. 4.7, 4.8) is several times at pellet diameter less than 50 μm, and decreases to about 10% at bigger pellet diameter. At the pellet diameter less than 40 μm the electron beam current of 500 mA is not optimal to obtain maximum luminosity that explains peculiarity of the curve in the Fig. 4.7. The dependence of the luminosity on the electron beam current will be discussed more detail below.

At big target density, when the cooling only slightly influences on the beam parameters during experiment, the cooling system can be used also for preliminary preparation the beam parameters before the target switching on. All the previous estimations were performed at the following initial beam parameters: emittances in both planes are 1 π·mm·mrad and momentum spread is 10^{-4}. The beam parameters corresponding to the equilibrium between electron cooling and intrabeam scattering are the foolowing: horizontal emittance is about 0.3 π·mm·mrad, vertical emittance - 0.1 π·mm·mrad and momentum spread is about $8 \cdot 10^{-5}$. The equilibrium is reached during 30 – 60 sec depending on initial beam parameters. Without the target the beam life is higher than 10^5 sec and permits to perform all required manipulations of the beam parameters.

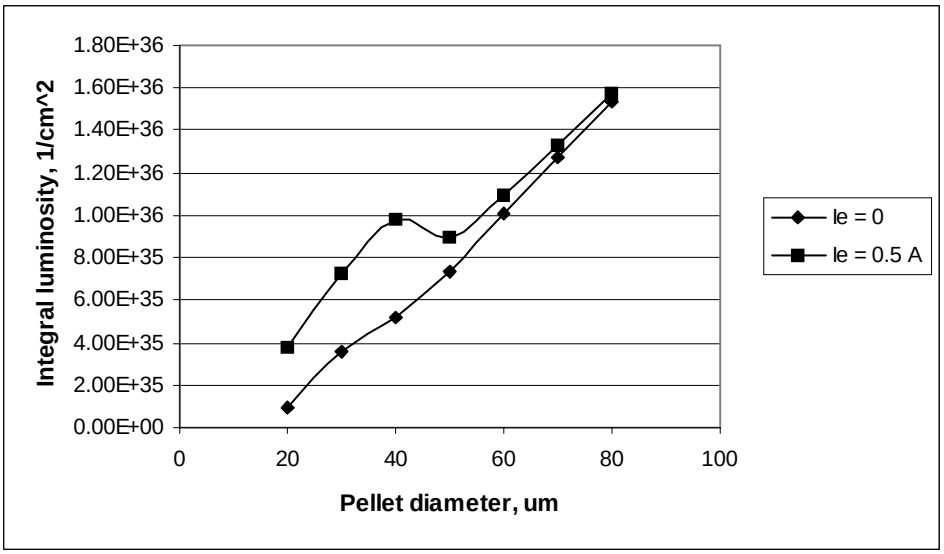

Fig. 4.7. Integral luminosity after five minutes of experiment as a function of the pellet diameter, beam energy is 2.7 GeV.

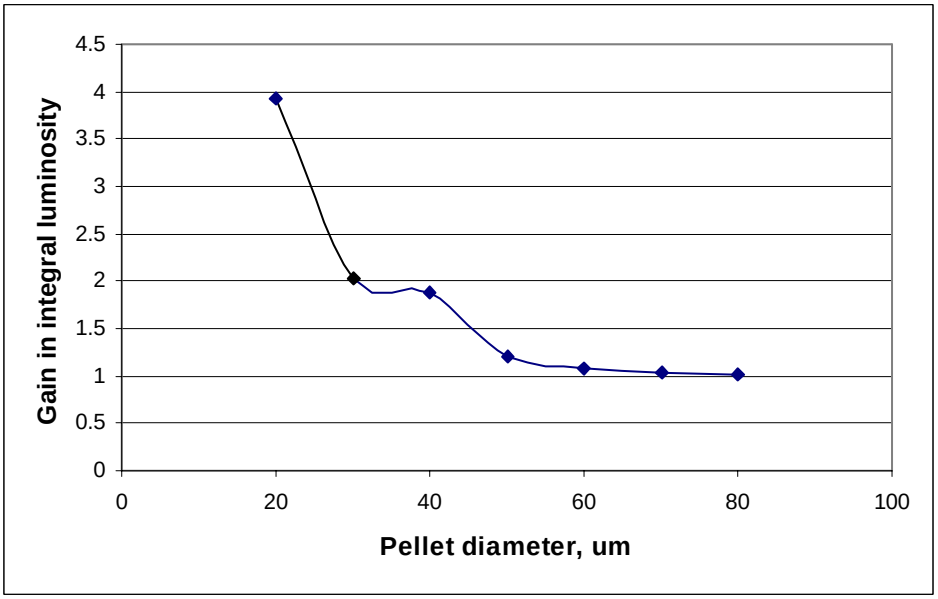

Fig. 4.8. Gain in the integral luminosity after five minutes of the experiment at electron beam current of 0.5 A, proton beam energy is 2.7 GeV.

In the Fig. 4.9 the integral luminosity was calculated under assumption that emittances in the both planes are the same and momentum spread is 10^{-4}. The integral luminosity monotonically increases with the decrease of the initial beam emittance and expected gain after five minutes of experiment due to initial preparation the beam before experiment is about 10%.

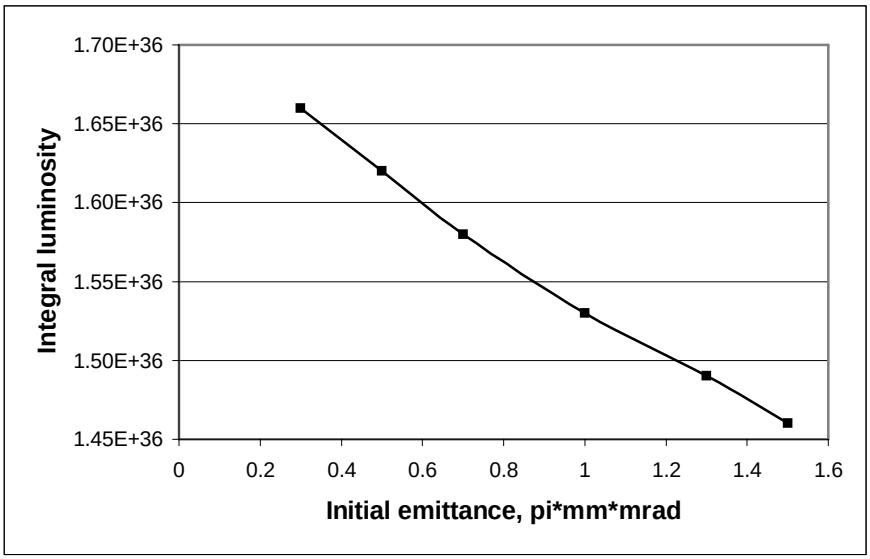

Fig. 4.9. Integral luminosity in $1/cm^2$ after five minutes of experiment without cooling as function of initial beam emittance, beam energy is 2.7 GeV, pellet diameter is 80 μm.

In order to obtain maximum integral luminosity one can to optimise the experiment duration also. The integral luminosity increases approximately as a square root from the experiment duration (Fig. 4.10). Maximum gain in the luminosity obtained due to beam cooling before experiment corresponds to short term of the experiment, and it decreases with increase of the experiment duration (Fig. 4.11).

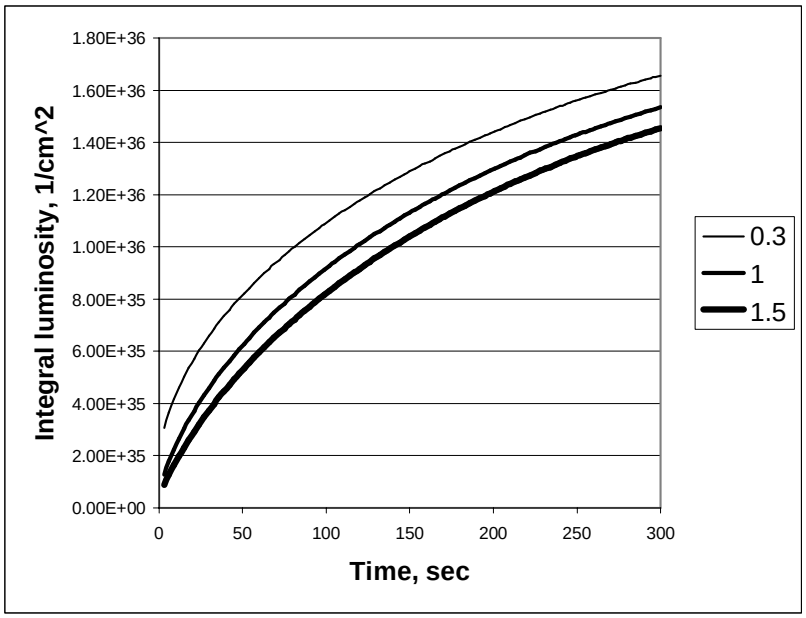

Fig. 4.10. Integral Luminosity as function of the experiment duration depending on initial beam emittance in π·mm·mrad, beam energy is 2.7 GeV, pellet diameter is 80 μm, cooling is off.

Thus, even at big target density, when the cooling power is not enough to suppress the heating due to interaction with the target, the experiment luminosity can be improved by preparation the beam parameters before the target switching on and by optimization of the experiment scenario.

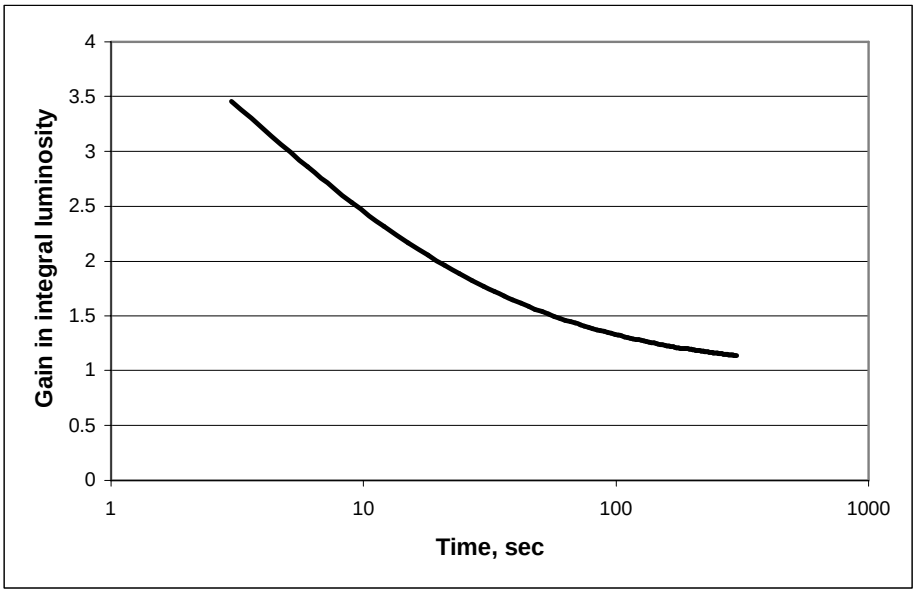

Fig. 4.11. The ratio between the integral luminosity at initial emittance of 0.3 π·mm·mrad and 1.5 π·mm·mrad versus experiment duration, beam energy is 2.7 GeV, pellet diameter is 80 μm, cooling is off.

At maximum experiment energy the luminosity increases with the electron beam current and maximum luminosity corresponds to maximum electron beam current. The electron cooling efficiency increases with decrease of the experiment energy (Fig. 4.12). And at minimum experiment energy it is not necessary to have maximum electron beam current to obtain the maximum luminosity – the luminosity dependence on the current has a saturation in the region of 400 mA (Fig. 4.13). The reason of the saturation can be explained by analysis of the luminosity time dependence (Fig. 4.14).

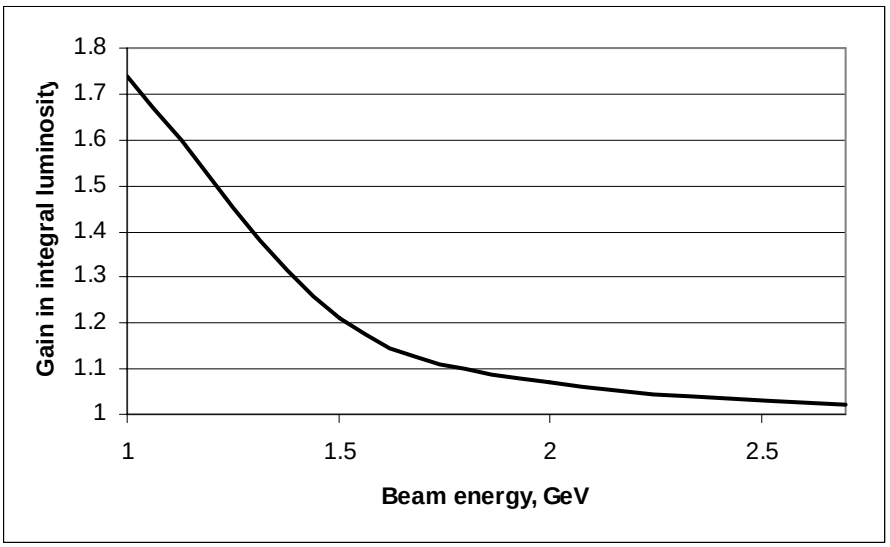

Fig. 4.12. Gain in integral luminosity after five minutes of experiment at electron beam current of 0.5 A, pellet diameter is 80 μm.

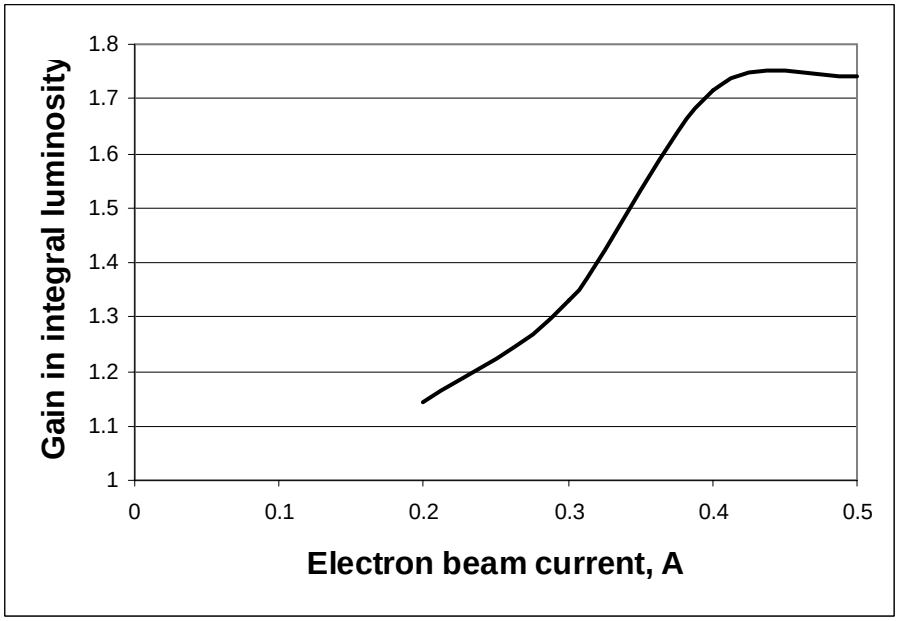

Fig. 4.13. The gain in integral luminosity after five minutes of experiment as function of electron beam current, beam energy is 1 GeV, pellet diameter is 80 μm.

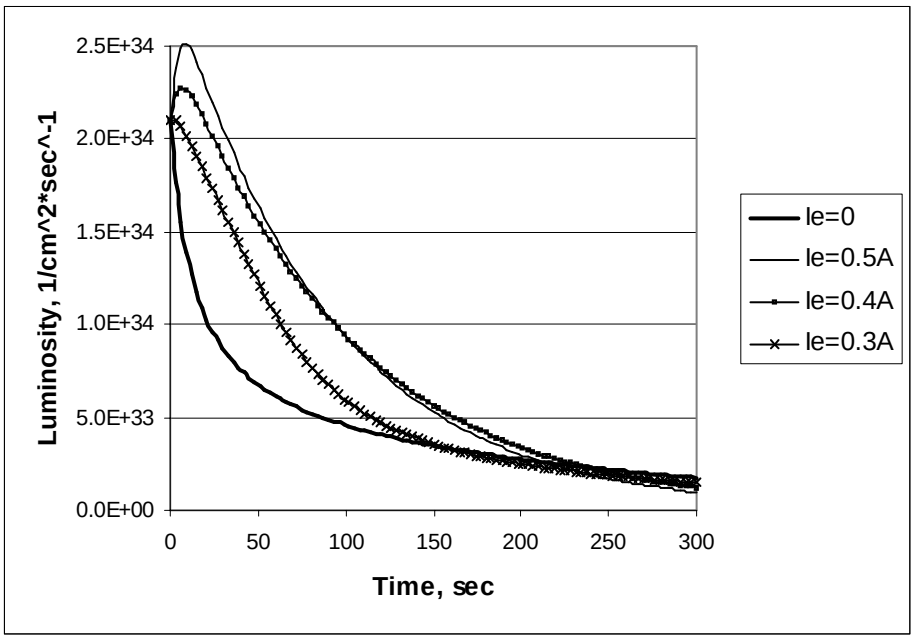

Fig. 4.14. Luminosity time dependencies at different electron beam current, beam energy is 1 GeV, pellet diameter is 80 μm.

At the electron beam current of 0.3 A the beam heating due to interaction with the target prevails on the cooling and beam emittance increases during experiment, but not so fast as without cooling. This "deceleration" of the emittance growth gives some gain in the luminosity life time in accordance with formula 4.4. At the electron beam current of 0.4 and 0.5 A the electron cooling completely suppresses the emittance growth and at the first stage of experiment (about 20 sec) the beam emittance decreases to the equilibrium value. The equilibrium is determined by the electron beam current and at 0.5 A it corresponds to about 0.62 π·mm·mrad in the horizontal plane and 0.88 π·mm·mrad in the vertical one. At the electron beam current of 0.4 A equilibrium emittances have some higher values: 0.7 π·mm·mrad - horizontal and 0.98 π·mm·mrad - vertical. After reaching the equilibrium luminosity decreases with the life time determined only by single scattering losses in the target. These losses is proportional to the probability of the particle cross the target, and, therefore, inversely proportional to the beam emittance. Thus, the initial gain in the luminosity, when the beam emittance decreases, is compensated by the shorter luminosity life time after reaching the equilibrium. It means that at the elevated beam energy and (or) relatively small target density the electron beam current has to be optimised to obtain maximum integral luminosity at each given experiment duration.

The possibility to vary the beam emittance during experiment can be investigated by comparison between the electron cooling rate and heating rate due to interaction with the target. In the Fig. 4.15 the dependencies of cooling and heating rate on the beam emittance at the beam energy of 2.7 GeV are presented.

At the pellet diameter of 80 μm (curve 4 in the Fig. 4.15) the heating always prevails on the cooling (curve 1), equilibrium is impossible and emittance of the beam increases to

acceptance of the ring. The cooling application can decrease the speed of the emittance growth only.

At the pellet diameter of 40 μm one can see the stable equilibrium point (point 1 in the Fig. 4.15) and unstable one (point 2). When the beam emittance value is less than certain value corresponded to the unstable equilibrium the emittance of the beam decreases under common action of the cooling and target to the stable equilibrium point. When the beam emittance is less than its value in the stable equilibrium, it increases, but the emittance increase is limited by the value corresponded to the stable equilibrium point.

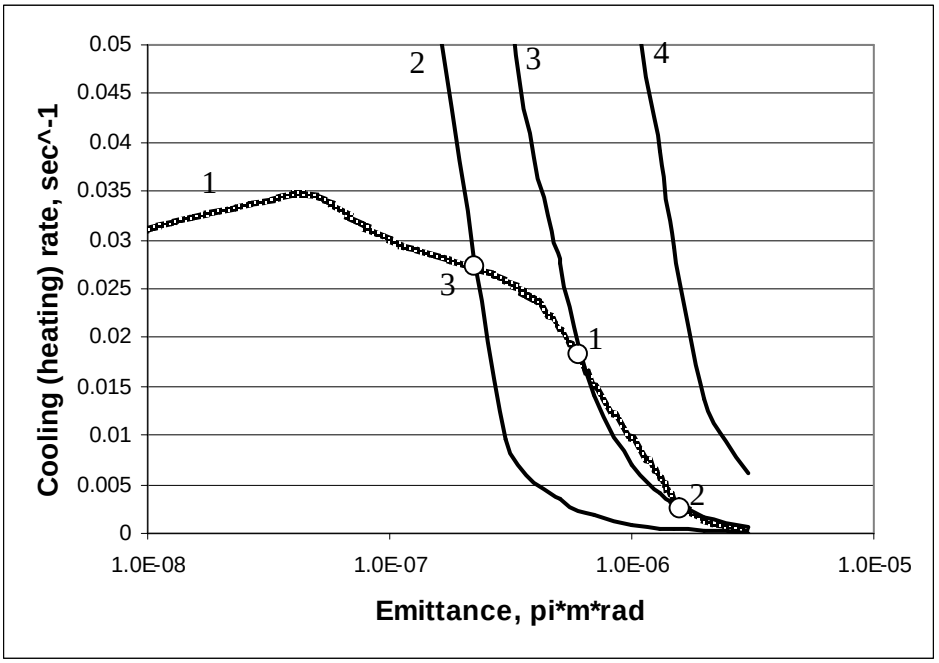

Fig. 4.15. Cooling rate at electron beam current of 0.5 A (1) and heating rate at pellet diameter of 20 μm (2), 40μm (3) and 80μm (4) as functions of the beam emittance, beam energy is 2.7 GeV.

At the pellet diameter of 20 μm the emittance value corresponded to the stable equilibrium (point 3 in the Fig 4.15) is less than in the previous case and unstable equilibrium lies outside the ring acceptance.

At low beam energy the maximum of the cooling rate is displaced to the region of higher emittances (this is a kinematical effect – the same emittance at low energy corresponds to low particle transverse velocity in the particle rest frame) and the maximum value increases due to strong dependence of the cooling time on the particle energy in the laboratory frame.

At the beam energy of 1 GeV the stable equilibrium points exist and unstable ones are outside the acceptance at all pellet diameters (Fig. 4.16). In this case the equilibrium beam emittance value can be varied by corresponding variation of the electron beam current. The range of the emittance variation is illustrated by the Fig. 4.17. At electron beam current of 150 mA the

stable equilibrium is reached at the emittance value of about 1.5 π·mm·mrad and the equilibrium displaces to the value of about 0.8 π·mm·mrad at the electron beam current of 500 mA. Thus, one can obtains the regime with permanent luminosity during the experiment compensating of the particle losses by corresponding increase of the electron beam current (and decrease of the beam emittance) (see formula 4.4).

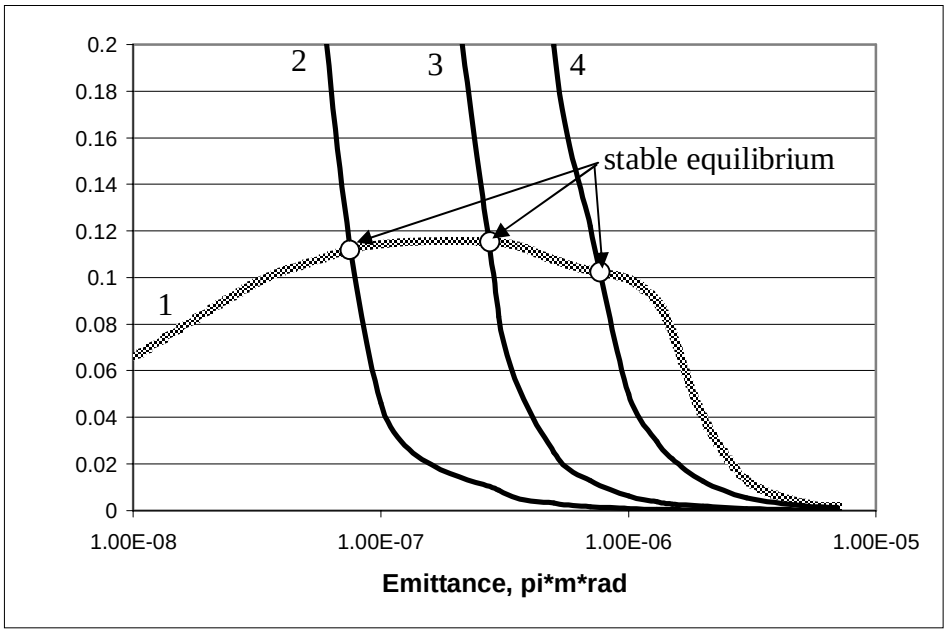

Fig. 4.16. Cooling rate at electron beam current of 0.5 A (1) and heating rate at pellet diameter of 20 μm (2), 40μm (3) and 80μm (4) as functions of the beam emittance, beam energy is 1 GeV.

The Fig. 4.15 – 4.17 are plotted without taking into account intrabeam scattering in the proton beam. However, the intrabeam scattering at the beam intensity up to 10^{11} particles slightly displaces the equilibrium position only.

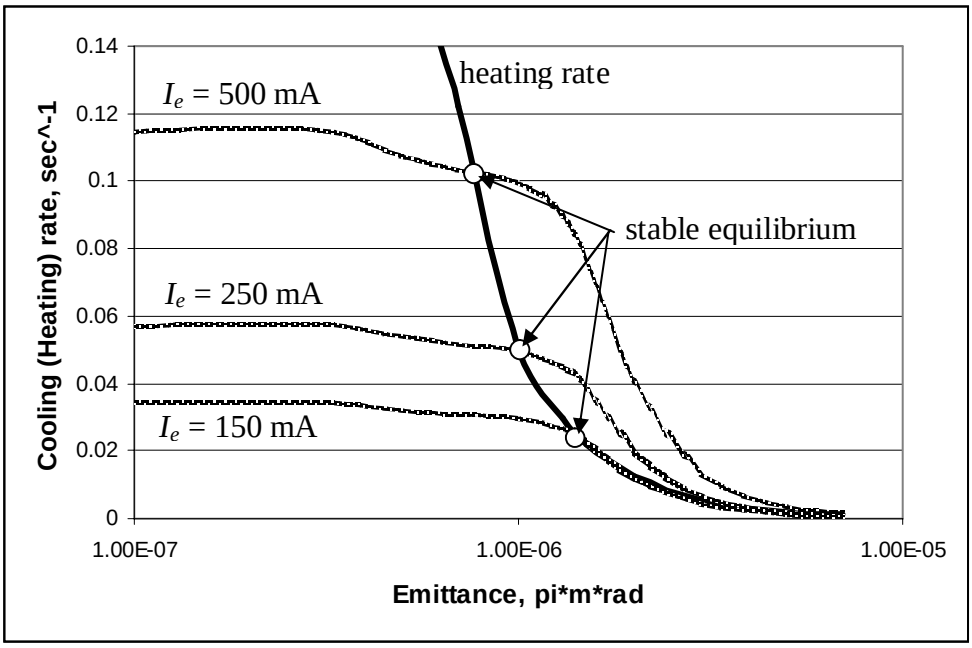

Fig. 4.17. The equilibrium position depending on the electron beam current. Pellet diameter is 80 μm, the beam energy is 1 GeV.

In the experiments with the deuteron beam the electron cooling gives a substantial gain in the luminosity even at big pellet diameter, due to small deuteron energy. But at deuteron beam energy of 2.11 GeV (Fig. 4.18) the electron cooling completely suppresses the beam heating only at maximum electron beam current of 500 mA and gain in the integral luminosity after five minutes of the experiment is about 50% (Fig. 4.18).

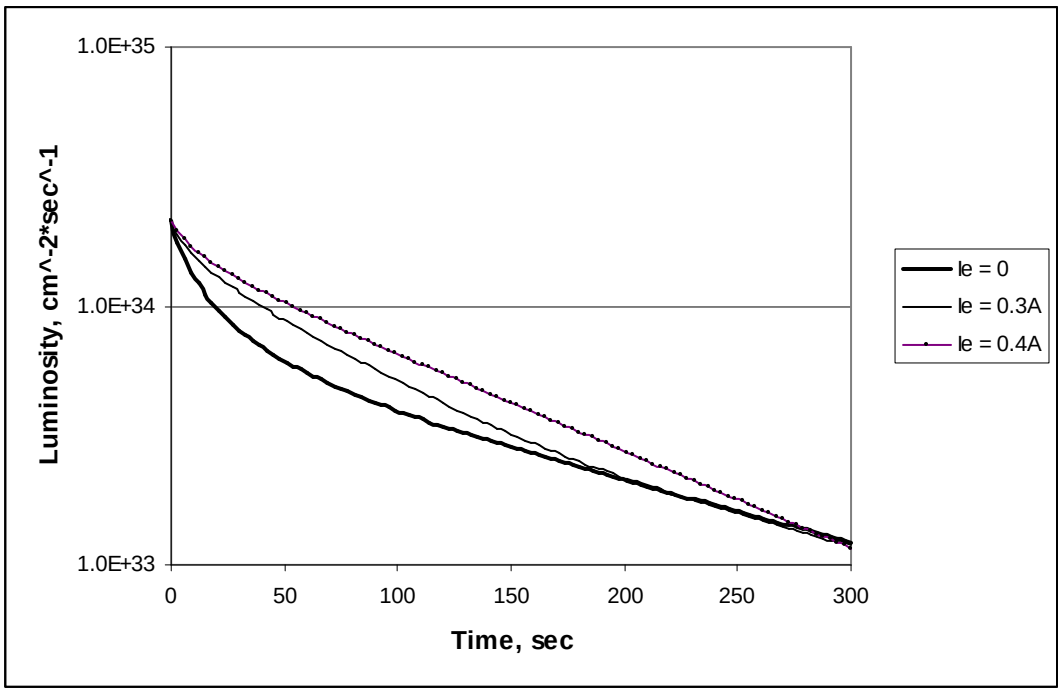

Fig. 4.18. Luminosity time dependence at different electron beam current. Deuteron beam energy is 2.11 GeV, the pellet diameter is 80 μm.

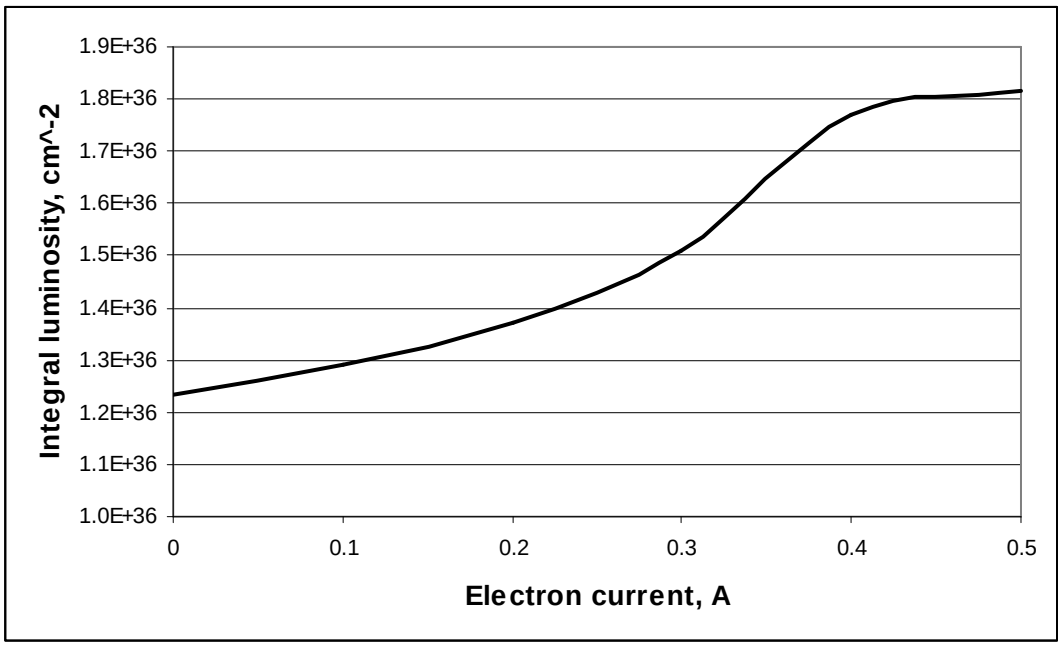

Fig. 4.19. Integral luminosity after five minutes of experiment as function of electron beam current. Deuteron beam energy is 2.11 GeV, the pellet diameter is 80 μm.

At less deuteron beam energy or at less pellet diameter the maximum gain in the integral luminosity can be achieved at less electron beam current and, as in the case with the proton beam, maximum expected gain in the luminosity can be 3 – 4 times.

4.3. Possible development of the existing electron cooling system

There are two possible design of the new cooling system:
- Traditional configuration of cooling system + HV accelerator,
- Cooling system with circulating electron beam.

Traditional configuration of the cooling system can provide electron beam at low transverse and longitudinal temperature, and the presented numerical results demonstrate its ability for ion beam parameters stabilization.

Electron cooling system with circulating electron beam has substantially low cost, but in such a system the electron beam quality is determined by a method of the beam acceleration, stability of electron motion in the electron storage ring, number of electrons and the ring circumference.

The required electron beam energy lies in the range from 0.5 to 1.5 MeV. Stable motion of the intensive electron beam at such relatively small energies can be provided only in the storage ring with longitudinal magnetic field. Electron beam acceleration can be provided using linear

RF accelerator which periodically fills up the ring with new portion of electrons, or directly in the electron storage ring using induction acceleration.

In the first case longitudinal temperature of the electron beam can be even higher than transverse one, and one of the general problems of this method is to adjust the momentum spread of the electron beam with the ring dynamic aperture on momentum deviation.

Induction acceleration of the electron beam permits to keep the flattened velocity distribution of the electrons and in principle provides the same longitudinal temperature as HV accelerator. However at constant value of the guiding magnetic field the working point crosses resonance regions of the Larmor oscillations. Due to this fact the transverse temperature of the electron beam can be higher than one in traditional cooling system by several orders of magnitude.

The design of the electron cooling system of traditional configuration was performed at COSY earlier [5]. The following chapters of this report are dedicated to investigation of cooling efficiency at relatively pure electron beam quality. The brief description of the cooling method with circulating electron beam and preliminary design of the installation are given.

5. Electron cooling system with circulating electron beam

The choice of the electron cooling system parameters is restricted by number of limitations. Part of them is common for both systems: with single pass and with circulating electron beam.

First of all it is requirement of the beam magnetisation, which limits the minimum value of the longitudinal magnetic field and maximum value of electron beam current.

Other limitations are related only to the system with circulating electron beam and particle dynamics in the storage ring with longitudinal magnetic field. Generals of them are the following:

- upper limit of the electron beam circulation period determined by increase of electron temperature during cooling process,

- upper limit of the electron beam momentum spread determined by dynamic aperture of the ring,

- upper limit of the electron beam current determined by threshold of microwave instability,

- limitations of the magnetic field and electron beam current due to longitudinal-transverse relaxation of the electron beam.

5.1. Magnetic field limitations

Electron beam magnetization is an efficient way of electron cooling rate increase using of longitudinal magnetic field [6] for transportation of the electron beam from the gun cathode to the collector through drift chambers including cooling section. The criterion of electron beam

magnetization has a clear physics meaning: radius of electron Larmor spiral in magnetic field has to be smaller of the mean distance between electrons [6]:

$$\rho \le (n_e)^{-1/3} \; when \; B > B_{\min 1} \equiv \frac{m}{e}\sqrt{T_\perp mc^2}\left(\frac{I_e}{\beta\gamma\pi a^2 ec}\right)^{1/3}. \qquad (5.1)$$

Here n_e is electron density in the electron rest frame, I_e – electron beam current, e, m – electron charge and mass, βc – electron velocity, $\gamma = \left(1-\beta^2\right)^{-1/2}$. Computer simulations with single pass electron beam show significant, up to several times, growth of cooling rate when $B \Rightarrow B_{min1}$ and its saturation $at \;\; B > B_{min1}$.

When electron beam is magnetized, electron drift caused by its own electric and guiding magnetic fields is sufficiently suppressed and does not exceed electron thermo velocity if

$$B > B_{\min 2} \equiv \frac{2I_e}{\beta\gamma a}\cdot\sqrt{\frac{m}{T_\perp}}. \qquad (5.2)$$

Comparing the criteria (3) and (4) one can see, that $B_{min1} > B_{min2}$, when

$$I < \frac{\beta\gamma ce}{\sqrt{\pi}\, r_e^{3/2}}\cdot\sqrt{a}\left(\frac{T_\perp}{2mc^2}\right)^{3/2} \approx 17.7\,\beta\gamma\sqrt{a_{[cm]}}\cdot(T_\perp)_{[eV]}^{3/2}, \qquad (5.3)$$

where r_e is electron classic radius. For COSY electron cooling system this condition is satisfied in the total range of the electron beam current required for effective cooling at minimum beam energy and minimum beam temperature. At reasonable electron beam transverse temperature (0.5 – 1 eV) the magnetic field value of 1 – 1.5 kG is big enough to provide beam magnetisation. More strong limitation of the magnetic field value follows from the requirement of suppression of the transverse-longitudinal relaxation in the electron beam during long circulation period. This process will be discussed below.

5.2. Principles of electron cooling with circulating electron beam.

The limitations of the electron beam circulating period are determined by the energy exchange between proton and electron beam due to the cooling process. The principle scheme [7] of the cooler with circulating electron beam (Fig. 5.1) includes an injector (“electron gun”), storage ring and electron collector (“electron dump”). The ring has straight section inserted in the structure of a hadron storage ring, where electron beam merges with proton one and cools it.

Due to interaction between the particles (antiprotons, ions) and electrons the particle temperature decreases when the electron one increases. The variation of both temperatures in Maxwellian plasma is described by the equations [7]:

$$\frac{dT_p}{dt} = \frac{4\sqrt{2\pi}\,\eta n_e z^2 e^4 L_C}{\gamma^2 mM}\cdot\frac{T_p - T_e}{\left(\frac{T_p}{M}+\frac{T_e}{m}\right)^{3/2}}; \qquad (5.4)$$

$$N_p \frac{dT_p}{dt} = - N_e \frac{dT_e}{dt}, \qquad (5.5)$$

where T_p , T_e are the particle and electron temperatures in the particle rest frame, m and M – their masses, N_p , N_e – the particle numbers in the rings, η is the ratio of the cooling section length to the circumference of the particle ring, L_C – Coulomb logarithm, n_e – the electron density, t – current time in Laboratory reference frame. The particle temperature in a cooler with single pass electron beam (and with Maxwellian velocity distribution!) decreases in accordance with the 1st equation, where T_e = *const.*

Therefore electron temperature in cooling process increase very fast and electron beam is to be renewed after electrons have got a significant temperature.

For typical parameters of the cooler the number of circulating electrons N_e is comparable with that one of the particles N_p circulating in COSY.

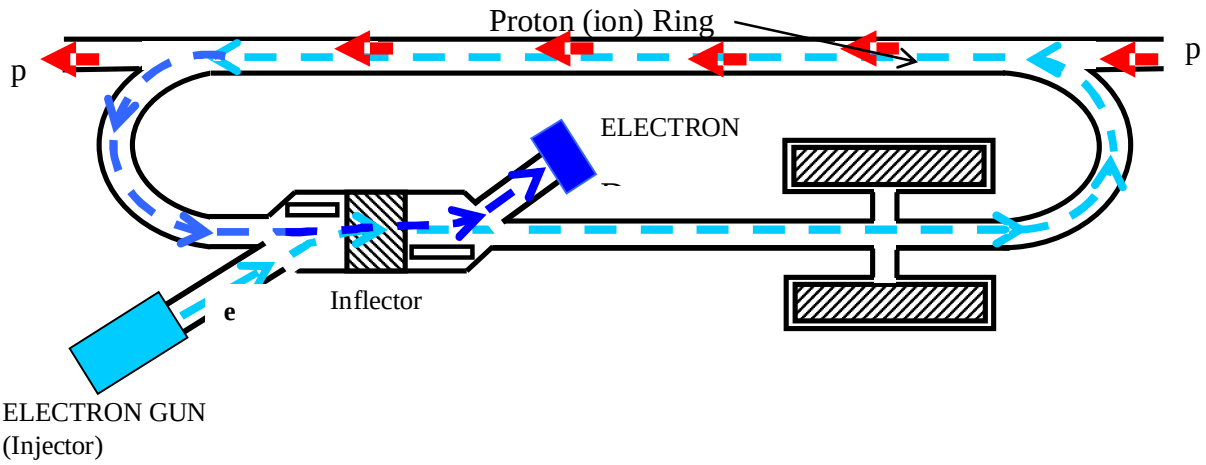

Fig. 5.1. Principle Scheme of Electron Cooler with Circulating Electron Beam

For electron beam with flattened velocity distribution electron beam parameter evolution during cooling process can be calculated as described in [1]. An example of the electron temperature variation during circulation is presented for COSY parameters in the Fig. 5.2.

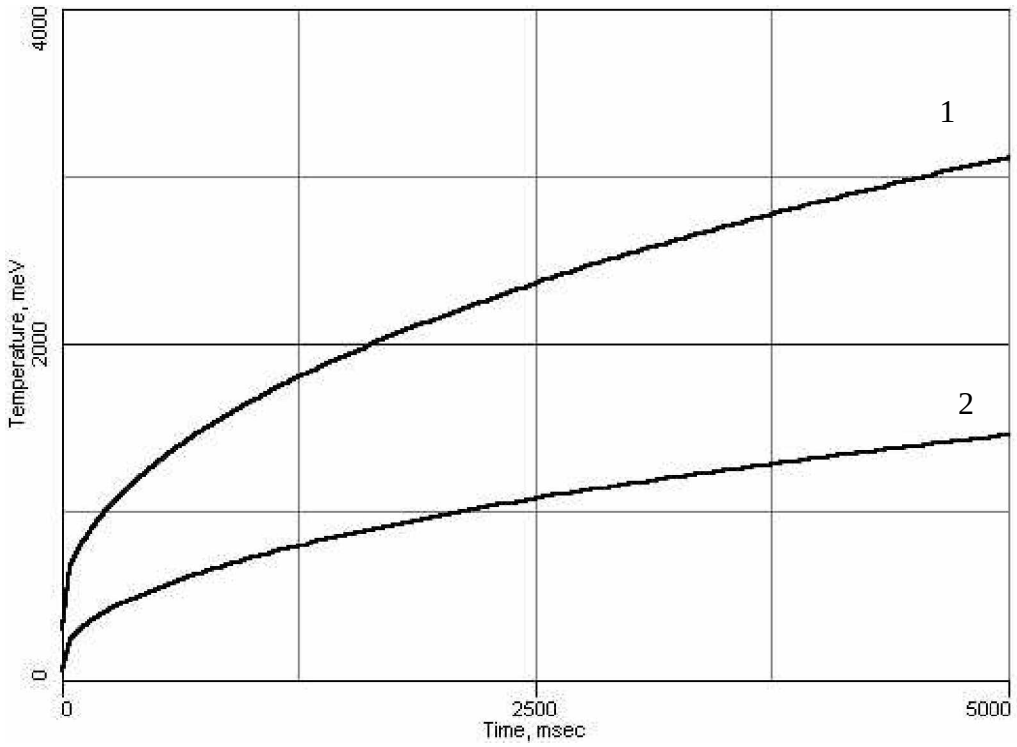

Fig. 5.2. Evolution of the transverse (1) and longitudinal (2) electron beam temperature during circulation. Proton beam energy is 1 GeV, proton number is 10^{11}, initial transverse electron temperature is 300 meV, longitudinal – 50 meV, electron beam radius is 0.5 cm, current – 0.5 A, electron ring circumference is 20 m, magnetic field is 1.2 kG, cooling section length – 1.4 m.

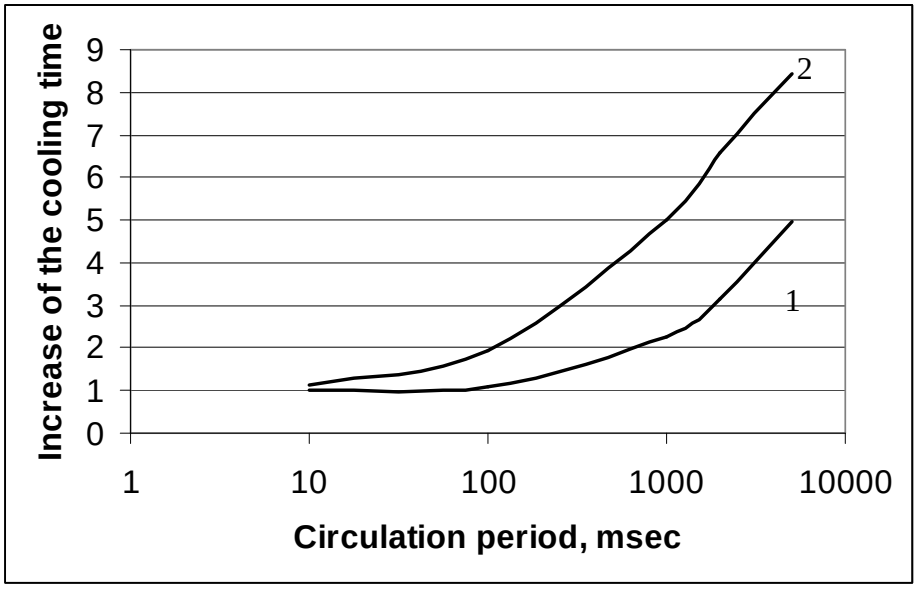

Fig. 5.3. Ratio of the characteristic cooling time of transverse degree of freedom providing by the cooling system with circulating electron beam to single pass one. Proton beam energy is 2.7 GeV (1) and 1 GeV (2), proton number is 10^{11}, initial transverse electron temperature is 300 meV, longitudinal – 50 meV, electron beam radius is 0.5 cm, current – 0.5 A, electron ring circumference is 20 m, magnetic field is 1.2 kG, cooling section length – 1.4 m.

The limitation of the circulation period is stronger at low beam energy. In the Fig. 5.3 the dependence of the cooling time on circulating period is presented at proton beam energy of 1 GeV and 2.7 GeV.

At circulation period shorter than 100 msec efficiency of the cooling system with circulating beam is practically the same as the single pass one (at minimum energy increase of the cooling time is less than two times). The cooling efficiency decreases during the circulation and after the period of time longer than approximately a few seconds further circulation of electrons does not influence practically on the proton beam parameters.

The circumference of the electron ring determines the total number of electrons and as a result the thermo capacity of the electron beam. In principle the electron beam circumference is to be as long as possible. The ring circumference of 20 meters is the minimum value, which permits to install in the ring injection and extraction systems, helical quadrupole lens for electron focusing and betatron yoke (if it is necessary).

The electron cooling system parameters determined by the requirements of beam magnetization and cooling efficiency are listed in the Table 5.1 and further calculations are performed at these parameters.

Table 5.1. General parameters of the electron cooling system with circulating electron beam

Electron ring circumference, m	20
Magnetic field, kG	1 – 1.5
Electron beam radius, cm	0.5
Maximum electron current, A	0.5
Effective length of the cooling section, m	1.4
Circulation period, msec	100 – 1000
Transverse electron temperature, meV	300 – 1000
Longitudinal electron temperature, meV	50 – 100

5.3. Storage ring with longitudinal magnetic field.

At electron energy of 10 MeV and higher usual strong focusing ring can be used for storage of electrons. In the case of low electron energy the storage ring with longitudinal magnetic field has some advantage (like electron magnetization) and provides a stable motion of circulating electrons. Such electron ring can be used simultaneously for preliminary acceleration of electrons. Then the injector delivers electrons of rather low energy. So called “modified betatron” is one of possible schemes of the storage ring with cooling electron beam. Combination of the ring with an injector provides an added bonus.

5.3.1 Particle dynamics in the ring with longitudinal magnetic field

Focusing system of the ring consists of straight and toroidal solenoids connected together as a racetrack. To form a closed orbit for a circulating particle the helical quadrupole winding is used. In the cooling section the quadrupole field is absent to avoid distortion of the cooling process. The helical winding can be placed in the straight section opposite to the cooling one.

Due to presence of the longitudinal and helical quadrupole magnetic fields the particle motion in the horizontal and vertical plane are strongly coupled. When the number of the spiral winding steps in the focusing section is integer the particle motion in the first approximation consists of two independent modes [8]:

a) fast Larmor rotation of every particle around "own" magnetic field line, which tune is equal to:

$$Q_{fast} \approx \frac{C}{2\pi\rho}, \tag{5.6}$$

$\rho = v/\omega_B, \omega_B = eB/\gamma mc$ is the electron cyclotron frequency, ρ is the electron Larmor radius, B is the longitudinal magnetic field averaged over the closed orbit, C is the ring circumference;

b) slow rotation of the beam as a whole around the axis of the helical quadrupole winding with the tune

$$Q_{slow} \approx \left(\frac{G}{B}\right)^2 \frac{L}{2k}, \tag{5.7}$$

L is the length of the sections with quadrupole field, G is the gradient of the quadrupole field, $k = 2\pi/h$, h is the step of the spiral winding.

For instance at typical parameters of the focusing system B = 1000 G, G = 20 G/cm, h = 60 cm, L = 120 cm, C = 20 m and at electron energy of 500 keV the working point corresponds to Q_{fast} = 109.4 (at maximum beam energy of 1.5 MeV Q_{fast} = 49.1), Q_{slow} = 0.24. In this case dispersion in the cooling section is relatively small: D_x = 10 cm, ellipticity of the electron beam cross section in the cooling section is less than 1%, i.e. circulating beam in the cooling section has round shape. Angular spread of the electron beam due to action of the helical quadrupole field can be reduced to the value less than 1 mrad by adiabatic variation of the gradient value at the entrance and at the exit of the quadrupole field region. Calculation of the ring lattice functions and beam parameters in the cooling section are provided numerically and the algorithm and computer code elaborated in JINR for this aim are described in [9]. Detailed design of the electron ring optics and accurate choice of the working point in the total range of electron energy can be a topic of further steps of the cooling system design and are not included in this report.

The motion stability conditions can be written as the following:

$$Q_{fast} \neq \frac{n}{2},\ Q_{slow} \neq \frac{k}{2},\ Q_{fast} \pm Q_{slow} \neq l \tag{5.8}$$

n, k, l are integer.

The resonant condition for the fast mode of oscillation (due to large value of its chromaticity) limits a dynamic aperture of the ring on momentum deviation. The particle momentum spread can not exceed the distance between nearest integer and half integer resonances. This value can be estimated by the following expressions:

$$\frac{\Delta Q_{fast}}{Q_{fast}} = -\frac{\Delta\rho}{\rho} = -\left(\frac{\Delta p}{p}\right)_{\max},\ \left|\Delta Q_{fast}\right| \leq \frac{1}{4}, \tag{5.9}$$

which gives us

$$\sigma_0 = \left(\frac{\Delta p}{p}\right)_{\max} \sim \frac{1}{4Q_{fast}} \quad . \tag{5.10}$$

Fig. 5.4 presents the dynamic aperture value at the ring circumference of 20 m. Width and power of resonances are determined by the errors of the focusing fields. Fast crossing of high order resonance leads to increase of the beam transverse temperature only. However, during a long circulation period the stability conditions (5.8) have to be satisfied to keep a good beam quality even at small instability increment.

At minimum electron beam energy and magnetic field of 1 – 1.5 kG the value of the ring dynamic aperture (Fig. 5.4.) is approximately equal to $2 \cdot 10^{-3}$ and such a value of the electron beam momentum spread has to be provided by the system of the electron beam acceleration. At maximum electron beam energy this limitation is not so strong.

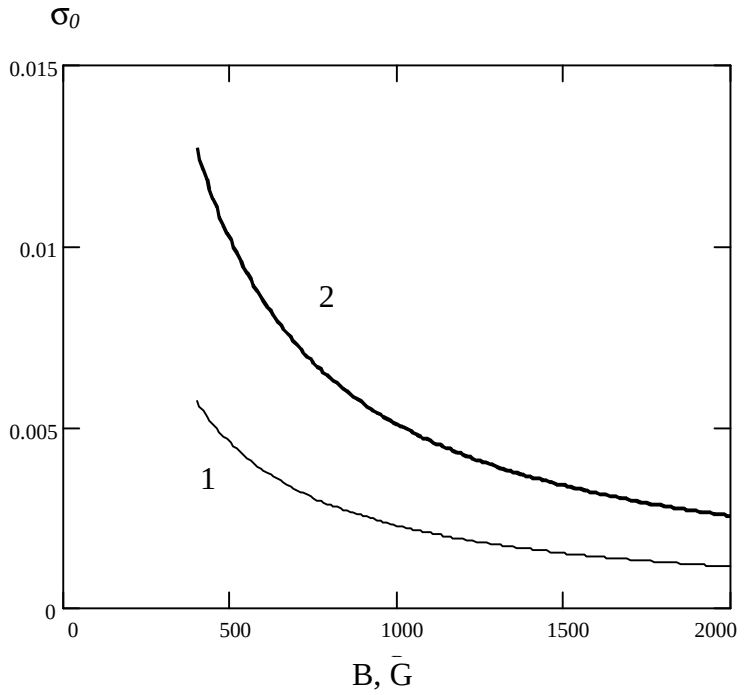

Fig. 5.4. Dynamic aperture on momentum deviation as function of longitudinal magnetic field, 1 – beam energy is 500 keV, 2 – beam energy is 1.5 MeV.

In principle, the maximum permitted value of momentum spread limits the circulating beam current because the momentum shift between particles at the axis and at the beam radius produced by the beam space charge has not to exceed $(\Delta p / p)_{\max}$. The shift in electron momentum due to electron beam space charge is equal to

$$\frac{\Delta p}{p} = (1 - \eta_n) \frac{eI}{\beta^3 \gamma m_e c^3}, \tag{5.11}$$

where η_n is neutralisation factor. Correspondingly, the maximum current of electron beam is limited by the value

$$I \le \frac{\beta^3 \gamma m_e c^2 \sigma_0}{(1-\eta_n)e} . \qquad (5.12)$$

However, even at zero neutralisation factor this condition practically does not limit a possible value of the beam current up to magnetic field value of several kG (Fig. 5.5).

More serious limitation of the circulating beam current is determined by the threshold of the microwave instability and it is discussed in the next chapter.

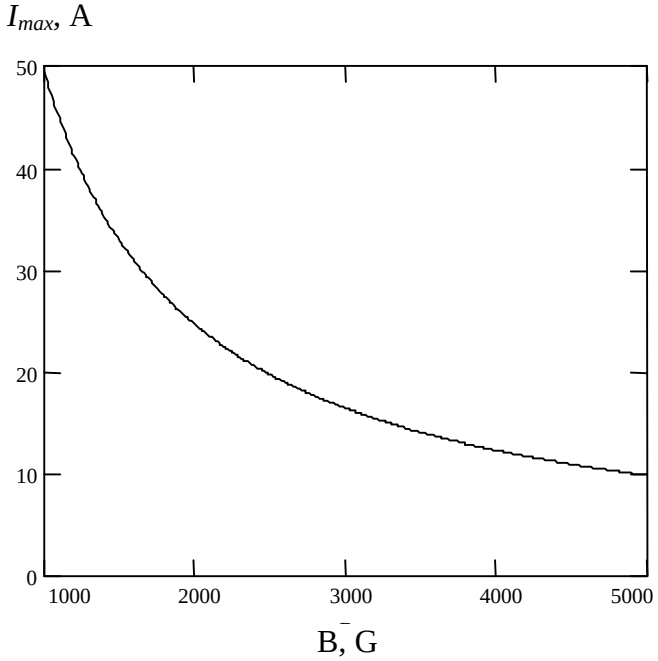

Fig. 5.5. Upper limit of the circulating beam current determined by momentum shift due to its space charge. Beam energy is 500 keV, neutralisation factor is equal to zero.

5.3.2 Current limitation due to microwave instability

At given maximum value of the momentum spread the longitudinal microwave instability limits the intensity of the circulating beam. Dynamics of longitudinal motion in the LEPTA is the same as in a standard strong focusing ring, and therefore we can use the usual criterion for longitudinal stability of the electron beam, which can be written as follows [10]:

$$I \le 4F_{long} \frac{mc^2 \beta^2 \gamma |\eta|}{e|Z_n / n|} \sigma_f^2 , \qquad (5.13)$$

σ_f is a spread in momentum deviation (half width on half height). Z_n is a longitudinal coupling impedance of the beam for a mode with number n. Factor F_{long} takes into account the real shape of the stability diagram. In standard Keil-Schnel criterium F_{long} = 1. However, when beam energy is less than critical one and momentum distribution function has a long "tails" F_{long} value can be significantly larger than unit. In this case with a good accuracy we can write:

$$F_{long} \cong \sigma_0^2 / 2\sigma_f^2 , \qquad (5.14)$$

where σ_0 is a dynamical aperture of the machine on momentum deviation. If the crossing of the half-integer resonance is impossible σ_0 is limited by the condition (5.10). The impedance for cylindrical beam and vacuum chamber is described with the formula:

$$\left|\frac{Z_n}{n}\right| = \frac{377}{2\beta\gamma^2}\left(1 + 2\ln\frac{b}{a}\right), \qquad (5.15)$$

where *b* and *a* are the radii of vacuum chamber and electron beam. This formula gives us about 250 Ohms at minimum beam energy.

For described focusing structure the transition energy of the ring can be estimated as $\gamma_{tr}^2 \cong \pm Q_{fast}\, Q_{slow}$ [8]. The sign of γ_{tr}^2 is determined by the directions of the longitudinal magnetic field and the qudrupole helical winding rotation, what permits to us choose the regime with $\eta > 0$ (no negative mass instability) in the total energy range. In this case the instability takes place due to finite conductivity of the vacuum chamber walls.

The threshold current (5.13) as a function of beam energy and longitudinal magnetic field is presented in the Fig. 5.6, the tune value of the slow mode of oscillations was chosen to be equal 0.2 in the total energy range. The threshold current decreases with the increase of magnetic field value due to dependence of σ_0 on the magnetic field (see Fig. 5.4).

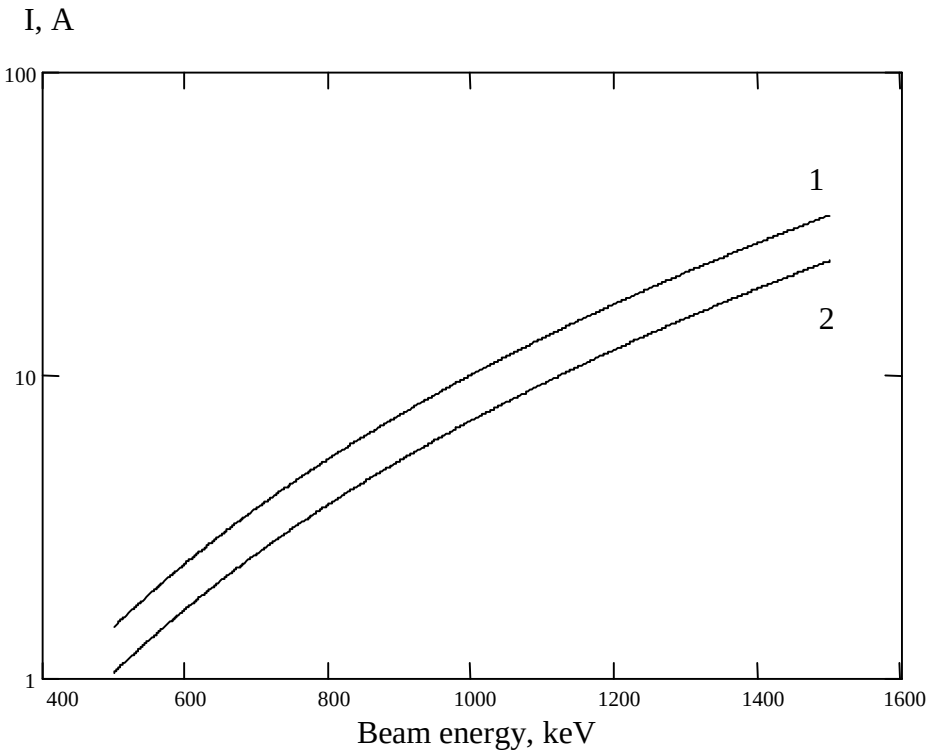

Fig 5.6. Threshold electron beam current of microwave instability: 1 – magnetic field is 1 kG, 2 – magnetic field is 2 kG.

At minimum electron beam energy the threshold beam current is higher than maximum designed value only by two times, however, even taking into account decrease of the cooling efficiency for the system with circulating electron beam, required value of electron beam current at minimum energy does not exceed 0.3 A.

5.3.3. Transverse-longitudinal relaxation of electron beam

In the magnetised electron beam intrabeam scattering is substantially suppressed by longitudinal magnetic field. Characteristic time of the temperature growth rate can be estimated by the following empirical expression [11]:

$$\frac{1}{\tau_{relax}} = \frac{1}{T_{\parallel}} \frac{dT_{\parallel}}{dt} \approx \frac{2\pi r_e^2 n_e mc^3 L_C}{T_{\parallel}} \sqrt{\frac{mc^2}{T_{\perp}}} e^{-2.8/\rho n_e^{1/3}}, \qquad (5.16)$$

where r_e is the electron classical electron radius, $L_c \sim 10$ is the Coulomb logarithm, n_e is the beam density, $\rho = \sqrt{2mc^2 T_{\perp}} / eB$ is the particle Larmor radius in the longitudinal magnetic field B. Exponential term in (5.16) leads to strong dependence of the relaxation characteristic time on the temperature of transverse degree of freedom and on the beam current (Fig. 5.7).

At electron beam current of 0.1 A the magnetic field value of 1.5 kG seems to be big enough to suppress intrabeam scattering of the electron beam during the period required for beam circulation. At maximum electron beam current the relaxation time is less than circulation period by about three orders of magnitude. It means that this process has to be taken into account in estimations of the cooling system efficiency.

The formula (5.16) describing the electron beam relaxation is half-empirical one and due to importance of this process for cooling system with circulating electron beam has to be carefully tested with the real installation. The process of the transverse – longitudinal relaxation in the cooling system with circulating electron beam will be experimentally investigated at LEPTA ring (see chapter 7).

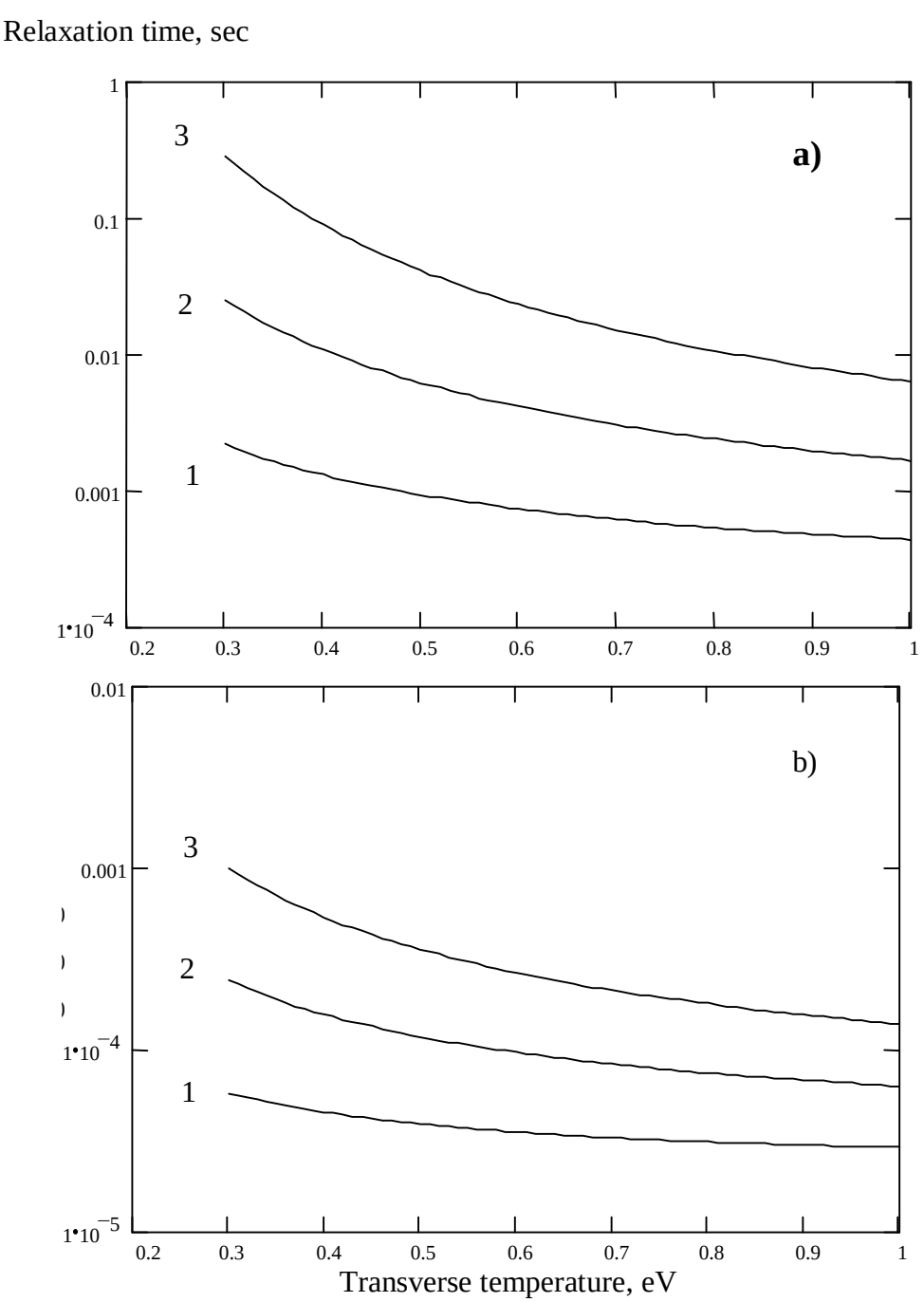

Fig. 5.7. Characteristic time of the transverse-longitudinal relaxation of the electron beam, magnetic field is 1 kG (1), 1.5 kG (2), 2 kG (3), longitudinal temperature is 50 meV, electron beam current is 0.1 (a) and 0.5 A (b).

5.4. Electron cooling with circulating electron beam in experiments with internal target

In experiments with internal target additional limit appears for the electron beam circulation period. It is connected with the coherent energy losses of the ion beam due to interaction with the target. Due to energy exchange between the ion beam and circulating electron one the beam velocities in the cooling section are the same. Correspondingly, the coherent energy variation of the electron and ion beams during the circulation period are connected in accordance with the relation:

$$\left(\frac{\Delta E}{E}\right)_e = \left(\frac{\Delta E}{E}\right)_i . \tag{5.17}$$

During the circulation period the energies of the ion and electron beams have to be inside the dynamic apertures on momentum deviation of corresponding ring. The dynamic aperture on momentum deviation of the electron ring with longitudinal magnetic field (σ_0 formula 5.10) is less than that one of the ion ring. Coherent momentum shift of the electron beam can be calculated as the following:

$$\frac{\delta p}{p} = \frac{1}{2}\frac{\Delta E}{E}\frac{T_{circ}}{T_{rev}}, \tag{5.18}$$

where ΔE is the ion energy loss after crossing the target (formula 1.2), E is the ion energy and T_{circ} is the electron beam circulation period. From the condition $\delta p/p \le \sigma_0$ one can write the condition for upper limit of the circulation period:

$$T_{circ} \le T_{\max,1} = \frac{T_{rev} E \rho_L}{2\Delta E C}, \tag{5.19}$$

where C is the electron ring circumference, ρ_L is the electron Larmor radius in the longitudinal magnetic field, T_{rev} is the ion revolution period. The dependencies of the maximum circulation period of the electron beam on the particle energy and the target density are presented in the Fig. 5.8. In the total range of the COSY experiment parameters the circulation period has to be less than about 1 second to avoid a resonance of the electron beam.

Other limitation connected with this effect is related to distortion of the cooling process after refresh the electron beam: the coherent momentum shift of the ion beam after circulation period has to be substantially less than its momentum spread. Only in this case the model using for cooling process simulation gives correct results for the system with circulating electron beam. The condition, when the used numerical model is valid for calculation of the cooling time for the system with circulating electron beam, can be expressed in the following form:

$$T_{circ} << T_{\max,2} = \frac{2T_{rev} E (\Delta p / p)_i}{\Delta E}. \tag{5.20}$$

The momentum spread of the ion beam $(\Delta p/p)_i$ depends on many parameters and can be varied by about one order of magnitude depending on experiment conditions. In the Fig. 5.9 the coherent energy shift of the proton beam as a function of the circulation period and beam energy is presented. One can see that at circulation period of about several hundreds of msec this effect can be ignored at all reasonable ion beam parameters.

a)

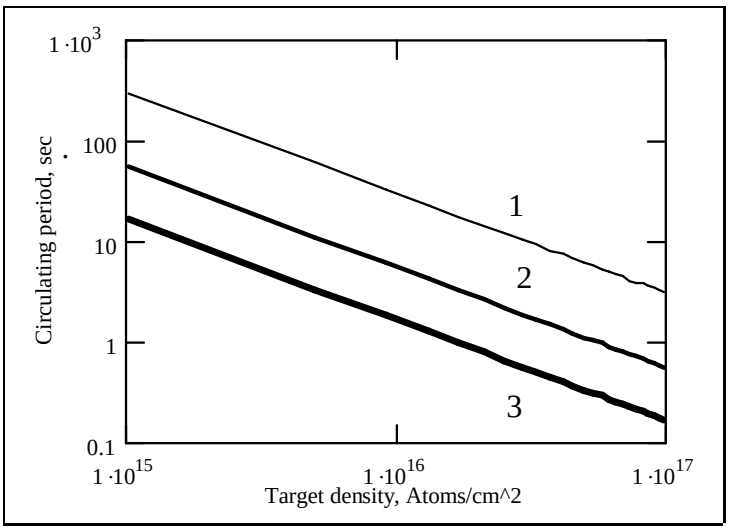

b)

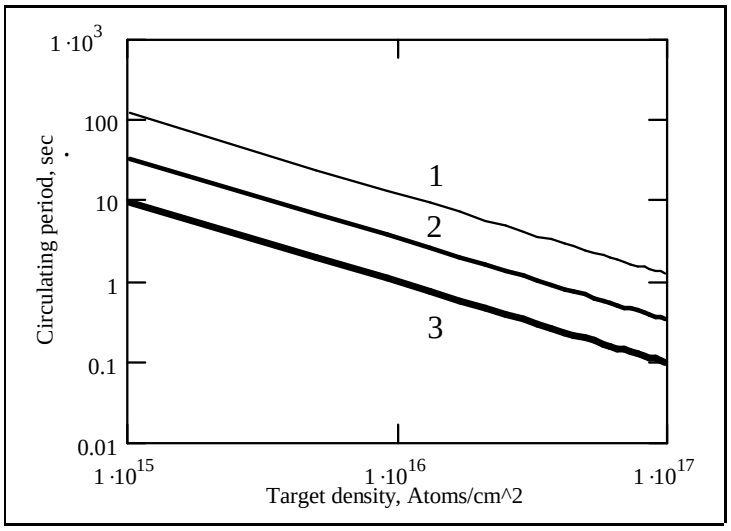

Fig. 5.8. Maximum circulating period of the electron beam as function of the target density:
a) proton beam at energy 2700 MeV (1), 1000 MeV (2), 500 MeV (3);
b) deuteron beam at energy 2100 MeV (1), 1000 MeV (2), 500 MeV(3).

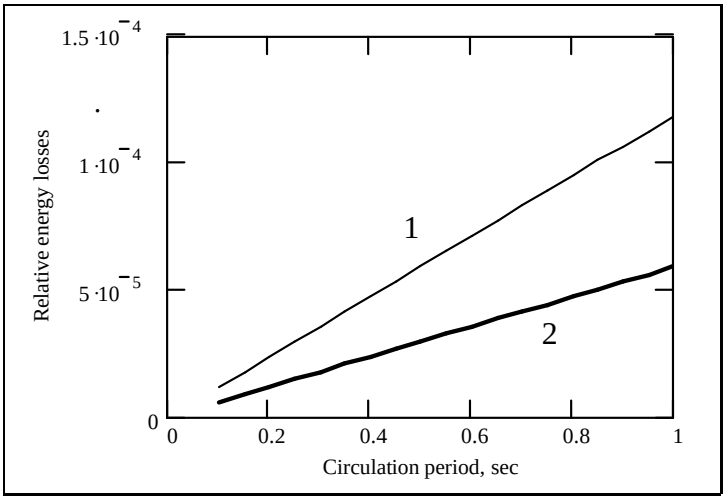

Fig. 5.9. Relative energy losses of the proton beam at target density of 10^{16} Atoms/cm^2, at energy 1000 MeV (1) and 2000 MeV (2).

5.5. Induction acceleration of the electron beam.

The electron acceleration can be provided using RF linac with further injection into electron ring or inside the electron ring using low frequency betatron acceleration. In the second case the energy spread of the accelerated electron beam caused by variations of the acceleration voltage during revolution period, is equal to [12]:

$$\Delta\varepsilon = e(\frac{\partial V}{\partial t}\tau_{rev})_{inj} - e(\frac{\partial V}{\partial t}\tau_{rev})_{fin}, \tag{5.21}$$

where V is the accelerating voltage, τ_{rev} is the electron revolution period. When $V=V_0 sin(\omega t)$ and initial and final phases of acceleration are symmetrically disposed around the voltage maximum, this formula gives us

$$\frac{\Delta\varepsilon}{\varepsilon} \approx \left(\frac{C\omega}{c}\right)^2 \frac{1-\beta_{inj}}{\beta_{inj}\bar{\beta}}. \tag{5.22}$$

In this case the acceleration voltage amplitude can be obtained by integration of the motion equation:

$$eV_0 = \frac{C\omega}{c}\frac{\varepsilon}{2\bar{\beta}\cos\omega t_{inj}}, \tag{5.23}$$

where C is the electron ring circumference, β_{inj}, $\bar{\beta}$ - initial and average electron velocity in the units of the speed of light.

Using the existing COSY high voltage power supply for injection one can accelerate electrons 0.5 msec from ε = 100 keV (injection) up to 1.5 MeV. The estimated momentum spread value caused by the voltage variation is negligible (Table 5.2).

Table 5.2. Parameters of the induction acceleration system

Injection energy, keV	100
Maximum energy, keV	1500
Electron ring circumference, m	20
Frequency of the acceleration voltage variation, kHz	1
Required amplitude of the acceleration voltage, V	500
Beam momentum spread caused by voltage variation	$2\cdot10^{-7}$

During the electron beam acceleration inside the ring with constant value of the longitudinal magnetic field the working point crosses series of the resonances of the fast mode of oscillation. The experiments at Modified Betatron Acceleratator in NRL (USA) [13] have shown that the crossing of the high order resonances does not lead to the particle losses. An increase of the beam transverse temperature in these experiments was not investigated and we plan to perform such investigations at LEPTA ring (see chapter 7).

6. Principles of the electron cooling system design

All general elements of electron cooling system with circulating electron beam are presented in the Fig. 6.1. If the electron acceleration is performed with RF electron linac, the betatron yoke is not necessary and instead of electron gun one needs to install the RF cavity and debunching system, if necessary to reduce $\Delta p/p$ (see [14]).

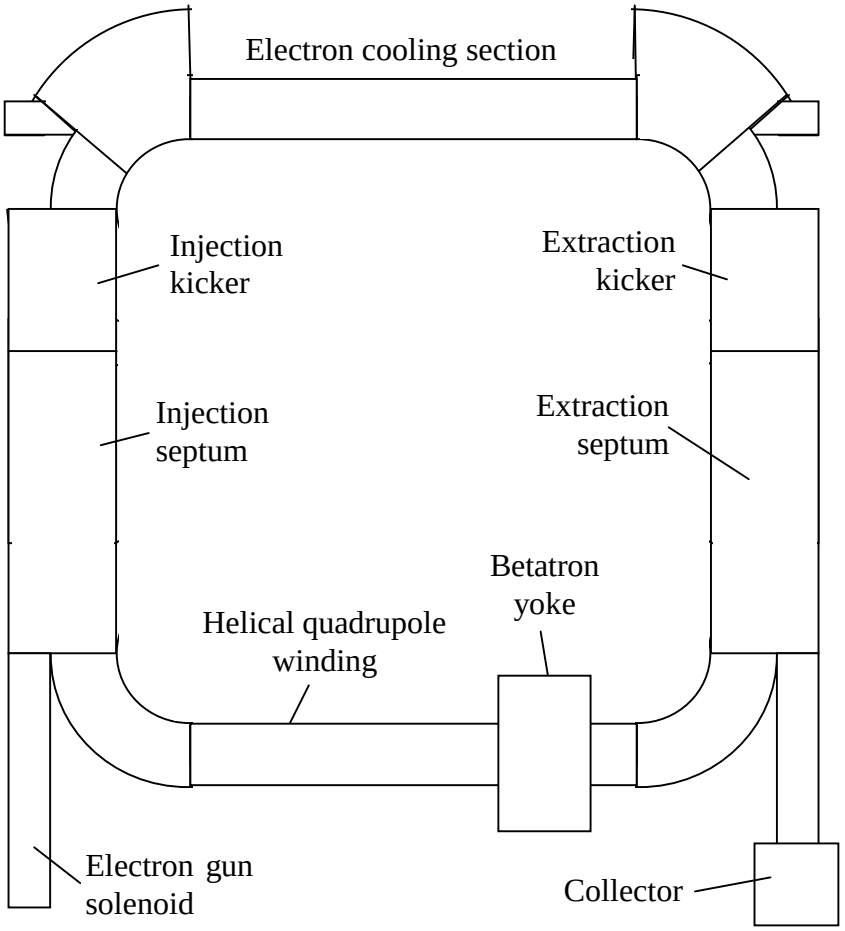

Fig. 6.1. Layout of the electron cooling system with circulating electron beam.

The electron beam injection into the ring is provided along the longitudinal magnetic field with transverse field of septum coils, which displace the electron beam to the vicinity of the equilibrium orbit at the distance of about diameter of the gun solenoid. Than the kicker plates displace the beam to the equilibrium orbit.

Inside the septum coil the electron beam drifts in the longitudinal magnetic field of the septum solenoid and transverse magnetic field of the septum coil. The field of the septum coil has a zero value at the orbit of circulating beam due to special coil design. Possible design of the septum coil is presented in the next chapter. The septum coils are operated in the DC mode.

The field of the kicker displaces the electron beam to the equilibrium orbit and after the beam occupies the total ring circumference the field of the kicker has to be switched off during the time substantially shorter than revolution period. Drift of the electrons inside the kicker can be performed by transverse magnetic field or by electric field. When electrostatic kicker is

applied the cooling system can be used also in the single pass mode of operation. In this case both kickers – injection and extraction are used in the DC mode and electron beam is displaced by injection kicker to the orbit inside the cooling section and after moving through the cooling section is displaced to extraction septum and to the collector by extraction kicker. Such a possibility looks like very attractive for COSY – it permits to use electron cooling system at injection energy in the single pass regime with existing electron gun and its power supply system. The example of the electrostatic kicker design is presented in the next chapter.

In the case of induction acceleration of the electron beam the existing COSY electron cooling system can be upgraded to medium energy electron cooling system by installation of several new solenoids and betatron yoke for electron acceleration. Two of the new solenoids (septum solenoids) are to be placed vertically above the existing toroidal solenoids. In each of these solenoids the coils of magnetic septum and electrostatic kicker are placed. Existing electron gun and collector with their solenoids are placed above these two new septum solenoids. To form a closed orbit for electron beam two toroidal and straight solenoids are connected with the septum solenoids. In the straight solenoid (which is placed opposite to the cooling section) the betatron yoke and helical quadrupole windings are placed.

In the regime with circulating electron beam the beam from the gun is directed to the closed orbit by injection septum and kicker plates. When the beam fills total circumference of the electron ring kicker voltage is switched off. After that beam is accelerated to required energy with the betatron yoke. Next current pulse applied to the betatron yoke coil decelerates the circulating electron beam and after deceleration the electron beam is extracted to the collector by the pulse applied to the extraction kicker.

The cooling system with induction acceleration has a lower cost in comparison with RF acceleration, but general problem of this system is beam quality degradation after crossing of number of resonances. This problem as well as optimisation of injection system can be experimentally investigated at LEPTA ring.

7. Program of experiments at LEPTA

7.1. LEPTA parameters

The general aim of the LEPTA ring construction (Fig. 7.1) is to provide storing low energy positrons, electron cooling of positrons and generation of the directed flux of positronium atoms. However at design study of the ring all the parameters were chosen such that we have a possibility to test beam parameters required for electron cooling system with circulating electron beam. The parameters of the ring in the mode with circulating electron beam (Table 7.1) are closed to the parameters of COSY cooling system and designed parameters of the betatron yoke cover the total energy range of the circulating beam required for COSY.

Adjustment of the injection and extraction system, investigations of an influence of the helical quadrupole winding will be performed during ring commissioning using optic method of the beam temperature measurement [3].

At the first stage of the LEPTA operation the study of the beam dynamics will be performed at the beam energy of 10 keV and variation of the beam energy will be provided using small RF cavity. Final test of the system will be performed after installation of the betatron yoke and it presumes the electron beam acceleration and test of the beam temperature at maximum required energy.

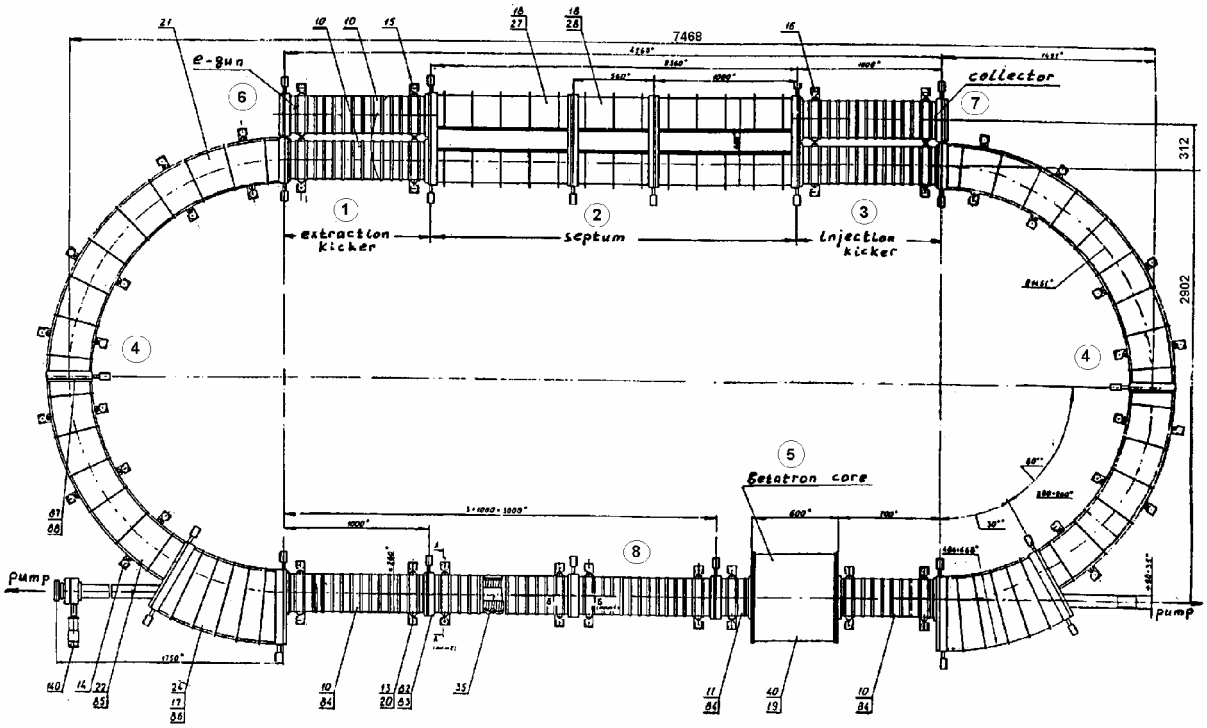

Fig 7.1. The assembly drawing of the LEPTA: 1 - extraction kicker, 2 - septum, 3 - injection kicker, 4 - toroidal sections, 5 - betatron core, 6 - electron gun, 7 - electron collector, 8 - cooling section.

Table 7.1. General parameters of the LEPTA.

Ring parameters		
Circumference, m	18.28	
Longitudinal magnetic field, G	1000	
Major radius of the toroids, m	1.45	
Bending magnetic field, G	1.75 – 124	
Gradient of the quadrupole magnetic field, G/cm	10 – 15	
Electron beam radius, cm	1.0	
Residual gas pressure, Torr	10^{-10}	
Electron beam parameters		
	At injection	After acceleration
Energy, keV	10	4360
Current, A	0.1	0.5
Revolution period, nsec	300	60
Acceleration cycle		
Induction voltage amplitude, V	50	
Repetition frequency, Hz	1	
Cycle duration, msec	10	

7.2. Preliminary program of the experiments.

General problems which have to be experimentally investigated before design of the full scale electron cooling system with circulating electron beam are the following:
- beam parameter distortion during injection,
- variation of the longitudinal beam temperature due to transverse-longitudinal relaxation,
- beam parameter distortion after crossing the resonances of the fast mode of oscillation.

The aim of the investigations is the final choice of the magnetic field value and the optimal position of the working point of circulating beam in the total range of the beam energy, accurate measurements of the maximum beam current which can circulate in the ring without loss the quality during required period of time. These experiments will be performed at the special test bench during the LEPTA assembling and with circulating electron beam during the ring commissioning.

7.2.1. Tuning of injection system and helical quadrupole winding

Injection system of the ring consists of magnetic septum (Fig. 7.2, Table 7.2) and electrostatic kicker (Fig. 7.3). Variation of the angle of the electron beam trajectory at the entrance and at the exit of the septum and kicker is about 15 mrad and only a resonance optics of these elements permits to keep electron beam quality after injection. In this case the integer number of the electron larmor rotations has to take plase at the length of the kicker and septum. Calculate of the effective length of the septum and kicker coils accurately is a complicated numerical problem and these values will be measured experimentally using optic method of the electron transverse temperature measurements.

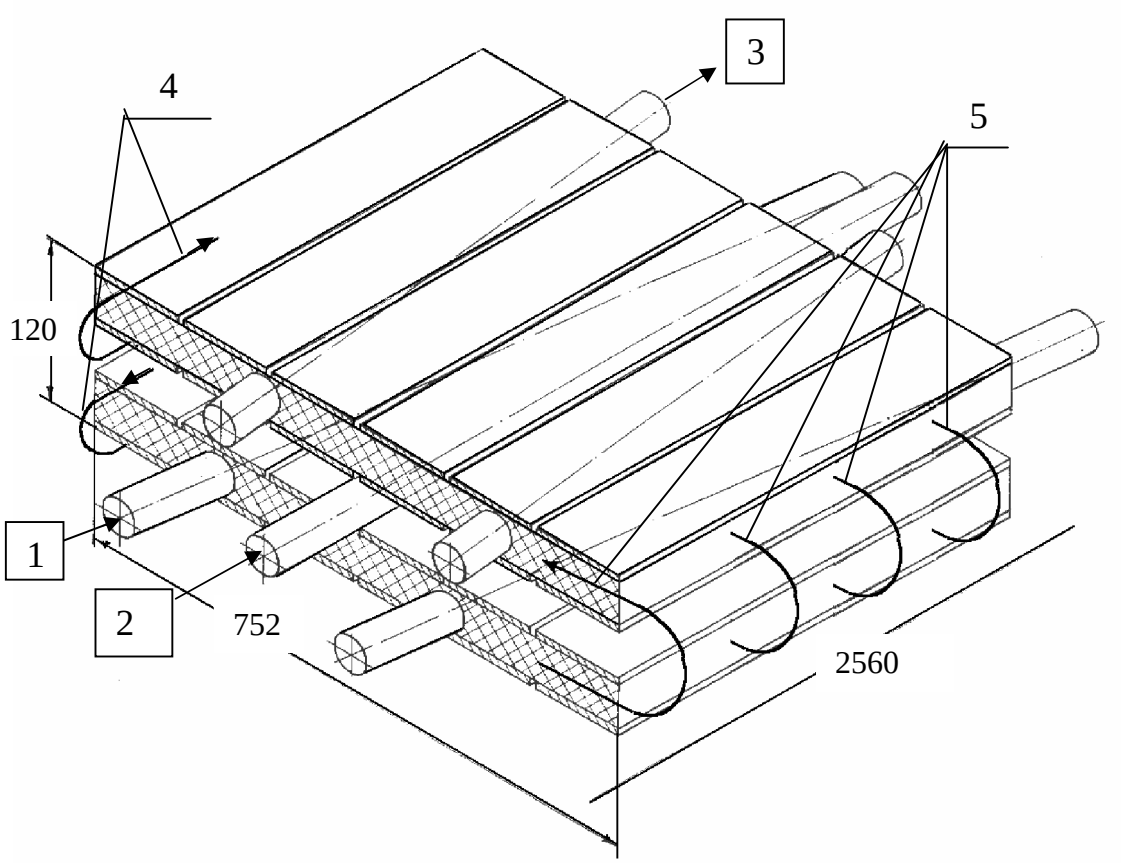

Fig.7.2. Septum design.1 -Beam from the gun, 2 - Circulating beam, 3 - Extracted beam, 4 -Current lines, 5 - Magnetic field lines.

Table 7.2. General parameters of the septum coils.

Magnetic field value, G	120
Current, A	1600
Number of turns	6
Conductor cross-section, mm	4 x 12
Beam displacement, mm	300

Initially the effective lengths of both coil fields will be measured independently by measurement of the magnetic field value corresponding to minimum distortion of the beam parameters after crossing the coil. After that the length of the kicker coil will be corrected to have an integer ratio between septum and kicker coil lengths.

The distortion of the angular spread of the circulating electron beam after crossing the helical quadrupole winding is minimised by adiabatic variation of the quadrupole field gradient at the entrance and at the exit of the coil. The designed and constructed helical quadrupole coil (Fig. 7.4) has in each crossection a geometry of "Panofsky lens" which provides a maximum linearity of the field. The gradient variation at the enetrance and exit of the coil is provided by corresponding variation of the number of winding turns. Accurate calculation of the particle dynamics in the coil is practically impossible due to difficulties in measurements of the fringe fields, and test of the coil and (if it would be necessary) correction of its design will be performed also using optic method of beam diagnostics. All these investigations will be performed at special test bench, which is under construction now.

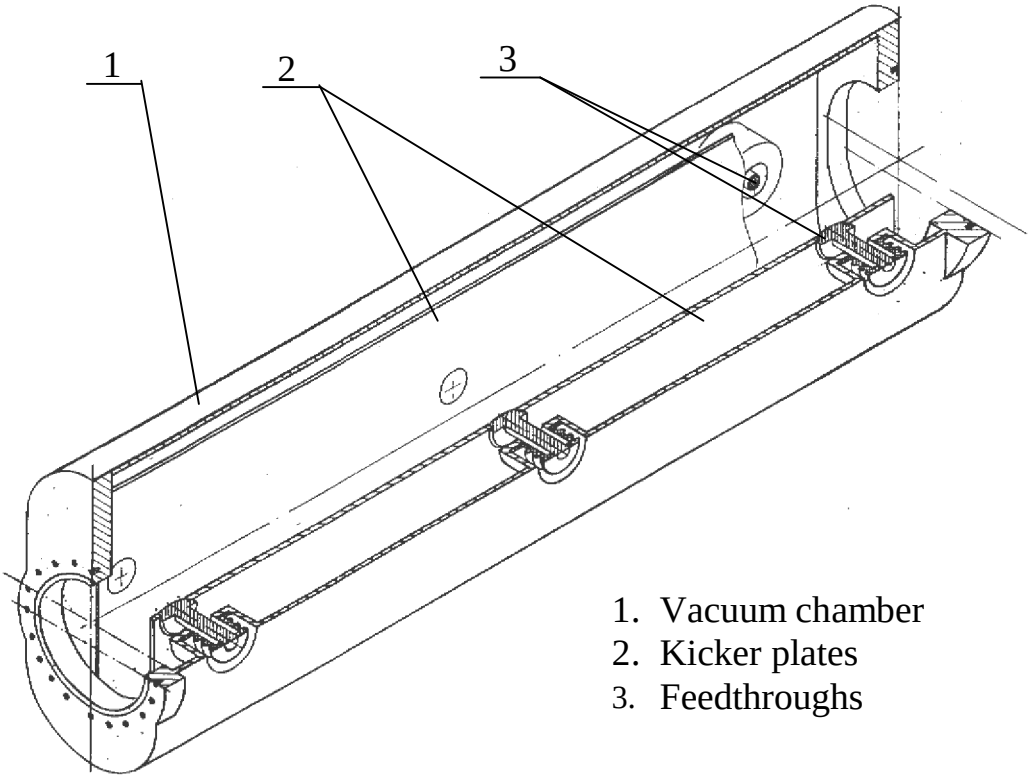

Fig. 7.3. Schematics of the kicker. Kicker length is about 90 cm, beam displacement is 6 cm.

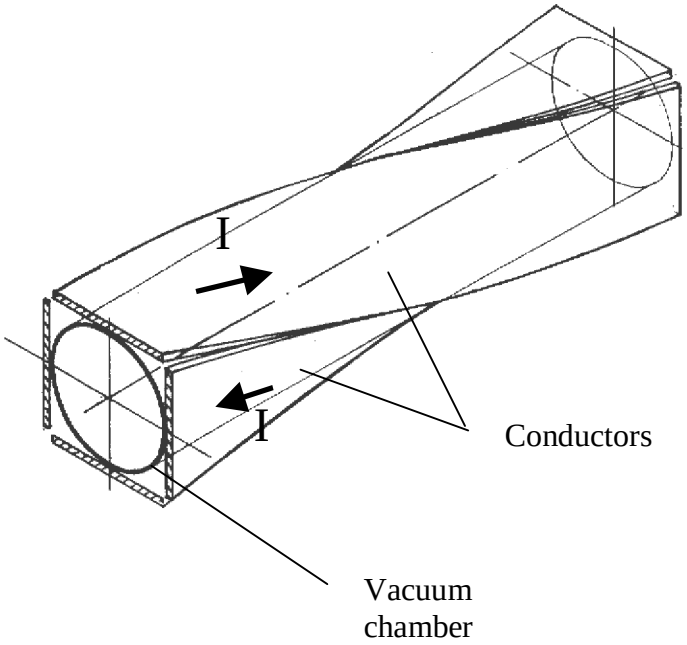

Fig. 7.4. Schematics of the helical quadrupole winding.

7.2.2. Study of the circulating beam dynamics

Stability diagram in the vicinity of the working point at injection energy of 10 keV is presented schematically in Fig 7.5. The most dangerous resonances are the integer (342 and 343) and half integer (342.5) ones of the fast mode of oscillations, the half integer and 1/3 nonlinear of slow mode of oscillations and the coupling resonance of the modes $Q_{fast} + Q_{slow} = 342$. Nonlinear resonances of the fast mode of oscillations have very high order and estimations show that they practically do not influence on beam parameters.

An accurate calculations of the position of the resonances and increments in their centre were performed using especially elaborated computer code BETATRON. Power of nonlinear resonance of slow mode of oscillations was calculated using averaging method. The nonlinear resonance appears due to sextupole component of the longitudinal magnetic field in the toroidal sections and leads to variation in time of the motion invariant corresponding to the slow mode of oscillation. Due to coupling between horizontal and vertical degrees of freedom the variation of slow invariant produces variation in time of the beam cross-section. In experiment the power of the resonance can be estimated by measurements of the frequency of beam cross-section variation.

Real width of the linear and coupling resonance is determined by the errors of the focusing fields. In the case of focusing by longitudinal magnetic field the errors can not to be calculated through the errors in the position of the focusing elements. The errors of the focusing field appear due to those in the solenoid winding and can be evaluated only by measurements of the real field distribution in each section of the solenoid. However the field measurements has to be performed in the position of the closed orbit which is known with accuracy of about a few millimetres.

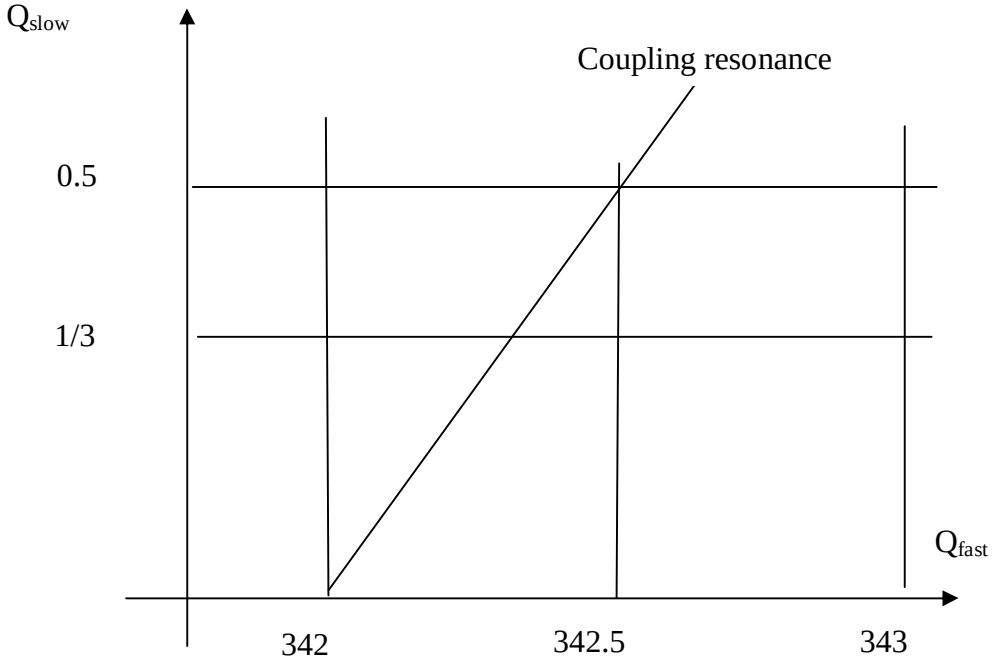

Fig 7.5. Stability diagram in the vicinity of the working point at beam energy of 10 keV and magnetic field value of 400 G.

Thus the dynamic behaviour of the ring can be investigated only experimentally. And such an investigation is of great importance for proposed cooling system. The width and power of the fast mode resonances in real structure are the key parameters in the problem of betatron acceleration of circulating beam. A possibility of the resonance crossing and beam parameters distortion in the resonance vicinity will determine the choice of acceleration regime. In the case of electron beam acceleration with RF accelerator the dynamics investigation will determine the requirements to the momentum spread of injected electron beam.

The tune of the slow mode of oscillation can be measured using pick up electrodes. The frequency of the slow oscillations at beam energy of 10 keV is about 700 kHz and corresponds to coherent oscillations of circulating beam. The tune of the fast mode of oscillations can not to be measured directly (characteristic value of the frequency of the fast mode of the betatron oscillations is about 1 GHz, and the signals produced by each particle on pick-up electrodes are incoherent.) Its measurements we plan to perform by displacement of the beam energy to the region of the coupling resonance which leads to increase of the amplitude of the slow mode. For this aim small RF cavity will be installed in the ring.

In order to test beam parameters variation after the resonance crossing the beam will be extracted from the ring and directed to the optic diagnostics for the beam temperature measurement.

The longitudinal temperature of the circulating electron beam will be measured using Schottky diagnostics. This permits to measure growth rate of the longitudinal temperature due to transverse-longitudinal relaxation, which is impossible in the case of single pass electron beam of a traditional electron cooling system. Experimental study of the relaxation process allows finding the limit of the maximum value of the electron beam current in the electron cooling devices with circulating electron beam.

Summary

1. Role of the cooling in experiments with internal targets

The beam energy and required target density in experiments with internal targets is determined by physical problem to be investigated. Investigations of nature of a_0-mesons are to be performed at maximum proton beam energy, required level of the luminosity is 10^{33} $cm^{-2} \cdot sec^{-1}$ and higher. This experiment can be provide using a pellet target. Measurements of the deuteron break-up, ω, η, K mesons production are performed in the wide energy range from 1 GeV to about 2 GeV, and with all the types of the ANKE targets. The effective density of the hydrogen cluster beam target, achieved in the experiment at January/February 2001, is about $2 \cdot 10^{15}$ Atoms/cm^2. Expected areal density of the gas storage cell is 10^{14} - 10^{15} Atoms/cm^2. Effective density of the frozen pellet target is expected to be between $3 \cdot 10^{14}$ and $2 \cdot 10^{16}$ Atoms/cm^2 at beam emittance of 1 $\pi \cdot mm \cdot mrad$.

In the experiments with the internal target the upper limit of the circulating beam life time (and, as a result, the experiment duration) is determined by single scattering on large angles with the target atoms. At the target density below 10^{15} Atoms/cm^2 the beam life time and characteristic times of the emittance growth due to interaction with the target are longer than one hour and experiment can be performed without cooling. At the effective target density over than approximately $2 \cdot 10^{16}$ Atoms/cm^2 the beam life time is shorter than expected cooling times at realistic parameters of the cooling system. In this case cooling cannot effect on the beam parameters effectively.

The range of the target density from 10^{15} to $2 \cdot 10^{16}$ Atoms/cm^2, in which cooling can be used for luminosity preservation, covers parameters of all types of the ANKE target practically. Only in the experiments with solid target the beam life time is so short that luminosity preservation using cooling seems to be unrealistic. The difference between the hydrogen and deuterium targets is not substantial because of the general processes which influences on the beam parameters are determined by interaction with the electrons of the target atoms.

In this report the possibility of the cooling application was investigated in two ranges of the target density: long term experiment (up to 1 hour) at the target density of 10^{15} Atoms/cm^2 and short term experiment (about 5 minutes) at the target density of 10^{16} Atoms/cm^2.

In the experiment with gas storage cell target, when the target dimensions coincide with the aperture of the vacuum chamber, the role of the beam cooling is to reduce the particle losses due to aperture limitation by suppression of the emittance growth. Maximum achievable gain in the experiment luminosity is determined by the relation between the beam life time and time of the emittance growth up to acceptance.

For proton beam at the target density of 10^{15} Atoms/cm^2 after one hour of experiment maximum possible gain in the beam intensity is more than two times at the energy below 2 GeV (up to one order of magnitude at 1 GeV), and about 50% at energy of 2.7 GeV.

For circulating deuteron beam the gain in intensity of about 50% can be obtained at energy of 2.11 GeV (which corresponds to the maximum magnetic rigidity). At intermediate energies the gain in the beam intensity is determined by suppression of the intrabeam scattering and for

deuteron beam is about two times less than the proton one, however at energy of 1 GeV the possible gain in the luminosity for deuteron beam is about 5 times.

Similar dependence on the particle energy takes place at the target density of 10^{16} Atoms/cm^2, but maximum expected gain in the beam intensity after five minutes of experiment is about 1.5 times higher.

The energy dependence of the maximum gain in the experiment luminosity is explained by the input of the intrabeam scattering into emittance growth. The role of this process fast decreases with the energy increase and at maximum beam energy emittance growth is determined by the single scattering with the target atoms mainly. Thus, the potential efficiency of a beam cooling increases with increase of the beam intensity and decreases with increase of the beam energy.

In the experiment with cluster beam target additional gain in the luminosity can be obtained due to the target dimension in the horizontal plane is 5 mm, which is less than beam dimension corresponded to acceptance limitation. Stabilisation of the horizontal beam dimension during experiment can give additional gain in the luminosity of about 50%.

In the experiment with the pellet target the luminosity is inversely proportional to the circulating beam cross section because of the beam cross section always larger than pellet one. In this case the beam cooling can provide increase the luminosity by several times. When the cooling prevails on the heating effects one can realise the regime with constant luminosity during the time of experiment via compensation of the particle losses by corresponding decrease of the beam emittance.

Thus, in the experiments with the gas jet and cluster beam targets the experiment duration can be about one hour without substantial loss of the luminosity and cooling application can give gain in the luminosity from 50% to 5 - 10 times at energy from 1 to 2.7 GeV. In the experiment with the pellet target the experiment duration can be about 5 minutes and cooling application can give a gain in the luminosity of about 2-3 times in the total range of the beam energy.

2. The possibility of the existing stochastic cooling system application

The effectiveness of the stochastic cooling strongly depends on the ion beam intensity. In this report the possibilities of the stochastic cooling were investigated under assumption that one of the chains is used for cooling of the horizontal degree of freedom, other one - for longitudinal. In this case the stochastic cooling system can be used for luminosity preservation at the target areal density of about 10^{15} Atoms/cm^2 up to ion beam intensity of about $2\text{-}3\cdot10^{10}$ particles. Maximum efficiency of the stochastic cooling corresponds to the maximum beam energy (due to dependence of the mixing factor on the off-momentum factor). The gain in the luminosity is close to the theoretical value and in the experiment with the gas jet target is about 20 – 50%, in the experiment with cluster beam target this value can be higher by about 1.5 times due to stabilisation of the horizontal beam dimension.

At the beam intensity of 10^{11} particles, which corresponds to expected value with new COSY injection system, or at high target density the existing stochastic cooling system is not powerful enough to expect a substantial effect from its application in the experiment with internal target.

3. The possibility of an electron cooling application

Electron cooling system at realistic parameters of the electron beam stabilises the parameters of the intensive (up to 10^{11} particles) ion beam at the target areal density of 10^{15} Atoms/cm^2 in the total energy range required for experiments. Maximum gain in the luminosity corresponds to the minimum beam energy. In the experiment with gas jet target for the proton beam expected gain in the luminosity after one hour of experiment is 2 – 3 times at 1 GeV and decrease to the value of 20 – 50% at 2.7 GeV. For deuteron beam expected gain in the luminosity is about 2 times at energy of 1 GeV and decreases to 50% at 2.11 GeV. In the experiment with cluster beam target additional gain in the luminosity can be obtained due to stabilisation of the horizontal beam dimension and its value is about 1.5 times.

In the experiment with the pellet target maximum gain in the luminosity is expected at minimum beam energy. In this case the experiment duration can be about 5 minutes and gain in the integral luminosity is 2 – 4 times depending on the pellet diameter. The expected average luminosity value exceeds 10^{33} cm^{-2}sec^{-1}. At these parameters one can realise the regime with permanent luminosity during the time of experiment via compensation of the particle losses by corresponding decrease of the beam emittance.

At maximum proton beam energy of 2.7 GeV the electron cooling compensates the beam heating due to interaction with target only at pellet diameter of 40 –50 μm, which corresponds to the luminosity value of 3 - $5\cdot10^{33}$ cm$^{-2}\cdot$sec^{-1}. At maximum pellet diameter the electron cooling does not suppress the beam heating, but it can be used for initial preparation of the beam parameters before the target switching on. In combination with the optimum experiment strategy it can give a gain in the integral luminosity of about 20%. It should be noted that all the simulations in this report were performed under assumption that each moment of time one pellet is in the beam. In the case of low frequency of the pellet production the effective target density has to be calculated taking into account the duty factor. Final conclusion can be expressed as follows: in the experiment with the pellet target at maximum proton beam energy an electron cooling gives substantial gain in the luminosity up to the luminosity level of about $5\cdot10^{33}$ cm$^{-2}\cdot$sec^{-1}.

For deuteron beam an electron cooling can be effectively used in the total energy range and at beam energy of 2.11 GeV and maximum target density the gain in the integral luminosity after five minutes of experiment is about 50% and it increases to several times at less energy or target density.

4. Electron cooling system with circulating electron beam

There are two possible design of new COSY cooling system:
- Traditional configuration of cooling system + HV accelerator,
- Cooling system with circulating electron beam.

Traditional configuration of the cooling system can provide electron beam at low transverse and longitudinal temperature, and the results of numerical simulations demonstrate its ability for ion beam parameters stabilisation.

Electron cooling system with circulating electron beam has substantially low cost, but in such a system the electron beam quality is expected to be rather less than in the HV system. The electron beam quality is determined by a method of the beam acceleration, stability of electron motion in the electron storage ring, number of electrons and the ring circumference.

General attention of this report was attracted to the possibility of the electron cooling system with circulating electron beam. In the electron energy range from 0.5 to 1.4 MeV only a longitudinal magnetic field can provide strong focusing of an intensive electron beam. General parameters of the electron ring with longitudinal magnetic field can be the following: magnetic field value is 1 – 1.5 kG, the ring circumference is about 20 m, electron beam radius is 0.5 mm, maximum current value is 0.5 A. The electron beam acceleration can be provided using RF electron linac or by induction acceleration of the electrons in the ring. The induction acceleration is more attractive from the side of the momentum spread of accelerated beam and installation cost, but it did not tested experimentally. The proposed design of the injection system of the electron ring permits to perform two modes of operation: with the single pass electron beam at injection energy and with the circulating electron beam at the energy of experiment. Some elements of the existing COSY electron cooling system can be used in the new cooling device.

General problems of the proposed cooling system are the following:
- distortion of the electron beam parameters during its injection into the ring,
- motion stability of the electron beam during circulation,
- heating of the electron beam due to its interaction with the cooled ion one,
- coherent energy losses of both beams – ion and electron – due to interaction of the ion beam with the target and energy exchange between beams,
- heating of the longitudinal degree of freedom of the electron beam due to intrabeam scattering.

In the case of induction acceleration of the electron beam more serious problem is to avoid beam heating during crossing of resonances of transverse particle motion.

The period of the electron beam circulation is limited by the heating due to interaction with the ion beam. When the circulation period is about 0.1 second the efficiency of proposed system is the same as one of the traditional electron cooling system. More serious limitation can appear due to transverse-longitudinal relaxation in the electron beam. This problem as well as the stability of the electron motion and electron beam distortion during injection requires experimental investigations. They can be performed at LEPTA installation, which construction is in the final stage in JINR. We plan to begin the experimental program next year and expected term of its completion is two years.

The cost of the cooling system with circulating electron beam estimated using the experience of construction of analogous system in JINR can lies between 1 and 1.5 M$.

Conclusion and recommendations

In the experiments with gas storage cell and cluster beam targets an electron cooling system can be effectively used for the luminosity preservation when the experiment duration is of the order of 1 hour. In this case expected gain in the luminosity is about 2 – 3 times at minimum and intermediate beam energy. At maximum beam energy the effect of cooling application decreases and at the target density below 10^{15} Atoms/cm^2 the experiment can be performed

without luminosity loss during long period of time without cooling. Electron cooling stabilises the beam parameters in the total energy rang and transverse dimensions of the ion beam during experiment can be 2 – 3 times less than in the case without cooling. This permits to decrease the aperture of the gas storage cell in order to increase the target density.

In the experiment with the pellet target at maximum proton beam energy an electron cooling gives substantial gain in the luminosity up to the luminosity level of about $5 \cdot 10^{33}$ $cm^{-2} \cdot sec^{-1}$ and at experiment duration up to five minutes. Using of an electron cooling system one can realise the regime with permanent luminosity during the time of experiment via compensation of the particle losses by corresponding decrease of the beam emittance. An electron cooling application gives a possibility to optimise the ion beam parameters and experiment duration in order to obtain maximum integral luminosity taking into account the time of the beam storage and acceleration.

The proposed scheme of the electron cooling system with circulating electron beam permits to provide the effective ion beam cooling in the total energy range and in the single pass mode of operation the beam cooling during storage process at injection energy. However the technical design of such a system can not be performed without an experimental test of its general elements.

References

1. Electron cooling application for luminosity preservation in an experiment with internal targets at COSY. Interim report, Dubna, 2001.
2. I.Meshkov, A. Sidorin, Electron cooling system with circulating electron beam. Workshop on Medium Energy Electron Cooling, Novosibirsk,1997, p. 183, G. Jackson, Modified Betatron Approach to Electron Cooling. Workshop on Medium Energy Electron Cooling, Novosibirsk,1997, p.171.
3. V.Golubev, I.Meshkov, V.Polyakov, I.Seleznev, A.Smirnov, E.Syresin ,The proceeding of the Workshop on Beam Cooling and Related Topics, CERN 94- 03, 26 April 1994
4. F. Hinterberger, D.Prasuhn, Analysis of internal target effects in light ion storage ring, NIM A 279(1989), 413-422
5. D.Anderson at al., The development of a prototype multi-MeV electron cooling system, T.Ellison at al., Multi-MeV electron cooling – a tool for increasing the performance of high energy colliders?, Fifth Annual International Industrial Symposium on the Super Collider, 6-8 may, 1993, San Francisco, California.
6. I.N.Meshkov, Fiz. Elem. Chastits At. Yadra 25 (1994) 1487 [Engl. transl. Phys.Part.Nucl.25 (6) (1994) 631], I.Meshkov, preprint RIKEN-AF-AC-2, January 1997.
7. Yu.V.Korotaev, I.N.Meshkov, S.V.Mironov, A.O.Sidorin, E. Syresin "The Modified Betatron Prototype Dedicated to Electron Cooling", 6th European Particle Accelerator Conference, Stockholm, 22-26 June, 1998., M.Chelnokov, V.Kalinichenko, Yu.Korotaev, I.Meshkov, S.Mironov, A.Petrov, I.Sedykh, A.Sidorin, A.Smirnov, E.Syresin, I.Titkova, G.Trubnikov, Modified Betatron Prototype Dedicated to Electron Cooling with Circulating Electron Beam, Proc. HEACC'98, Dubna, 1999, p. 413, I.Meshkov, Electron cooling with circulating electron beam in GeV energy range, NIM A 441(2000), p.255.
8. I.Meshkov, A.Sidorin, A.Smirnov, E.Syresin The particle dynamics in the low energy storage rings with longitudinal magnetic field, 6th European Particle Accelerator Conference, Stockholm, 1998, p. 1067,
9. I.N.Meshkov, A.O.Sidorin, A.V.Smirnov, E.M.Syresin, G.V.Trubnikov , "Betatron program for simulation of particle dynamics in storage ring with strong coupling of transverse coordinates", proceedings of ICAP2000, Darmstadt, to be published in Phys.Rev. (Accelerators & Beams)
10. I.Meshkov, A.Smirnov, A.Sidorin, E.Syresin, E.Mustafin, P.Zenkevich, The Stability of the Circulating Electron Beam in the Electron Cooling System Based on the Modified Betatron, Proc. HEACC'98, Dubna, 1999, p.416.
11. A.V.Aleksandrov, N.S.Dikansky, N.Ch.Kot, V.I.Kudelainen, V.A.Lebedev, P.V.Logachev, Proc. Workshop on Electron Cooling and New Cooling Techniques, Legnaro, 1990 (World Scientufic, 1991) p. 279
12. JINR electron cooling group, "The report of the Designing of the Modified Betatron Prototype", JINR, Dubna, 1997.
13. C.Kapetanakos, et.al., The Naval Research Laboratory Modified Betatron Accelerator and Assessment of its Results, Phys. Fluids B 5(7), 1993, p.2295.
14. K.Balewski, et. al., Preliminary Study of Electron Cooling Possibility of Hadronic Beam at PETRA, 6th European Particle Accelerator Conference, Stockholm, 22-26 June, 1998, p.1079

Annex I

Electron cooling application for luminosity preservation in an experiment with internal targets at COSY.

Interim report

JINR I.N.Meshkov, Yu.V.Korotaev, A.L.Petrov, A.O.Sidorin, A.V.Smirnov, E.M.Syresin, G.V.Trubnikov, S.V.Yakovenko

COSY H.J.Stein

Dubna, 2001

CONTENTS

Abstract 3

Introduction 4

1. General description of the physical model 4
1.1. Beam emittances and particle number evolution 4
1.2. Particle losses and emittance calculation in the presence of beam scrapers 5

2. Heating processes involved into calculations 7
2.1. The interaction with the target atoms 7
2.1.1. Description of the COSY internal targets 7
2.1.2. Emittance growth and beam lifetime 8
2.1.3. Target parameters calculation 9
2.2. Intrabeam scattering of the ion beam 11
2.2.1. Piwinski model 11
2.2.2. Martini model 12
2.3. Ion multi scattering on residual gas atoms 14
2.4. Tune resonances of the ion betatron motion 15
2.5. External heating 15

3. Particle losses calculation 16
3.1. Nuclear scattering on residual gas atoms 16
3.2. Single scattering on large angles 16
3.3. Recombination in the electron cooling section 17
3.4. Other particle losses 17

4. Cooling processes involved into calculations 17
4.1. Stochastic cooling 17
4.1.1 Transverse cooling time 17
4.1.2 Longitudinal cooling time 18
4.1.3. Power limited cooling 18
4.2. Electron cooling 18
4.2.1 Electron cooling with single pass electron beam 18
4.2.2 Electron cooling with circulating electron beam 22

5. Calculations of the beam stability characteristics 25

6. Description of the program 27

References 31

Abstract

The synchrotron and storage ring COSY delivers proton beams with momenta between 300 and 3500 MeV/c for internal and external experiments. It is operating both with electron and stochastic cooling. The electron cooling is used mainly at injection energy with 22 keV electrons to increase the intensity of the polarized proton beam with a combined cooling/stacking injection. In addition, the electron-cooled proton beam is used for diagnostic purposes of machine parameters. The stochastic cooling for COSY is working in the proton momentum range between 1.0 and 3.4 GeV/c (energy from 0.4 to 2.5 GeV) and is used for experiments with thin internal targets and at a long flat top time.

The general aim of this work is to estimate a feasibility to extend the energy of electron cooling application up to maximum proton beam energy of 2.6 GeV (maximum electron beam energy is about 1.4 MeV) and to use electron cooling in combination with stochastic one for luminosity preservation in experiments with internal targets. It presumes:
- numerical calculation of the ion beam parameter variation under common action of different heating and cooling processes with and without electron cooling, which permits to estimate the gain in luminosity and its life time value due to electron cooling application,
- comparison of efficiency of two medium energy electron cooling methods: with single pass electron beam and circulating one,
- preliminary design of the electron cooling system for COSY at energy range required for experiments with internal target,
- elaboration of the experimental program dedicated to investigation of the electron beam dynamics in electron cooling system with circulating electron beam using the LEPTA ring, which is under construction in JINR.

This report includes description of the numerical methods and computer program developed for beam parameter calculations.

Introduction

Luminosity of an experiment with an internal target in an ion storage ring at conventional experiment setting up is limited in time due to the growth of the circulating beam emittance and momentum spread related to different heating effects. Other limitation is connected with particle losses during experiment.

General heating effects are the following:
- interaction of the beam ions with the target atoms,
- intrabeam scattering of the ion beam,
- ion multi scattering on residual gas atoms,
- high order tune resonances of the ion betatron motion due to space charge tune shift.

The sources of the particle losses:
- nuclear scattering on the target and residual gas atoms,
- single scattering by large angles on the target and residual gas atoms,
- electron capture (recombination) in the electron cooling section.

Cooling processes:
- stochastic cooling (both – transverse and longitudinal),
- electron cooling – with single pass and circulating electron beams.

1. General description of the physical model

1.1. Beam emittances and particle number evolution

The influence of all the processes determining the luminosity variation can be investigated in the frame of the physical model used in BETACOOL program elaborated in JINR [1].

The model is based on the following general assumptions:
1) the ion beam has Gaussian distribution by all degrees of freedom, which does not change during the process;
2) algorithm of the problem analysis consists in the solution of the equations for root mean square values of the beam phase space volumes of three degrees of freedom;
3) maxima of all distribution functions coincide with equilibrium orbit.

The evolution of the ion beam parameters during its motion inside the storage ring is described by the following system of four differential equations:

$$\begin{cases} \dot{N} = N\sum_j \frac{1}{\tau_{life,j}}, \\ \dot{\varepsilon}_x = \varepsilon_x \sum_j \frac{1}{\tau_{x,j}}, \\ \dot{\varepsilon}_z = \varepsilon_z \sum_j \frac{1}{\tau_{z,j}}, \\ \dot{H}_{lon} = H_{lon} \sum_j \frac{1}{\tau_{lon,j}}, \end{cases} \tag{1.1}$$

where N is the particle (protons) number in the ring, ε_i is the particle beam emittance in the corresponding transverse plane, $i = x, z$. For longitudinal degree of freedom invariant of motion H_{lon} is given by the following expression:

$$H_{lon} = \begin{cases} (\frac{\Delta p}{p})^2, & \textit{coasting beam;} \\ (\frac{\Delta p}{p})^2 + \frac{1}{\Omega_s^{\,2}}[\frac{d}{dt}(\frac{\Delta p}{p})]^2, & \textit{bunched beam.} \end{cases} . \tag{1.2}$$

In Eq. (1.2) upper line corresponds to coasting beam, lower line to bunched beam with constant parameters. Thus we limit our consideration with the case of small synchrotron oscillations, which corresponds to a well cooled beam. A change of the synchrotron frequency Ω_s requires to use adiabatic invariant instead of energy. Thus depression of the synchrotron tune due to action of the beam space charge is not taken into account during dynamics simulation in the present consideration. Characteristic times are functions of all three emittances and particle number and have positive sign for a heating process and negative for cooling one. The negative sign of the lifetime corresponds to the particle loss and the sign of the lifetime can be positive in the presence of particle injection, when particle number increases.

Index j in the system (1.1) is the number of process involved into calculations. The program structure is designed in such a way that permits to include into calculation any process, which can be described with cooling or heating rates.

Numerical solution of the system (1.1) is performed using Euler method with automatic step variation. The use of high order Runge-Kutt methods meets certain problems related to a long time of the equation right parts calculation.

1.2. Particle losses and emittance calculation in the presence of beam scrapers

The emmitance growth and the particle survival probability are dependent of the presence of beam scrapers, which limit the amplitudes of particle betatron oscillations. Maximum admissible betatron amplitude value Y can be calculated from the ring acceptance as follows:

$$Y_{x,z} = \sqrt{A_{x,z}\beta_{x,z}}\,, \tag{1.3}$$

where $A_{x,z}$ are the ring acceptances in the corresponding planes, $\beta_{x,z}$ are the beta functions at the scraper position.

The survival probability of the particle after one revolution in the ring can be estimated by the following expression [2]:

$$P(\zeta) = 2\sum_{k=1}^{\infty} \frac{1}{\lambda_k J_1(\lambda_k)} \exp(-\lambda_k^2 \zeta), \tag{1.4}$$

where J_1 is the Bessel function of the first kind and λ_k is the k-th root of the equation $J_0(\lambda) = 0$. The dimensionless variable ζ is connected with the mean square amplitude of the betatron oscillations. In the case of Rayleigh distribution function of the beam particles over betatron amplitudes:

$$\rho(y) = \frac{2}{\sigma^2} y \exp\left(-\frac{y^2}{\sigma^2}\right) \tag{1.5}$$

where the $\langle y^2 \rangle = 2\sigma_y^2 = \varepsilon\beta$ mean square amplitude, ε is so called "two sigma beam emittance", σ_y is mean value of Gaussian distribution function in the space of co-ordinate, one can calculate

$$\zeta = 0.25\langle y^2 \rangle / Y^2 = 0.25\varepsilon / A, \tag{1.6}$$

Then calculating $P(\zeta)$ overestimate slightly the particle loss by including a small loss, which would have occurred without any emmitance growth. However this overestimation is negligible as long as $\langle y^2 \rangle \le 0.1Y^2$. If particle loss occur in both transverse planes the total survival probability P_{tot} is the product of two one-dimensional probabilities:

$$P_{tot} = P_x(\zeta_x) P_z(\zeta_z). \tag{1.7}$$

The particle loss on scrapers can be included into calculations at emittance growth ($\dot{\varepsilon} > 0$) by introduction of the lifetime:

$$\frac{1}{\tau_{life}} = \frac{1 - P_{tot}}{T_{rev}}, \tag{1.8}$$

where T_{rev} is the revolution period.

In the case of particle loss on scrapers the emittance growth has to be corrected in accordance with:

$$\varepsilon_{scr} = Af(\zeta). \tag{1.9}$$

The function $f(\zeta) = \varepsilon/A$ for $\zeta < 0.05$ and tends rapidly to the constant asymptotic value of 0.3084. The asymptotic value is in accordance with the theoretical expectation for a homogeneous density distribution with a smooth cutoff near the amplitude limit [2].

2. Heating processes involved into calculations

2.1. The interaction with the target atoms

2.1.1. Description of the COSY internal targets

COSY experiments are performed in the energy range from 0.5 to 2.6 GeV (polarized or unpolarized protons). There are various "heating effects" caused by the various targets (solid strip targets, cluster and pellet targets, and a storage cell used especially for polarized atoms). There are four experimental areas with internal targets: ANKE, COSY-11, COSY-13 and EDDA [3]. The types of the targets being used in the experiments are listed in the Table 1.

Table 1. The type of targets used in the different internal experiments at COSY

Target	COSY 13	EDDA	COSY 11	ANKE
strip or filament	strip	filament		strip
cluster			x	x
pellet				x
atomic beam		x		x
storage cell		x		x

At the first stage of numerical calculations we plan to investigate the beam parameters evolution in the ANKE experiments. The results for the cluster target will be compared with the COSY-11 experiment.
The cluster beam of the COSY-11 cluster target has always the maximal density of 10^{14} atoms/cm^3. The cluster beam is round with a diameter of 9 mm.

ANKE is the experiment where all types of targets will be applied in time. Up to now solid strip targets (Table 2) and the cluster target (H, D) were used.

Table 2. The ANKE solid targets

Type	Density, μg/cm^2
CH_2	200
C (in form of polycristalline diamond)	500...1000 (maximum density is not clear, 1.7 or 3.5 g/cm^3 or in between)
Cu	200
Au	400

The solid targets were flat stripes, of 18-mm length, and shaped in form of a triangle. (2-mm width above with the tip at the lower end in order to minimize the beam target overlap as few as possible.) The targets were positioned above the beam axis and the p beam was moved into the target with beam orbit deformation. Typical cycle times were of 1 minute. The experiments were also run with a constant target rate by applying a feedback loop.

The ANKE cluster beam apparatus is very similiar to COSY 11, however, it has different dimensions. It is of rectangular shape, 5 x 10 mm^2 (10 mm longitudinally). We take in calculations the maximum value of the areal density equal to 5 x 10^{13} atoms/ cm^2.

The pellet target is planned to have parameters listed in the Table 3.

Table 3. Parameters of frozen pellet target

Diameter of pellet [μm]	20 - 80
mass [g]	$3*10^{-10} – 2*10^{-8}$
total number of atoms per pellet	$1.8*10^{14} – 1.1*10^{16}$
Speed, m/s	40 - 100
Pellet flux, pellet/sec	10^5

The storage cell at ANKE will be fed by an atomic beam source (10^{12} atoms/cm^3). The maximum areal density of 10^{14} atoms/cm^2 is expected. The cell cross section is 30 x 10 mm^2 (10 mm horizontal), the length along the beam is 400 mm.

2.1.2. Emittance growth and beam lifetime

The parameters of the circulating ion beam vary at single pass through the target in accordance with the following expression [4]:

$$\begin{cases} \Delta\varepsilon_{hor} = \beta_{hor}\theta_{str}^2 + H_{hor}\left(\dfrac{\Delta p}{p}_{target}\right)^2 \\ \Delta\varepsilon_{vert} = \beta_{vert}\theta_{str}^2 \\ \Delta\varepsilon_{long} = \left(\dfrac{E_{str}}{\beta^2\gamma A E_0}\right)^2 + 2\left(\dfrac{\Delta p}{p}_{target}\right)^2 \end{cases}, \qquad (2.1.1)$$

where $\Delta p/p_{\text{target}}$, θ_{str}, E_{str} are the target parameters, β_{hor}, β_{vert} are horizontal and vertical beta functions in the target position, $H_{hor} = \dfrac{(1+\alpha_{hor})^2}{\beta_{hor}} D^2 + 2\alpha_{hor} DD' + \beta_{hor} D'^2$, α_{hor}, D are the alpha function and the dispersion in this point. The target parameters $\Delta p/p_{\text{target}}$, θ_{str}, E_{str} are calculated for the given width and material of the target parameters and particle energy, either can be introduced into the program as input parameters.

We assume that the circulating beam crosses the target during multiturn injection n_{target} times and the injection pulses follow with the repetition period is T_{target},. Then one can calculate the emittance growth times:

$$\frac{1}{\tau_{i,target}} = \frac{1}{\varepsilon_i}\frac{n_{target}\Delta\varepsilon_i}{T_{target}} P(\varepsilon), \qquad (2.1.2)$$

where $P(\varepsilon)$ is the probability of the target crossing by an individual particle (see below, Formula 2.1.3). The parameters n_{target} and T_{target} are introduced to have a possibility to calculate beam parameters variation at charge exchange injection, when the stored beam crosses the target only during injection period and is cooled between the cycles of injection. In the case of an experiment with internal target the particle crosses the target every turn, therefore $n_{target} = 1$, $T_{target} = T_{rev}$ in this case (T_{rev} is the particle revolution period).

The probability $P(\varepsilon)$ is introduced to take into account a situation when the target cross-section is less than that one of the circulating beam. The value $P(\varepsilon)$ can be estimated as a ratio

between beam cross section and the target one without any assumption about real geometry of the target point:

$$P(\varepsilon) = \begin{cases} 1 & if \quad S_b \le S_t \\ \dfrac{S_t}{S_b} & if \quad S_b > S_t \end{cases}, \tag{2.1.3}$$

where S_t is the target cross-section, $S_b = \pi\sigma_{hor}\sigma_{vert}$, is the r.m.s. beam cross-section σ_{hor} and $\sigma_{hor} = \sqrt{\sigma_{hor,bet}^2 + D^2\sigma_p^2}$ are the horizontal and vertical r.m.s. beam dimensions.

Particle lifetime due to interaction with a target can be estimated as follows:

$$\frac{1}{\tau_{life,target}} = -\frac{n_{target}}{\tau_t P(\varepsilon)}\frac{T_{rev}}{T_{target}}, \tag{2.1.4}$$

where τ_t is the target parameter, which also can be introduced as input parameter for calculations.

2.1.3. Target parameters calculation

The parameters $\Delta p/p_{\text{target}}$, θ_{str}, E_{str} can be calculated in accordance with the following formulae [2]:

$$\theta_{str}^2 = 2Nx\pi\left(\frac{Z_T Z_P r_e}{\beta c}\right)^2\left[\ln\left(\frac{\alpha_2^2}{\chi^2}\right) - 1 + \Delta b\right], \tag{2.1.5}$$

$$E_{str}^2 = \xi\Delta E_{\max}\left(1 - \frac{\beta^2}{2}\right), \tag{2.1.6}$$

$$\left(\frac{\Delta p}{p}\right)_{target}^2 = \left(\frac{\gamma}{\gamma + 1}\right)^2\frac{E_{str}^2}{E^2}. \tag{2.1.7}$$

Here, Nx is the number of targets atoms per unit area, Z_P and Z_T are the charge number of projectile and target atoms, p and E is the particle momentum and kinetic energy, r_e is the electron classic radius. The parametrs α_2, χ and Δb are given by the equations:

$$\alpha_2 = \frac{a}{\left(A_T^{1/3} + A_P^{1/3}\right)r_0}, \tag{2.1.8}$$

where $a = \lambda / p$ is De Broglie wavelength, A_T and A_P are the mass numbers of the target and the projectile, r_0 = 1.3 fm,

$$\chi^2 = 1.13\alpha_1^2\left[1 + 3.33\left(\frac{Z_T Z_P}{137\beta}\right)^2\right], \tag{2.1.9}$$

where

$$\alpha_1 = \frac{a}{0.885 a_0 \left(Z_T^{2/3} + Z_P^{2/3}\right)^{1/2}}, \tag{2.1.10}$$

$a_0 = 0.529 \cdot 10^{-8}$ cm denotes the Bohr radius,

$$\Delta b = \frac{1}{Z_T}\left\{\ln\left[\frac{1130\beta^2}{Z_T^{4/3}(1-\beta)^2}\right] - u_{in} - \frac{\beta^2}{2}\right\}, \tag{2.1.11}$$

where u_{in} is a constant determined by the electron configuration of the target atom (from the Thomas-Fermi model one finds u_{in} = -5.8, for the H-atom exact calculation yields u_{in} = -3.6, for Li- and O-atoms the values of u_{in} are -4.6 and -5.0, respectively). E_{max} is the maximum energy loss in a head-on collision of the projectile with a target electron:

$$E_{\max} = \frac{2 m_e c^2 \beta^2 \gamma^2}{1 + 2\gamma \frac{m_e}{M} + \left(\frac{m_e}{M}\right)^2}, \tag{2.1.12}$$

with m_e is the electron mass and M - the projectile mass. ξ is a quantity which is proportional to the areal density ρx of the target (ρ – target density in g/cm^3):

$$\xi = 0.1535 \frac{MeV\, cm^2}{g} \frac{Z_1^2}{\beta^2} \frac{Z_2}{A_2} \rho x\,. \tag{2.1.13}$$

2.2. Intrabeam scattering of the ion beam

Two modes for the calculations of the IBS growth rate can be used in the present version of the program.

At smoothed lattice structure (without variation of the beta and dispersion functions) the rates are calculated by numerical evaluation of corresponding integrals in accordance with Piwinski model [5]. For real lattice of the ring the algorithm described in [6] is used.

2.2.1. Piwinski model

For the smoothed focusing approximation only the mean values of the lattice functions are used and they are determined as follows:

$$\beta_{h,v} = \frac{R}{Q_{h,v}},\ D = \frac{R}{Q_h^2},\ \alpha_{h,v} = 0,\ D' = 0\,. \tag{2.2.1}$$

In accordance with Piwinski model the growth rates are calculated in accordance with the following expressions:

$$\frac{1}{\tau_p} = \frac{1}{2\sigma_p^2}\frac{d\sigma_p^2}{dt} = nA\frac{\sigma_h^2}{\sigma_p^2} f(a,b,c)$$

$$\frac{1}{\tau_x} = \frac{1}{2\sigma_{x\beta}^2}\frac{d\sigma_{x\beta}^2}{dt} = A\left[f\left(\frac{1}{a},\frac{b}{a},\frac{c}{a}\right) + \frac{D^2\sigma_p^2}{\sigma_{x\beta}^2} f(a,b,c)\right] \qquad (2.2.2)$$

$$\frac{1}{\tau_z} = \frac{1}{2\sigma_z^2}\frac{d\sigma_z^2}{dt} = Af\left(\frac{1}{b},\frac{a}{b},\frac{c}{b}\right)$$

where $n = 1$ for a bunched beam and $n = 2$ for an coasting beam,

$$A = \frac{r_i^2 c N_b}{64\pi^2\sigma_s\sigma_p\sigma_{x\beta}\sigma_z\sigma_{x'}\sigma_{z'}\beta^3\gamma^4} \text{ - bunched beam} \qquad (2.2.3)$$

and for coasting beam one needs to use a substitution $\frac{N_b}{\sigma_s} \to \frac{2\sqrt{\pi}N}{C}$.

The standard deviations are determined here as follows:

$$\sigma_{x_\beta,z} = \sqrt{\frac{\varepsilon_{x,z}\beta_{x,z}}{2}}\ ,\ \sigma_{x'_\beta,z'} = \sqrt{\frac{\left(1+\alpha_{x,z}^2\right)\varepsilon_{x,z}}{2\beta_{x,z}}}\ , \qquad (2.2.4)$$

and σ_p is the r.m.s. momentum spread, $\varepsilon_{x,z}$ are the beam two sigma emittances. The function f is the following integral:

$$f(a,b,c) = 8\pi^2\int_0^1\left[\ln\left(\frac{c^2}{2}\left(\frac{1}{\sqrt{p}}+\frac{1}{\sqrt{q}}\right)\right) - 0.577\right]\left(1-3x^2\right)\frac{dx}{\sqrt{pq}}\,. \qquad (2.2.5)$$

The following relations determine normalized parameters used in the Formula 2.2.5:

$a = \frac{\sigma_h}{\gamma\sigma_{x'}}$, $b = \frac{\sigma_h}{\gamma\sigma_{z'}}$, $c = \beta\sigma_h\sqrt{2\frac{d}{r_i}}$, $\frac{1}{\sigma_h^2} = \frac{1}{\sigma_p^2} + \frac{D^2}{\sigma_{x\beta}^2}$,

$p = a^2 + x^2\left(1-a^2\right)$,

$q = b^2 + x^2\left(1-b^2\right)$,

and the maximum impact parameter d is about 0.5 beam height. Integral (2.2.5) is calculated numerically.

2.2.2. Martini model

To calculate the IBS with the Martini model one needs to use the lattice functions of the COSY for different modes of its operation. The lattice parameters are imported to the program from the files presented by COSY (see for instance Fig. 2.1).

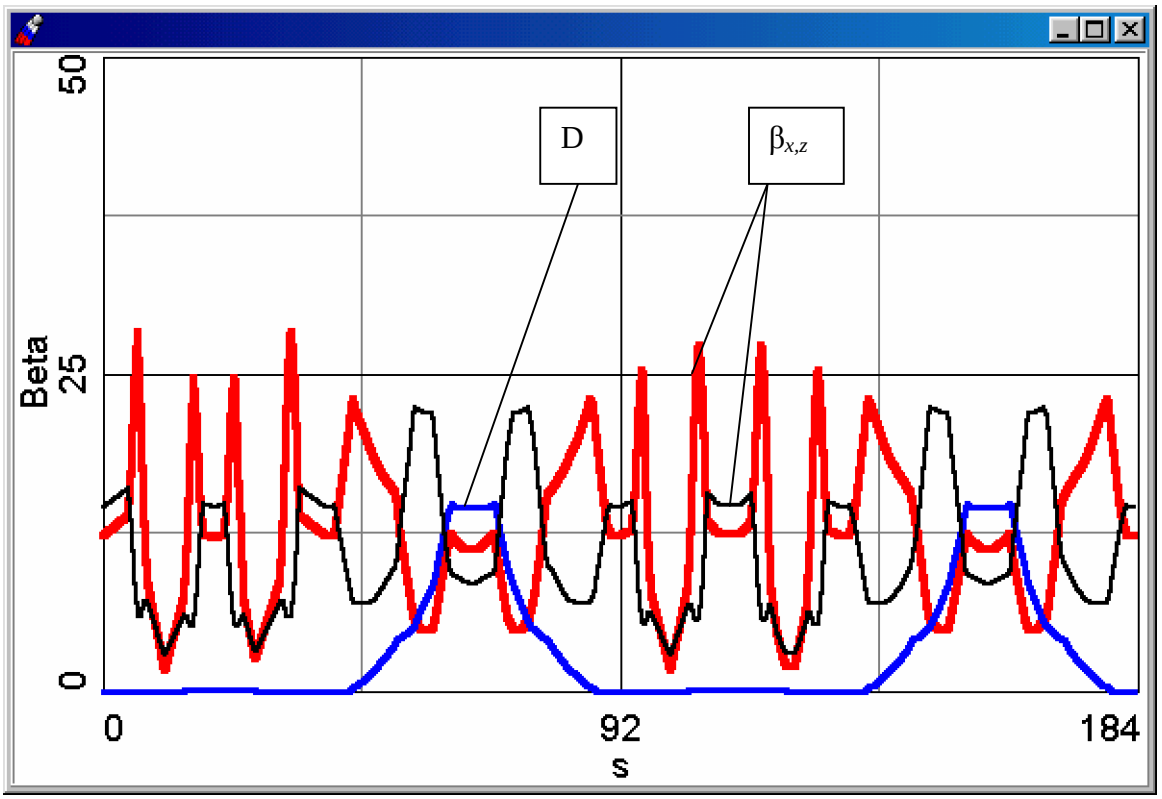

Fig. 2.1. The optical functions for an ideal COSY lattice with dispersion-free telescopic sections obtained by non-symmetric operation of the 6 unit cells in the arcs, superperiodicity S = 2.

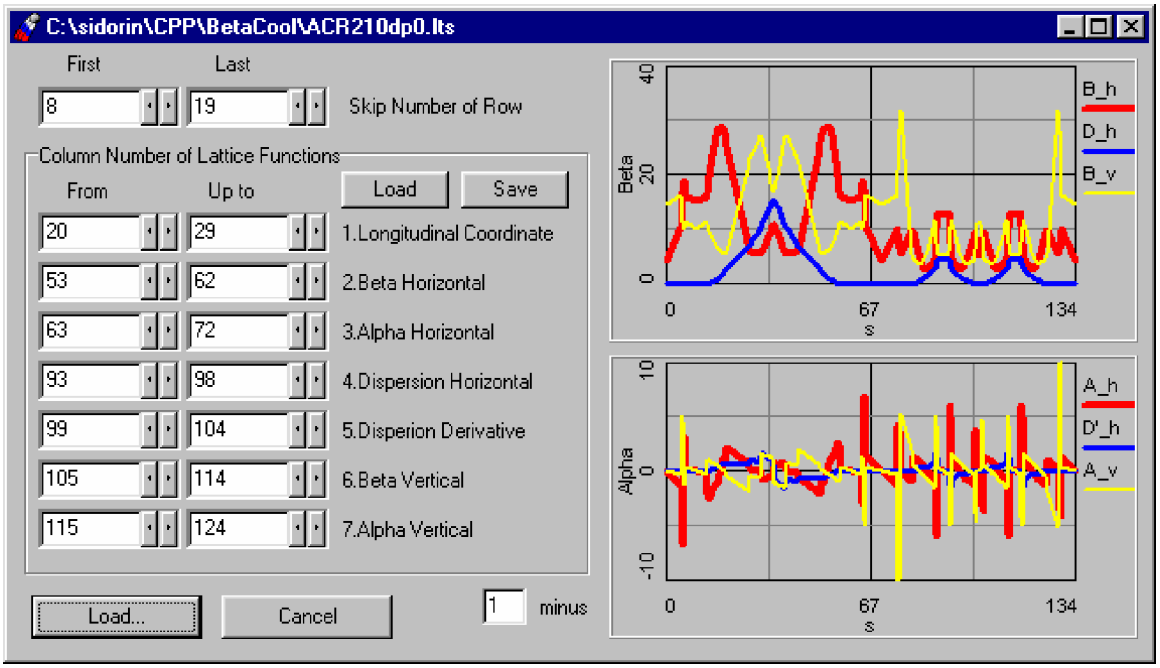

Fig. 2.2. The lattice parameters imported from the MAD output file.

In order to read the lattice functions from the file in text format a special visual form was elaborated (Fig. 2.2). Using it user can specify positions of the corresponding parameters in input file, read the file and check a validity of the data presented in the numerical or graphic format.

In accordance with the Martini model the growth rates can be inserted into the code in the form of the corresponding characteristic times:

$$\frac{1}{\tau_p} = \left\langle \frac{nA}{2}\left(1-d^2\right) f_1 \right\rangle$$
$$\frac{1}{\tau_{x'}} = \left\langle \frac{A}{2}\left[f_2 + \left(d^2 + \tilde{d}^2\right) f_1 \right] \right\rangle \qquad (2.2.6)$$
$$\frac{1}{\tau_{z'}} = \left\langle \frac{A}{2} f_3 \right\rangle$$

where angular brackets mean averaging over the ring circumference, n = 1 for a bunched beam and n = 2 for coasting beam,

$$A = \frac{\sqrt{1+\alpha_x^2}\sqrt{1+\alpha_z^2}\, c r_i^2 \lambda}{16\pi\sqrt{\pi}\sigma_{x_\beta}\sigma_{x'_\beta}\sigma_z\sigma_{z'}\sigma_p\beta^3\gamma^4} \qquad (2.2.7)$$

λ is the linear ion density:

$$\lambda = \begin{cases} N/L, & \textit{for coasting beam} \\ N_b/\left(2\sqrt{\pi}\sigma_s\right), & \textit{for a bunched beam} \end{cases}. \qquad (2.2.8)$$

The functions f_i are integrals of the following form:

$$f_i = k_i \int_0^\infty \int_0^\pi \int_0^{2\pi} \sin\mu\, g_i(\mu,\nu) \exp\left[-D(\mu,\nu) z\right] \ln\left(1+z^2\right) d\nu\, d\mu\, dz\,, \qquad (2.2.9)$$

with the coefficients $k_1 = 1/c^2$, $k_2 = a^2/c^2$, $k_3 = b^2/c^2$, and

$$D(\mu,\nu) = \frac{\left[\sin^2\mu\cos^2\nu + \sin^2\mu\left(a\sin\nu - \tilde{d}\cos\nu\right)^2 + b^2\cos^2\mu\right]}{c^2}, \qquad (2.2.10)$$

$$g_1(\mu,\nu) = 1 - 3\sin^2\mu\cos^2\nu\,, \qquad (2.2.11)$$

$$g_2(\mu,\nu) = 1 - 3\sin^2\mu\sin^2\nu + 6\tilde{d}\sin^2\mu\sin\nu\cos\nu/a\,, \qquad (2.2.12)$$

$$g_3(\mu,\nu) = 1 - 3\cos^2\mu\,. \qquad (2.2.13)$$

The normalized parameters are to be calculated from the following expressions:

$$a = \frac{\sigma_y}{\sigma_{x'_\beta}}\sqrt{1+\alpha_x^2}\,,\ b = \frac{\sigma_y}{\sigma_{z'}},\ c = q\sigma_y,\ d = \frac{\sigma_p}{\sigma_x}D,\ \tilde{d} = \frac{\sigma_p}{\sigma_x}\tilde{D},$$

where $\tilde{D} = \alpha_x D + \beta_x D', \sigma_x^2 = \sigma_{x_\beta}^2 + D^2\sigma_p^2,\ \sigma_y = \dfrac{\sigma_p\sigma_{x_\beta}}{\gamma\sigma_x}$ and $q = 2\beta\gamma\sqrt{\dfrac{\sigma_z}{r_i}}$.

The integration over z – variable can be approximately performed analytically due to small value of the function $D(\mu,\nu)$:

$$\int_0^\infty \exp[-D(\mu,\nu)z]\ln(1+z^2)dz \approx 2\int_1^\infty \exp[-D(\mu,\nu)z]\ln z dz =$$
$$-\frac{2}{D(\mu,\nu)}\left(C+\ln D(\mu,\nu)+\int_0^{D(\mu,\nu)}\frac{e^{-t}-1}{t}dt\right),$$

where C is the Euler constant.

The integration (2.2.9) over other two variables is performed numerically.

2.3. Ion multi scattering on residual gas atoms

The characteristic time of the emittance grows rate is calculated using the following formula [7]:

$$\frac{1}{\tau_i}=\frac{1}{\varepsilon_i}\frac{\partial\varepsilon_i}{\partial t}=\frac{8\pi\beta_i}{\varepsilon_i}n_{ms}\ln\left(\frac{280}{\alpha}\right)r_e^2\frac{(m_ec^2)^2}{\beta cp^2}. \qquad (2.3.1)$$

Here

$$n_{ms}=\sum_i n_i\frac{Z^2\ln\left(280/\left(\alpha(AZ)^{1/3}\right)\right)}{\ln(280/\alpha)} \qquad (2.3.2)$$

is the multiple scattering density with a given residual gas composition (in the program three components of the residual gas atoms can be introduced), α is the fine structure constant, β_i is the mean beta function in corresponding plane.

2.4. Tune resonances of the ion betatron motion

The tune resonances are often associated with beam losses, but if the resonance is weak enough or it is crossed quickly enough it may lead to an amplitude growth only which is equivalent to heating.

The maximum amplitude growth time (e-folding) due to a nonlinear one-dimensional resonance is [7]:

$$\tau_Q=\frac{N}{\pi\Delta Q_N}\frac{C}{\beta c}\frac{1-e^{2-N}}{N-2},\ N>2 \qquad (2.4.1)$$

Here N is the order of resonance, C – ring circumference, ΔQ_N is the resonance width, βc is the particle velocity.

2.5. External heating

During proton beam injection in the beginning of the stacking process the beam in COSY is additionally heated longitudinally with a white noise frequency band around the harmonic by USE-kicker and transversely by noise applied to the stripline until for the tune measurement. This parallel heating results in a higher intensity of the cooled beam. The noise heating can be characterized with the diffusion power P and the corresponding heating rates are calculated as follows:

$$\frac{1}{\tau_{x,z}} = \frac{2P_{trans}}{\varepsilon_{x,z}^2}$$
$$\frac{1}{\tau_{long}} = \frac{2P_{lon}}{H_{lon}^2}. \qquad (2.5.1)$$

The heating effects caused by interaction with residual gas and target atoms lead to linear increase with time of the beam emittances. The emittance deviation can be calculated in accordance with corresponding formulae or measured experimentally and introduced into calculation as an external linear heating:

$$\frac{1}{\tau_{x,z}} = \frac{\partial\varepsilon / \partial t}{\varepsilon_{x,z}}$$
$$\frac{1}{\tau_{long}} = \frac{\partial H_{lon} / \partial t}{H_{lon}}, \qquad (2.5.2)$$

where $\partial\varepsilon / \partial t$ and $\partial H_{lon} / \partial t$ are the heating power in the transverse and longitudinal degrees of freedom correspondingly.

3. Particle losses calculation

3.1. Nuclear scattering on residual gas atoms

The cross-section for nuclear scattering can be approximated by the expression [7]:

$$\sigma_{a,[mb]} = A^{2/3}\left(\frac{53}{p_{[GeV/c]}} + 66\right) \qquad (3.1.1)$$

Introducing the nuclear scattering density:

$$n_{ns} = \sum_i n_i A_i^{2/3} \qquad (3.1.2)$$

we can express the life time as the following:

$$\tau_{ns} = \frac{1}{\beta c n_{ns} \sigma_{ns}}, \qquad (3.1.3)$$

where σ_{ns} is the hydrogen cross-section (A = 1).

3.2. Single scattering on large angles

The cross-section for single scattering with an angle larger than the acceptance angle θ is:

$$\sigma_{sc} = 4\pi\left(\frac{Zr_p}{\gamma\beta^2}\right)^2 \frac{1}{\theta^2}, \tag{3.2.1}$$

where Z is the charge number of the nucleus of the rest gas atoms, r_p is the proton classic radius. The average acceptance angle in eliptical vacuum chamber is given by

$$\frac{1}{\theta^2} = \frac{1}{2\theta_x^2} + \frac{1}{2\theta_z^2}, \text{ where } \frac{1}{\theta_{x,z}^2} = \frac{2\beta_{x,z}}{\varepsilon_{accept,x,z}} \tag{3.2.2}$$

The beam life time due to single Coulomb scattering

$$\tau_{life} = \frac{\gamma^2\beta^3\varepsilon_{accept}}{4\pi r_p^2 c\left(\langle\beta_x\rangle + \langle\beta_z\rangle\right)n_{sc}} \tag{3.2.3}$$

where

$$n_{sc} = \sum_i Z_i^2 n_i . \tag{3.2.4}$$

3.3. Recombination in the electron cooling section

The recombination rate in the laboratory frame for the radiative recombination is described by the following formula:

$$\frac{1}{\tau_{life}} = \frac{1}{N_i}\frac{dN_i}{dt} = -\frac{\alpha_r n_e \eta_L}{\gamma^2} \tag{3.3.1}$$

where α_r is the recombination coefficient (see Formula (3.3.2) below), $n_e = I_e/(e\pi a^2\beta c)$ is electron beam density in the cooler, a, I_e – electron beam radius and current correspondingly, η_L is the ring fraction occupied by the electron beam. Assuming a flattened electron velocity distribution one can express the formula for α_r in a simple form [8]:

$$\alpha_r = 3.02\cdot 10^{-13}\frac{cm^3}{s} Z^2 \sqrt{\frac{1}{T_\perp}}\left[\ln\left(\frac{11.32Z}{\sqrt{T_\perp}}\right) + 0.14\left(\frac{T_\perp}{Z^2}\right)^{1/3}\right], \tag{3.3.2}$$

here $T_\perp$ is measured in eV.

3.4. Other particle losses

All the processes leading to exponential decrease of the particle number can be summarized in the calculations by introducing an equivalent particle lifetime in the ring. This value can be included into calculations using a special process called "DECAY".

4. Cooling processes involved into calculations.

4.1. Stochastic cooling

4.1.1 Transverse cooling time

At the optimum gain of the of the feed back system the optimum cooling rate is [2]:

$$\frac{1}{\tau_{opt}} = \frac{1}{\varepsilon}\frac{d\varepsilon}{dt} = -\frac{W}{N \cdot M} \tag{4.1.1}$$

where W is the bandwidth of the cooling system, N is the particle number,

$$M = \frac{3}{4}\frac{f_0}{W|\eta|\delta}, \tag{4.1.2}$$

f_0 is the mean frequency, $\eta = \frac{1}{\gamma_{tr}^2} - \frac{1}{\gamma^2}$, δ denotes the absolute relative momentum spread of the protons.

4.1.2 Longitudinal cooling time

At the optimum gain of the of the feed back system the optimum cooling rate is the following:

$$\frac{1}{\tau_{opt}} = \frac{1}{H_{long}}\frac{dH_{long}}{dt} = -\frac{W}{N} \tag{4.1.3}$$

4.1.3. Power limited cooling

In the case when optimum cooling time can not be obtained due to power limitation of the amplifiers, the cooling time in first approximation is not dependent of particle number and beam parameters. To take into account this case in the program the cooling times can be input directly and kept constant during calculations.

4.2 Electron cooling

4.2.1 Electron cooling with single pass electron beam

Electron cooling rates are calculated in the BETACOOL program through averaging of the action of the friction force inside the electron cooler over phases of betatron and synchrotron oscillations and over Gaussian distribution function of the particles in the space of the motion invariants.

The cooling rates calculation was performed under the following general assumption:

1) the ion coordinates are kept constant during ion passing the cooling section;

2) the motion of each particle is described by two Courant-Snyder invariants:

$$I_i = \frac{1+\alpha_i^2}{\beta_i} i_\beta^2 + 2\alpha_i i_\beta i'_\beta + \beta_i i'^2_\beta,\ i = x, z, \qquad (4.2.1)$$

where x, z are horizontal and vertical co-ordinates, α_i and β_i are alpha and beta functions in the cooling section. The invariant corresponding to synchrotron motion can be introduced in accordance with (1.2) as follows:

$$I_s = m\left(\frac{\Delta p}{p}\right)^2_{\max}, \quad m = \begin{cases} 1 - \textit{coasting beam}, \\ 2 - \textit{bunched beam}. \end{cases}$$

$I_s = H_{lon}$, if $(\Delta p/p)_{max} = \sigma_p$, where σ_p is the r.m.s. momentum spread.

The ion "betatron" coordinates and momentum inside the cooling section can be calculated in accordance with

$$x_\beta = \sqrt{I_x \beta_x}\sin\varphi, \quad x'_\beta = \sqrt{\frac{I_x}{\beta_x}}\left(\cos\varphi + \alpha_x \sin\varphi\right)$$

The same expressions are used for z co-ordinate with substitution of corresponding alpha and beta function value. The total value of x-co-ordinate is equal to

$$x = x_\beta + D(\Delta p/p),\ x' = x'_\beta + D'(\Delta p/p),\ \frac{\Delta p}{p} = \frac{\Delta p}{p}_{\max}\cos\phi,\ s - s_0 = \sigma_s \sin\phi,$$

where s_0 is longitudinal coordinate of the bunch center, $x' = p_x/p$.
A relative change of the ion momentum components after passing the cooling section can be expressed with the following formula:

$$\begin{pmatrix} \frac{\delta p_x}{p} \\ \frac{\delta p_z}{p} \\ \frac{\delta p_s}{p} \end{pmatrix} = \overset{\circ}{\Phi}(x, z, s - s_0, x', z', \Delta p/p), \qquad (4.2.2)$$

where the functions Φ can be calculated in the BETACOOL program using one of three different analytical formulae for friction force of non magnetized [9] or magnetized electron beam [9, 10]. User of the program can make a choice of the formula which he prefers to use in calculations. For instance, Fig 4.1 presents a shape of the friction force of the magnetized electron beam given in [10].

The dependence of the friction force (or "drag rate") on particle coordinates appears due to space charge effects of the ion and electron beams. Calculations are performed taking into account these effects as described in [1, 11]. To speed up the program run time user can

exclude from the calculations the ion beam space charge effects. Electron beam neutralization is taken into account under assumption of parabolic profile of the residual gas ions distribution inside the electron beam. Influence of electron beam space charge introduces an electron momentum shift and electron drift velocity – both are the functions of ion radial position inside the electron beam. In presence of dispersion in the cooling section an asymmetry between vertical and horizontal degrees of freedom appears. At last, in the case of an intense ion bunched beam the friction force depends on the ion distance from the bunch center.

The variation of the motion invariants after single passing the cooling section are given by the following expressions:

$$\delta I_x = -2\left(x_\beta \left(\frac{\left(1+\alpha_x^2\right)}{\beta_x} D + \alpha_x D' \right) + x'_\beta \tilde{D} \right) \frac{\delta p}{p} + \\ + \frac{\left(D^2 + \tilde{D}^2\right)}{\beta_x} \left(\frac{\delta p}{p} \right)^2 + 2\left(\beta_x x'_\beta + \alpha_x x_\beta\right) \frac{\delta p_x}{p} + \quad , \qquad (4.2.3)$$
$$+ \beta_x \left(\frac{\delta p_x}{p} \right)^2 - 2\tilde{D} \frac{\delta p}{p} \frac{\delta p_x}{p}$$

$$\delta I_z = 2\left(\beta_z z'_\beta + \alpha_x z_\beta\right) \frac{\delta p_z}{p} + \beta_z \left(\frac{\delta p_z}{p} \right)^2 , \qquad (4.2.4)$$

$$\delta I_s = 2m \frac{\delta p}{p} \frac{\Delta p}{p} + m \left(\frac{\delta p}{p} \right)^2 , \qquad (4.2.5)$$

where $\frac{\delta p}{p} = \delta \frac{\Delta p}{p}$, D and D' are dispersion and its derivative in the cooling section, $\tilde{D} = \alpha_x D + \beta_x D'$.

The expressions (4.2.3) - (4.2.5) include the diffusion terms proportional to the square of momentum deviations. These terms determine equilibrium beam parameters in absence of other heating effects. In presence of more powerful heating processes, like IBS or scattering on residual gas atoms we can ignore the diffusion effects and speed up the program runtime excluding them from the calculations.

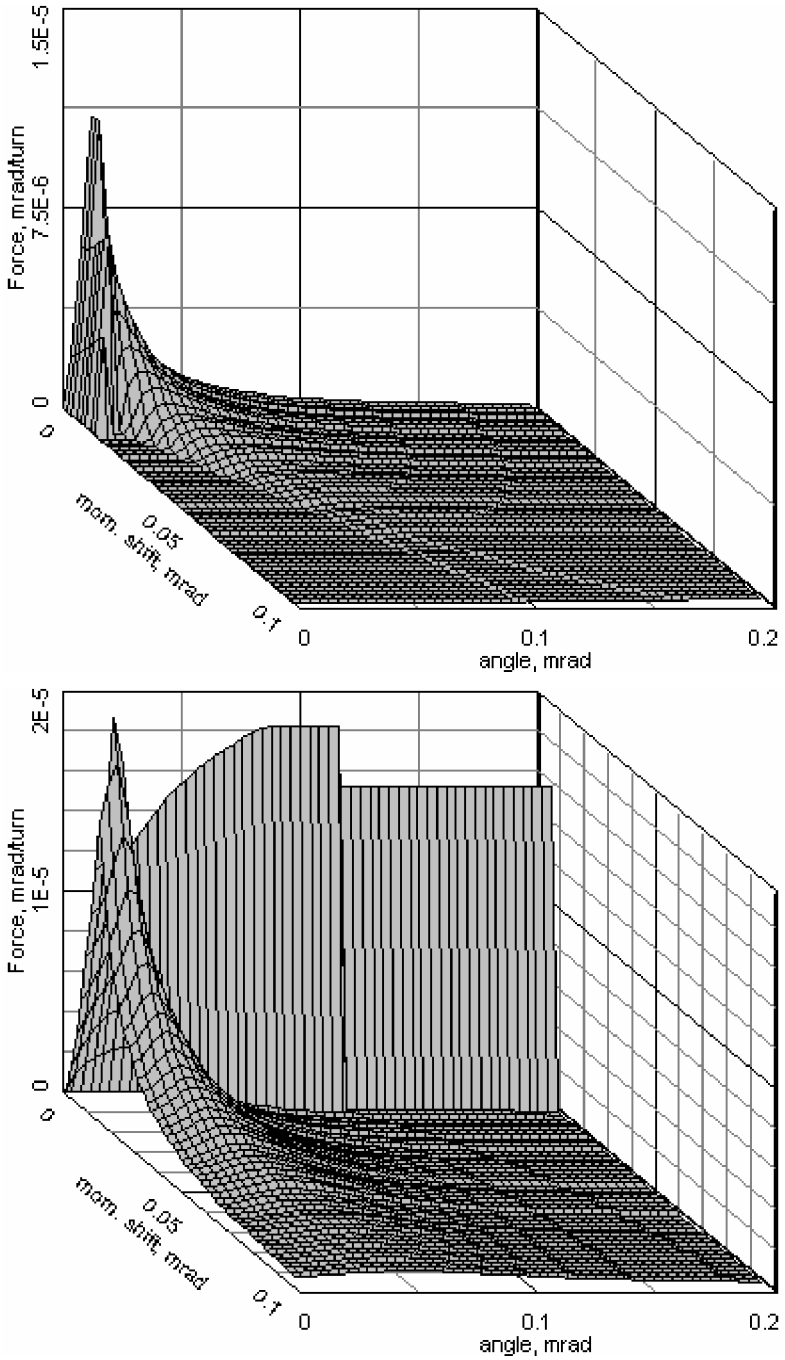

Fig.4.1. An example of the dependencies of the transverse (upper picture) and longitudinal (lower picture) components of the friction force on the ion momentum and angular shiftcalculated with friction force formulae from Ref. 10.

Under assumption, that the ion distribution over betatron and synchrotron phases is uniform in an interval [0, 2π] (a stationary beam) we can calculate average invariant deviation for ions having the same invariants of motion:

$$\left\langle \delta \overset{\circ}{I} \right\rangle = \frac{1}{8\pi^3} \int_0^{2\pi} \iint \delta \overset{\circ}{I} \left(\overset{\circ}{I}, \varphi_x, \varphi_{z,} \varphi_s \right) d\varphi_x d\varphi_z d\varphi_s \,. \tag{4.2.6}$$

These values calculated with invariants of motion are equal to beam emittances and can be used for evaluation of so called "single particle" cooling rate:

$$\frac{1}{\tau_{cool,sp}} = \frac{1}{I} \frac{\langle \delta I \rangle}{T_{rev}}, \tag{4.2.7}$$

where T_{rev} is the particle revolution period in the storage ring.

The cooling rates for ion beam with Gaussian distribution are calculated in BETACOOL by averaging (4.2.6) over distribution function in the space of invariants:

$$\delta\varepsilon_i = \frac{1}{\varepsilon_x \varepsilon_z \varepsilon_s} \int_0^{\infty} \langle \delta I_i \rangle e^{-I_x/\varepsilon_x - I_z/\varepsilon_z - I_s/\varepsilon_s} dI_x dI_z dI_s \,. \tag{4.2.8}$$

The cooling time value is equal to:

$$\frac{1}{\tau_{cool,i}} = \frac{1}{\varepsilon_i} \frac{d\varepsilon_i}{dt} = \frac{1}{\varepsilon_i} \frac{\delta\varepsilon_i}{T_{rev}} \,. \tag{4.2.9}$$

It should be noted, that emittance used in Formula (4.2.8) as a parameter of distribution function contains 63% of particles and is twice higher than r.m.s. value and this has to be taken into account in calculations of the standard deviation values.

Both possibilities can be used in the simulations: cooling time can be calculated in accordance with (4.2.9) or, to speed up the calculations, in accordance with (4.2.7).

4.2.2 Electron cooling with circulating electron beam

Due to interaction between the particles (antiprotons, ions) and electrons the particle temperature decreases when the electron one increases. In accordance with energy conservation low the temperatures of the ion and circulating electron beam are connected together as follows:

$$N_p \frac{dT_e}{dt} = - N_e \frac{dT_e}{dt}, \tag{4.2.10}$$

where T_p, T_e *are the particle and electron temperatures in the particle rest frame,* N_p, N_e – *the particle numbers in the rings.*

"Thermodynamics" of the cooling process in approximation of uniform two component Maxwellian plasma was investigated in [12]. The variation of both temperatures in this plasma is described by the equation:

$$\frac{dT_p}{dt} = \frac{4\sqrt{2\pi}\eta_L n_e z^2 e^4 L_C}{\gamma^2 mM} \cdot \frac{T_p - T_e}{\left(\frac{T_p}{M} + \frac{T_e}{m}\right)^{3/2}}, \qquad (4.2.11)$$

where m *and* M – *the electron and ion masses,* η_L *is the ratio of the cooling section length to the circumference of the particle ring,* L_C – *Coulomb logarithm,* n_e – *the electron density,* t – *current time in Laboratory reference frame. This approach leads to Budker's formula for friction force [13].*

To solve the system (4.2.10 – 4.2.11) we have to introduce two additional parameters of the cooler: electron ring circumference *C,* and period of electron circulation τ_c. During the electron circulation period the electron beam temperature increases due to relaxation with ion beam, after that the electron ring is filled up with new portion of cold electrons. The number of electrons in the electron ring is calculated using the expression:

$$N_e = \frac{CI}{\beta c}. \qquad (4.2.12)$$

Initial ion beam temperature is to be calculated from given values of the transverse and longitudinal emittances of the ion beam. The relation between the mean particle kinetic energy and emittance depends on emittance definition used in the calculations. Here we use the standard deviation of the particle distribution function in the invariant space as an

emittance definition. The corresponding phase space contains 63% of particles and relates with r.m.s. beam dimensions in accordance with (4.2.8).

The mean kinetic energy for single transverse degree of freedom in the particle rest frame is connected with the beam emittance by the following relations:

$$\varepsilon_{x,z} = 2\theta^2\beta_{x,z} = 2\left(\frac{p_{x,z}}{p}\right)^2 \cdot \beta_{x,z} = \frac{4E^*_{x,z}}{\beta^2\gamma^2 Mc^2} \cdot \beta_{x,z} \tag{4.2.13}$$

where $\beta_{x,z}$ *is mean beta function in corresponding plane. The number of particles inside* $T_{x,z}$ *has the same value as inside the emittance when the kinetic energy of the particles is connected with the beam transverse temperature as* $E^*_{x,z} = T_{x,z}$ *.And we have for transverse temperature the following relation with the beam emittance:*

$$T_{x,z} = E^*_{x,z} = \beta^2\gamma^2 Mc^2 \frac{\varepsilon_{x,z}}{4\beta_{x,z}}. \tag{4.2.14}$$

Summarizing by all degrees of freedom we have:

$$3T_p = E_{kin} = Mc^2\beta^2\gamma^2\left(\frac{\left((\Delta p / p)^2\right)}{\gamma^2} + \frac{\varepsilon_x}{4\beta_x} + \frac{\varepsilon_z}{4\beta_z}\right) \tag{4.2.15}$$

Using this definition of the ions and electron temperature (in both beams the temperature is averaged over degrees of freedom) as an initial values we can solve the system (4.2.10 –

4.2.11) during circulation period. Under assumption that circulating period is substantially shorter than the cooling time and that all degrees of freedom are cooled uniformly we can determine the cooling time as follows:

$$\frac{1}{\tau_{cool,circ}} = \frac{1}{\varepsilon_x}\frac{\partial \varepsilon_x}{\partial t} = \frac{1}{\varepsilon_z}\frac{\partial \varepsilon_z}{\partial t} = \frac{1}{H_{long}}\frac{\partial H_{long}}{\partial t} = \frac{1}{\tau_c}\frac{T_{p,fin} - T_{p,in}}{T_{p,in}}, \qquad (4.2.16)$$

where $T_{p,in}$ *and* $T_{p,fin}$ *are initial and final beam temperatures correspondingly. In this model the effects of the flattened velocity distribution and magnetization of electron beam are neglected and temperatures of all degrees of freedom of the ion beam are supposed to be near the thermal equilibrium.*

In the case of magnetized electron beam with flattened velocity distribution the cooling time of the system with circulating electron beam can be calculated using the following procedure. The circulation period is divided into n *short intervals of time and we assume that during each of them electron temperature is constant. The change of emittance during this period of time can be calculated using cooling time calculated for single pass electron beam:*

$$\delta\varepsilon = \frac{\varepsilon}{\tau_{cool,\sin glepass}} \cdot \frac{T_c}{n} \qquad (4.2.17)$$

The change of the ion beam temperature is calculated in accordance with (4.2.15):

$$3\Delta T_p = Mc^2\beta^2\gamma^2\left(\frac{\delta H_{lon}}{\gamma^2} + \frac{\delta\varepsilon_x}{4\beta_x} + \frac{\delta\varepsilon_z}{4\beta_z}\right) \qquad (4.2.18)$$

Assuming that the energy obtained by electron beam is divided between degrees of freedom in the equal parts we can calculate new electron temperature:

$$\Delta T_{e,\parallel} = -\frac{1}{3}\frac{N_p}{N_e}\Delta T_p,$$

$$\Delta T_{e,\perp} = \Delta T_x + \Delta T_z = -\frac{2}{3}\frac{N_p}{N_e}\Delta T_p \qquad (4.2.19)$$

At the next period of time the change of emittance is calculated at new electron temperature and so on. Finally the cooling time is calculated using the following expression:

$$\frac{1}{\tau_{cool,circ}} = \frac{1}{\tau_c}\frac{\varepsilon_{fin} - \varepsilon_{in}}{\varepsilon_{in}}. \qquad (4.2.20)$$

Here ε_{in} and ε_{fin} are the ion beam emittance value at the begining of the circulation period τ_c and at it's end.

5. Calculations of the beam stability characteristics

During the numerical solving of the system (1.1) the following parameters characterizing the beam stability are calculated.

Incoherent tune shift is calculated using well known formula:

$$\Delta Q_{sc} \approx \frac{r_i}{2\pi}\frac{N_b}{\beta^2\gamma^3\varepsilon_z(1+\sqrt{\varepsilon_x/\varepsilon_z})B_f}, \qquad (5.1)$$

where N_b is the particle number in the case of coasting beam and product of the particle number per bunch and harmonic number in the case of bunching beam, B_f - the bunching factor (relation of average current to peak current).

As a characteristics of a longitudinal stability of the beam the following parameter is calculated:

$$KS = \left(4F_L\frac{U_p}{(|Z_L|/n)}\frac{A_i}{Z_i I}\gamma\beta^2|\eta|(\frac{\Delta p}{p})^2\right)^{-1} \le 1. \qquad (5.2)$$

Here F_L is the factor depending on the form of distribution function and the impedance phase (in "Keil-Schnell" criterion it is assumed that F_L=1), U_p = 938 MV, $\eta = 1/\gamma^2 - 1/\gamma_{tr}^2$, Z_n is the longitudinal coupling impedance at $\omega = n\omega_0$.

Criterion for transverse beam stability is calculated as follows

$$SZ = \left(8F_t\frac{U_p}{Z_t R}\frac{A_i}{Z_i I}\beta\gamma Q\Delta Q_n\right)^{-1} \le 1. \qquad (5.3)$$

Here the effective spread of betatron tune for *n*-th mode ($\omega_n = n\omega_0$) ΔQ_n is defined by

$$\Delta Q_n \approx \sqrt{[(n-Q)\eta+\xi]^2\left(\frac{\Delta p}{p}\right)^2+\Delta Q_{non}^2}\,, \tag{5.4}$$

Z_t is transverse coupling impedance at $\omega=(n-Q)\omega_0$, and ξ is the rind chromaticity, F_t is the factor depending on form of distribution function and the impedance phase.

At the regime of the storage ring with the bunched ion beam the influence of the space charge fields on synchrotron motion is estimated with numerical calculations also. For calculation of linear synchrotron tune Q_s the model of the beam with linear longitudinal space charge field and parabolic dependence of linear charge density on longitudinal coordinate is applied. The synchrotron tune is calculated as follows

$$Q_s = Q_s^{\,0}\sqrt{1-N_b/N_b^{\max}}\,, \tag{5.5}$$

where N_b is ion number per bunch, its maximal value - $N_b^{\max}$ is given by the expression:

$$N_b^{\max} = \frac{1}{3\pi G_L}\cdot\frac{q(eU)\sigma_s^{\,3}\gamma^2}{Z_i E_0 r_p R^2}\,, \tag{5.6}$$

$G_L = 1+2\ln(\frac{b}{a})$, U is RF voltage, q is RF harmonic number, E_0 and r_p are the proton rest energy and classical radius, Z_i is an ion charge number. The tune $Q_s^{\,0}$, which appears due to RF field, is

$$Q_s^{\,0} = \frac{1}{\beta}\sqrt{\frac{q\eta eZ_iU}{2\pi E_0 A_i\gamma}}\,, \tag{5.7}$$

here A_i is the ion atomic number. R.m.s momentum spread is connected to σ_s by the formula:

$$\sigma_p = Q_s\frac{\sigma_s}{\eta R}\,. \tag{5.8}$$

Now for calculation of the bunch length the tune Q_s^0 is used, the value (5.7) is displayed as well as the values (5.1), (5.2) and (5.3) in graphic form for estimation of the influence of the beam space charge on the particles motion.

6. Description of the program

The BETACOOL program developed on the base of BOLIDE system using C++ Builder 4 and works now under Microsoft Windows operation system. The BOLIDE version for Unix is under development presently. In the program only the standard C++ and BOLIDE commands are used for connection of algorithmic and interface parts. In future the program can be recompiled to Unix version without any modifications.The numerical algorithm is realized on the base of Object Oriented Programming method and the program structure consists of several basic objects. For input and visual presentation of parameters of each object special forms were developed. The tools of the BOLIDE system to load and save data into hard disc, for output the data into two and tree dimensional plots during the calculations and to control of the calculation process are used. Below we discuss briefly general objects of the program.

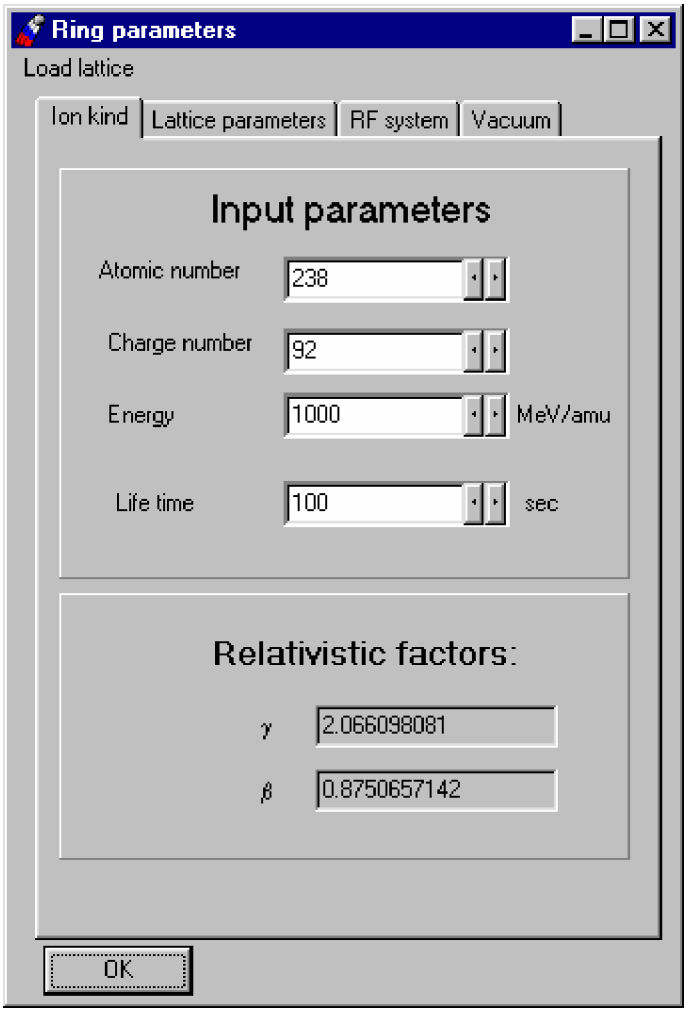

Fig.6.1. The form for input and output of the parameters of the storage ring in numerical format.

The object "Ring" includes the general parameters of the storage ring, methods of import of the parameters from external file and control of its validity, methods for calculation of required parameter. The parameters are divided by several groups in accordance with general systems of the storage ring: parameters of the stored ions, lattice parameters - mean and

imported from external file, radio frequency and vacuum system parameters. View of the form for input of the ring parameters is presented in the Fig.6.1.

The object "Beam" includes general beam parameters: particle number, values of the emittances and momentum spread, methods for calculation of beam parameters characterizing beam stability and luminosity, for general parameters visualization in numerical and graphic form. The methods use only ring parameters as input. Fig. 6.2, 6.3 present the forms for input and output of the beam parameters.

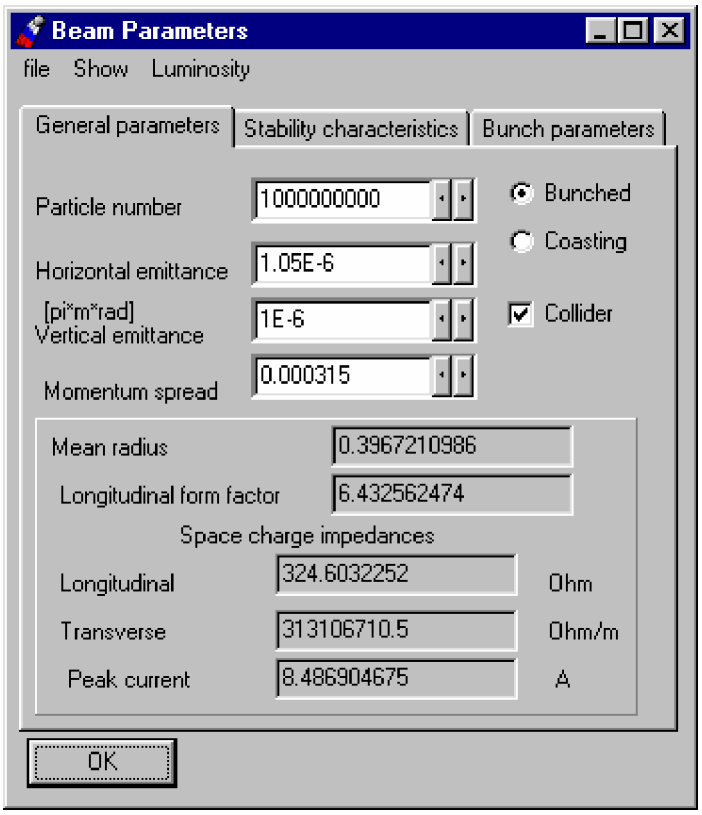

Fig. 6.2. The form for input and output of the beam parameters in the numerical format.

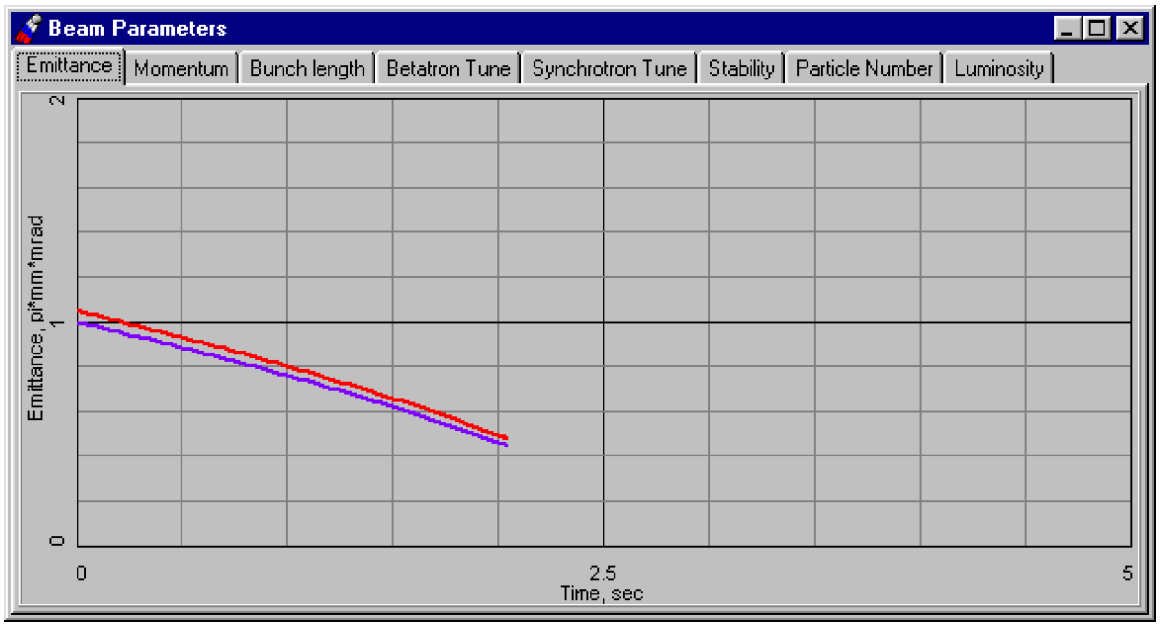

Fig. 6.3. The form for output of the beam parameters in the graphic format.

Each process involved into calculation of the beam parameters evolution is performed as an independent object also. This object includes the parameters of the corresponding process or device and methods of these parameters optimization and visualization. For instance, object "Electron Cooling" includes parameters of the cooling section, parameters of the electron beam and lattice functions in the cooling section. To optimize cooling time calculations user can choose physical model of the process and mode of the cooler operation. The dependence of friction force on ion angular and momentum deviation is output as a three dimensional plot, and for mode with circulating electron beam the time dependence of electron temperature is displayed in graphic format also. The view of the form for input of the electron cooling system parameters is presented in the Fig. 6.4.

All objects describing a beam parameters evolution are developed on the base of the ancestor class "Effect", which has a virtual function using Beam and Ring objects as input variables, and returning array of the rates: particle loss, two emittances and momentum spread variation. In each descendants class corresponding to concrete process this function is reloaded by its individual one. All variables of the class effect are automatically included into array of the effects, and class effect includes the method, which calculates the sum of the rates in the cycle. This ancestor class includes also methods for output of the rates in numerical and graphical format (see Fig. 6.5).

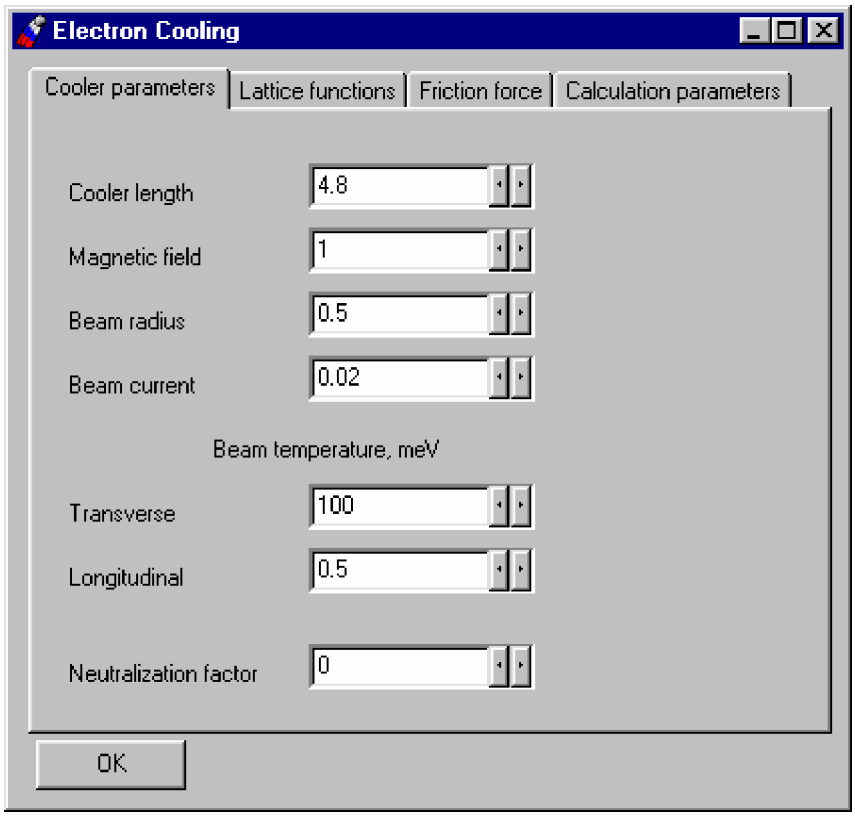

Fig. 6.4. The form for input of the electron cooling system parameters.

In order to realize this approach in the program the special class BTemplate for the storage of object pointers was elaborated. The declaration and constructor of this template are presented here:

```
template <class B>
class BTemplate
{ public:
   static B **BItems;
   static int BCount;
   int BIndex;
   BTemplate();
   virtual ~BTemplate();
};

template <class B>
BTemplate<B>::BTemplate()
{ B** newItems = new B*[BCount+1];
   for (int i = 0; i < BCount; i++)
      newItems[i] = BItems[i];
   newItems[BCount] = (B*)this;
   if (BCount) delete []BItems;
   BItems = newItems;
   BIndex = BCount;
   BCount++;
}
```

All `Effect` classes are the descendants from `BTemplate`. Simulation tasks do not use standard variable names of different `Effect` classes. They use the pointer array `BItems` of `BTemplate`. This structure permits to include very easy new effects without any changes in the program.

Such approach is useful and widely used in our program codes as the base of Object Oriented Programming.

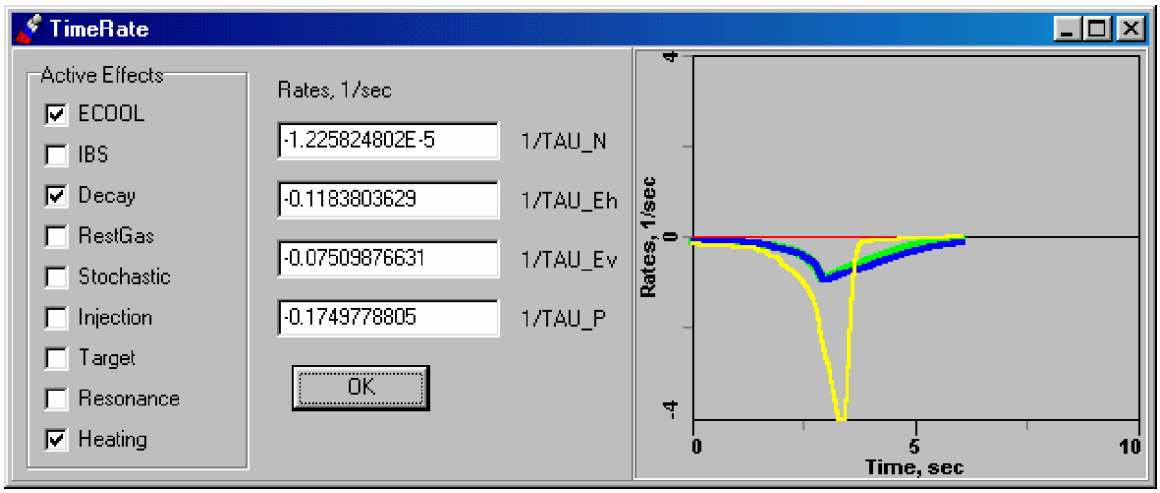

Fig. 6.5. The form for visualization of the effect array and output of the sum of the rates of the active effects.

Another group of objects called “Task” corresponds to investigation of the beam parameter variation due to common action of the active effects (Fig. 6.5). These objects get the array of the rates from the list of effects, calculate the beam parameters and use the methods of the Beam object for their visualization. Only one object of this type is realized now in the program “Dynamics”, which includes method and parameters necessary for numerical solution of the system of differential equations (1.1) and for visualization of the results of calculations.

User manual will be included as an addendum into a final report.

References

[1] A. Lavrentev, I.Meshkov “The computation of electron cooling process in a storage ring”, preprint JINR E9-96-347, 1996.

[2] F. Hinterberger, D.Prasuhn, Analysis of internal target effects in light ion storage ring, NIM A 279(1989), 413-422

[3] COSY Annual report, 1997.

[4] P.Zenkevich et al., Modeling of electron cooling by Monte-Carlo method, to be published.

[5] A.Piwinski, Proc. 9th Int. Conf. on High Energy Accelerators, p. 105, 1974.

[6] M. Martini “Intrabeam scattering in the ACOOL-AA machines”, CERN PS/84-9 AA, Geneva, May 1984.

[7] N.Madsen, D.Moehl at al, Equilibrium beam in the Antiproton Decelerator (AD), NIM A (20000, 54-59.

[8] A.Wolf, et al., Recombination in electron coolers, NIM A 441(2000), 183

[9] I.N.Meshkov, Fiz. Elem. Chastits At. Yadra 25 (1994) 1487 [Engl. transl. Phys.Part.Nucl.25 (6) (1994) 631].

[10] V.Parkhomchuk, New insights in the theory of electron cooling, NIM A 441 (2000), 9-17.

[11] A.Sidorin, I.Meshkov, T.Katayama, P.Zenkevich. Ion Bunch Stability in the Double Storage Ring. RIKEN-AF-AC-19, February 2000.
[12] I.Meshkov, Electron cooling with circulating electron beam in GeV energy range, NIM A 441(2000), p.255.

Annex II User manual for BETACOOL program

A.Sidorin, A.Smirnov, G.Trubnikov

Contents

Introduction 2
1. The BETACOOL files 3
2. Main form 4
3. Main menu → File 6
3.1. File→ Open 6
3.2. File→ Save 6
3.3. File→ Save as 6
3.4. File→ Save On Exit 7
3.5. File→ Save DeskTop 7
3.6. File→ Graf as Data 7
3.7. File→ Open Dialog 7
3.8. File→ Exit 7
4. Main menu → Parameters 8
4.1. Parameters→ Ring 8
4.2. Parameters→Beam 11
4.3. Parameters→Beam evolution 13
4.4. Parameters→ Load Lattice 14
5. Main menu → Effects 16
5.1. Effects→ ECool 16
5.1.1. Tab sheets **Cooler parameters** and **Lattice functions** 17
5.1.2. Tab sheet **Friction force** 17
5.1.3. Tab sheet **Calculation parameters** 23
5.1.4. Menu item **Circulating electron beam** 24
5.1.5. Effects→ ECool→ Circulating electron beam→ Show temperature button 25
5.2. Effects→ IBS 25
5.3. Effects→ RestGas 26
5.4. Effects→ Stochastic 26
5.5. Effects→ Target 27
5.5.1. **Target** form 27
5.5.2**. Target material** form 28
5.6. Effects→ Injection 29
5.7. Effects→ External heating 30
6. Main menu → Task 31
6.1. Task→ Rates 31
6.2. Task→ Dynamics 32
7. Main Menu→ Tools 35
8. Graphics and process parameters 37
8.1. 2D graph 37
8.2. 3D graph 40
8.3. Process control 42

Introduction

BETACOOL program developed on the base of **BOLIDE** system using C++ Builder 4 is the **Windows 9x/NT** application dedicated to calculate an ion beam parameter evolution in a storage ring under the common action of different heating and cooling effects. The description of the physical model using in the calculation is in the ref. 1. All the parameters and references to the formulae in this manual are described in accordance with [1]. The tools of the **BOLIDE** system and **Windows** for loading and saving data to hard disk, for output the data into two and tree dimensional plots during the calculations and for controlling the calculation process, are used.

BOLIDE (Beam Optics Library & Interface Development Environment) is the kit of program modules, developed for quick creation of new applications in Borland C++ Builder3 under Windows95/98/NT in physical and mathematical applications. The main task of this pack is relief of functioning (working) the physicists and mathematicians during creation of new programs. Herewith as ready modules are such possibilities like creation of 2d- and 3d-graphs, management by parallel processes, loading and saving of data into files, that with the power of visual applications development in the ambience of Borland C++ Builder3 allows quickly to create and easy develop program software. More detail information you can get in the LEPTA web site **http://nuweb.jinr.ru/~lepta/bolide.htm**

To start the calculations with **BETACOOL** please follow next steps:
- start the **BetaCool.exe** file;
- load input parameters from ***.eta** file and modify them if necessary using the menu items **Parametrs** and **Effects**;
- load the ion ring lattice parameters from ***.lts** file, which specification can be loaded from the ***.llf** file;
- specify the effects taken into account in the calculations in the visual form **Rates**;
- input the step of the integration over the time in the visual form **Dynamics**;
- start the calculations using the button **Run** in the visual form **Dynamics**;
- the results of the calculations are presented in the visual form **Beam parameters** (time dependencies of general ion beam parameters) and in the visual form **Rates** (time dependencies of characteristic times).

To stop the calculations click the button **Stop** in the visual form **Dynamics**.

The calculations results can be saved in the graphic format using the buttons combination **Alt-PrintScreen**, or in the text format – using the graphic interface, which is described in the chapter 8 of this manual.

The edited file of input parameters can be saved with new name, or automatically saved with the same name after exit of **BetaCool.exe** file.

The manual includes description of all visual forms of the **BETACOOL** program, all input parameters using in calculations, the tools for graphic and calculation process control elaborated in the frame of **BOLIDE** system.

1. The BETACOOL files

Executed file of the program

BetaCool.exe (1.14 Mb)

requires for its work only standard **Windows** libraries.

Input parameters for calculations are presented in the text format file. The program does not check extension of the input file and in principle the extension can be arbitrary. During the load and save processes the file of parameters in the “Open” and “Save as” windows the files in the current directory with extension ***.eta** are automatically indicated. If you save a file without specification of file extension the program automatically generates the extension ***.eta**.

When program starts the file

Betacool.eta

is automatically loaded if exists in the current directory. When the file loaded all the editing windows in all the form of the program are filled with the data from input file. Modifying the existing file and saving it with new name one can generate new input file.

The files

Betacool.grf, Betacool.srf

contain the parameters of all the plots in the program (scale of the axis, intervals and so on) and are automatically loaded when program starts. If these files do not exist in the current directory the plot parameters are generated automatically, and when the program has been closed these files are generated and saved in the current directory.

The file

Betacool.top

contains the status of all the forms of the program during the previous session.

The files with extension

***.lts, *.llf**

are used in the case of intrabeam rates calculation. File ***.lts** contains lattice parameters of the storage ring in text format and can be generated by different programs of particle dynamics simulation (for instance MAD). File ***.llf** contains specification of the ***.lts** file and must be generated by user in accordance with the format of using ***.lts** file.

All the files required by BETACOOL program (except the *.lts file) can be generated during the program work and only **BetaCool.exe file** is needed for operation, however it is more convenient to have all the files specified in this chapter.

2. Main form

Main form of the **BETACOOL** program is presented in Fig. 2.1. It contains the name of current file with parameters and **Main Menu**.

Fig. 2.1. Main form of the BETACOOL program.

Main menu:

Menu item **File** contains the following sub items:
Open
Save
Save as
Save On Exit
Save DeskTop
Graf as Data
Open Dialog
Exit

This item of menu is standard for all applications developed with **BOLIDE** system.

Menu item **Parameters** contains the following sub items:
Ring
Beam
Beam evolution
Load Lattice

It is intended for input general parameters of the storage ring (**Ring, Load Lattice**), ion beam parameters (**Beam)** and representation on the screen beam parameters in the graphic format during calculations (**Beam evolution**).

Menu item **Effects** contains the following sub items:
Ecool
IBS
RestGas
Stochastic
Target
Injection
External heating

Each sub item is intended for input the general parameters of corresponding cooling or heating effect used in the calculations.
Menu item **Task** contains the following sub items:
Rates
Dynamics

The sub item **Rates** is used for specification of the task, which is solved in the current calculation and visualisation in the graphic format the particle life time and heating or cooling rates for beam parameters.
The sub item **Dynamics** is used for input parameters of the numerical algorithm for beam parameter dynamics simulation and for control of the calculation process.

Menu item **Tools** contains the following sub items:
Calculator
Periodic Table
Constants
Game

The sub items are not used in the calculations directly, but can help in the preparation of the initial parameters. **Calculator** is the programming calculator with general algebraic functions. **Periodic Table** contains Mendeleev's Periodic Table of elements. **Constants** – the table of numerical values of a number of physical constants. **Game** is included into program especially for our Japanese colleges and presents the version of Ren Dzu game in the field 40x40.

3. Main menu → File

3.1. File→ Open

This sub item calls the standard **Windows** open dialog window (Fig. 3.1.).

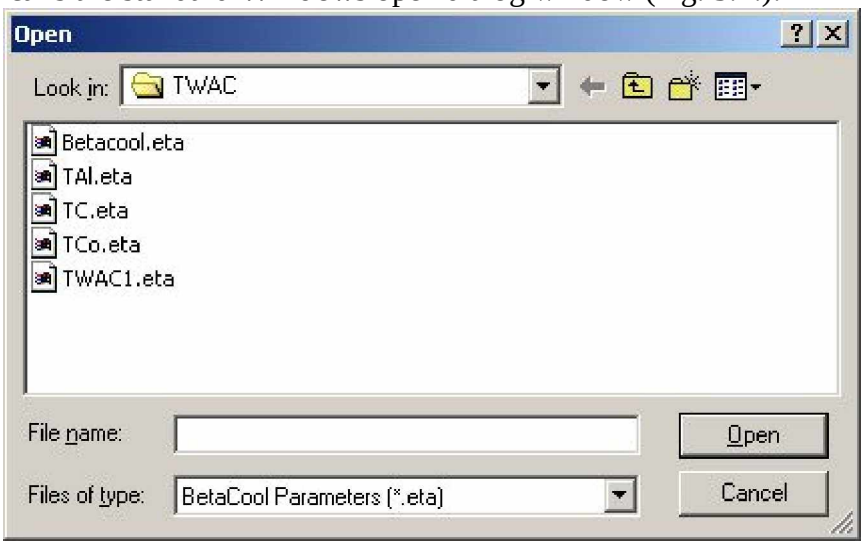

Fig. 3.1. Open dialog window.

Look in indicates the current directory.

File Name edit box is used for input the file name, or file name can be chosen from the list.

Files of type: default parameter is ***.eta** and it can be changed by **all types** or arbitrary extension.

3.2. File→ Save:

This sub item is used for saving of current parameters in the file, which name is indicated in the left corner of the main form (Fig. 2.1).

3.3. File→ Save as

This sub item calls the standard **Windows** save dialog window (Fig. 3.2). All the parameters are the same as in chapter 3.1.

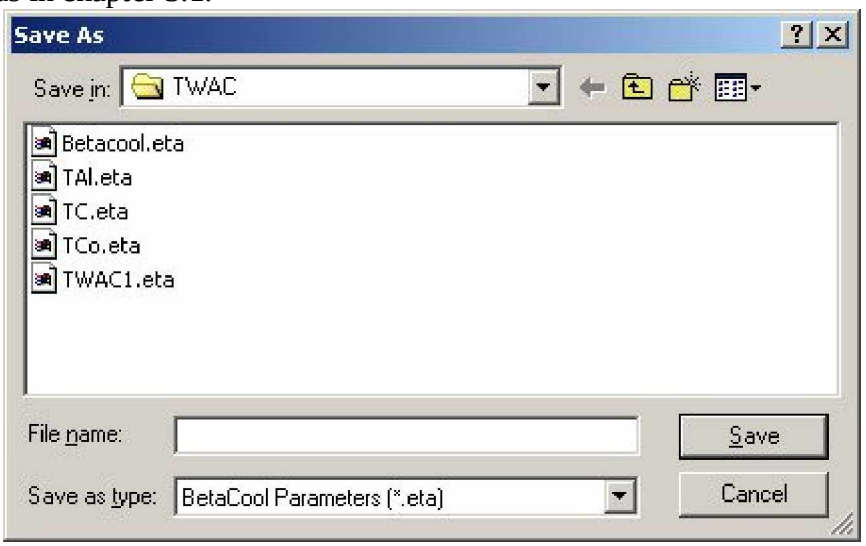

Fig. 3.2. Save dialog window.

3.4. File→ Save On Exit

If this sub item is checked all the parameters are saved after exit in the file, which name is indicated in the left corner of the main form (Fig. 1).

3.5. File→ Save DeskTop

If this sub item is checked the current positions and parameters of all the forms of the program are saved in the file **Betacool.top.**

Note: when the visual form parameters are not correct you need to delete the **Betacool.top** file in the directory where the **BetaCool.exe** is located. After that the default parameters will be used for all the forms and after exit the **BETACOOL** new file **Betacool.top** will be generated automatically.

3.6. File→ Graf as Data

When this sub item is checked the parameters of 2D and 3D plots are saved in the files, which names coinside with the name of curren ***.eta** file after exit of the program. At the next run of the program these files will be loaded with corresponding ***.eta** file.

3.7. File→ Open Dialog

If this sub item is checked the **open dialog window** (chapter 3.1) is called at the beginning of the program work.

3.8. File→ Exit

Exit from the program.

4. Main menu → Parameters:

4.1. Parameters→ Ring

This sub item calls the form for input the storage ring parameters (Fig. 4.1).

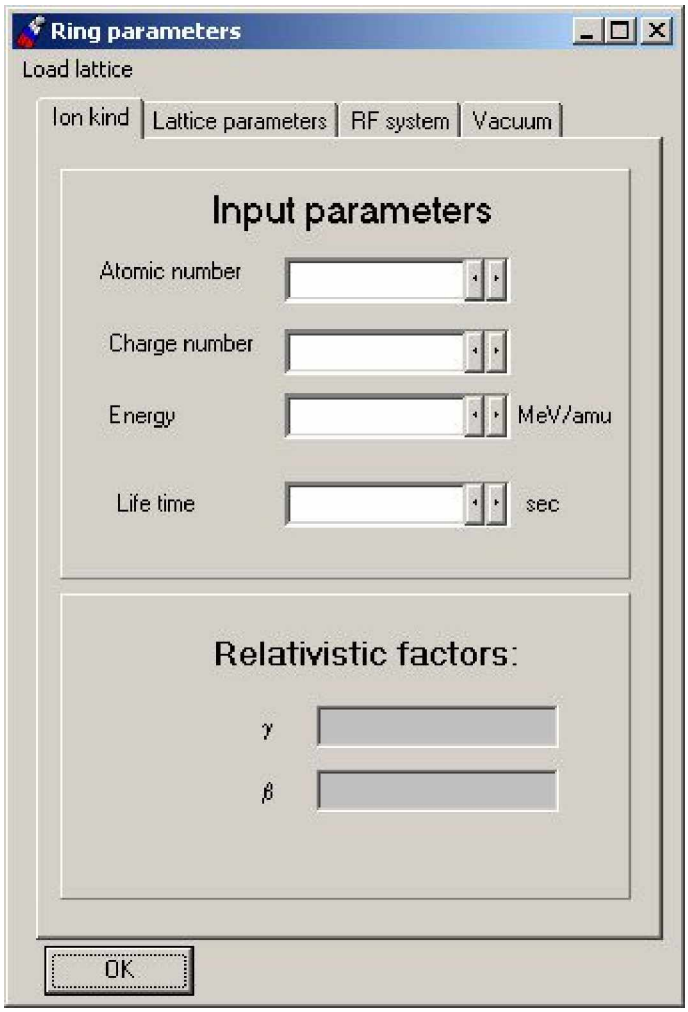

Fig. 4.1. Form for input the storage ring parameters

The form contains four tab sheets:
Ion kind
Lattice parameters
RF system
Vacuum
and menu item **Load Lattice.**

The menu item calls the same form as the main menu sub item **Parameters→Load Lattice** and it is described in the chapter 4.4.

The tab sheet **RF system** is visible only in the case when in the **Beam Parameters** form (Fig. 4.2) the option **Bunched** is chosen.

The parameters indicated in the edit boxes of the **Ring Parameters** form are specified in the tables 4.1 – 4.4.

Table 4.1. Tab sheet **Ion kind**			
Input parameters			
Atomic number	A		Ion atomic number
Charge number	Z		Ion charge number
Energy	E	Mev/Amu	Ion energy
Life time	τ_{life}	sec	Life time of the radioactive ion that is used in the calculation when the process **Decay** is chosen in the list of the processes in the form **Rates** (chapter 6.1)
Relativistic factors			
gamma	γ		The usual relativistic factors – output parameters
beta	β		

*Table 4.2. Tab sheet **Lattice parameters***			
Input parameters			
Circumference	C	m	Ion ring circumference
Gamma transition	γ_{tr}		Lorenz factor corresponded to transition energy
Horizontal Q	Q_x		Horizontal betatron tune
Vertical Q	Q_z		Vertical betatron tune
Horizontal Acc	A_x	[m*rad]	Horizontal and vertical acceptances that are used for particle losses calculation in accordance with ref.1 chapter 1.2, when the option **Beam scrapers** is chosen in the **Dynamics** form (chapter 6.2.)
Vertical Acc		[m*rad]	
Horizontal Hromaticity	ξ_x		Horizontal and vertical hromaticities are used for tune spread calculation (formula 5.1 in ref. 1)
Vertical Hromaticity	ξ_z		
Mean ring parameters (output parameters)			
Radius	R	m	The mean ring parameters are used for intrabeam rates calculation in accordance with chapter *2.2.1.* ref.1, when the option **Piwinski** is chosen in the **Intra Beam Scattering** form (chapter 5.2)
Horizontal beta function	β_x	m	
Vertical beta function	β_z	m	
Dispersion	D	m	
Revolution period	T_{rev}	Sec	
Off momentum factor	η		$1/\gamma^2 - 1/\gamma_{tr}^2$

*Table 4.3. Tab sheet **RF system***			
Input parameters			
Harmonic number	q		Are used for synchrotron tune calculation (formulae 5.6, 5.7 in ref. 1)
RF voltage	U	kV	
Calculated parameters			
Separatrix length	l_{sep}	m	$l_{sep} = C/q$
Synchrotron tune	Q_s^0		Formula 5.7 in ref. 1.

*Table 4.4. Tab sheet **Vacuum***			
Input parameters			
Mean chamber radius	b	cm	Is used for calculation of longitudinal form factor G_L, chapter 5 in ref. 1.
Pressure	P	Torr	Residual gas pressure
Residual gas composition			
$\%_1$	n_1/n_0	%	It is assumed that residual gas composition includes three kinds of atoms
$\%_2$	n_2/n_0	%	
$\%_3$	n_3/n_0	%	
A_1			
A_2			
A_3			
Z_1			
Z_2			
Z_3			
Calculated parameters			
SS density	n_{ss}	$1/sm^3$	Formula 3.2.4 in ref. 1.
MS density	n_{ms}	$1/sm^3$	Formula 2.3.2 in ref. 1.

4.2. Parameters→Beam

This sub item calls the form for input the storage ring parameters (Fig. 4.2).

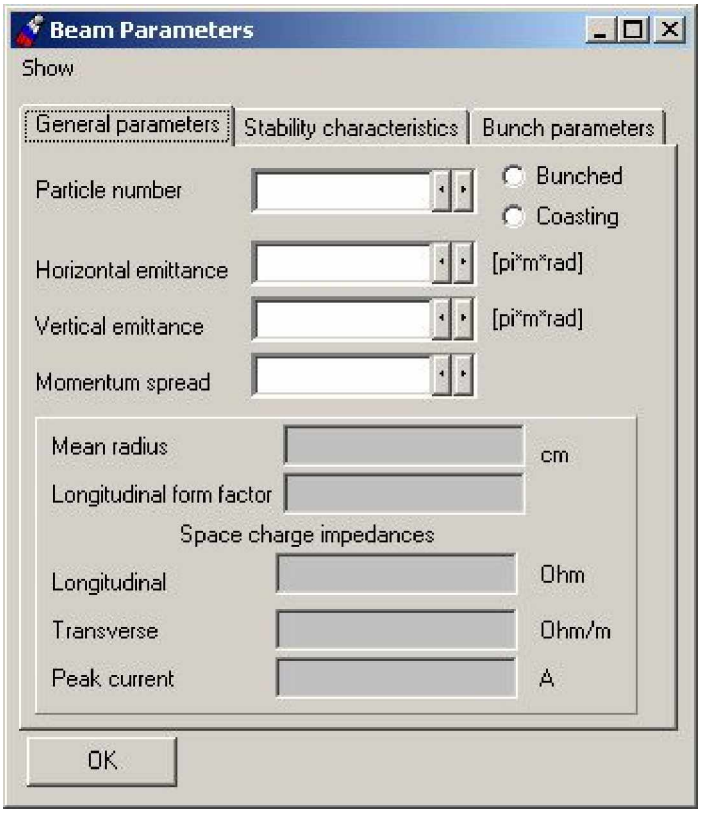

Fig. 4.2. The form for input the storage ring parameters.

The form contains three tab sheets:

General parameters
Stability characteristics
Bunch parameters
and menu item **Show.**

The menu item **Show** calls the same form as the main menu sub item **Parameters→Beam evolution** and it is described in the chapter 4.3.

The tab sheet **Bunch parameters** is visible only in the case when the option **Bunched** is chosen.

The parameters indicated in the edit boxes of the **Beam Parameters** form are specified in the tables 4.5 – 4.7.

Table 4.5. Tab sheet **General parameters**			
Particle number	N		Number of ions, in the case of bunched beam – number of particles in the bunch
Horizontal emittance	ε_x	[π·m·rad]	"Two sigma" emittances: $\sigma = \sqrt{\frac{\varepsilon\beta}{2}}$, σ is standard deviation
Vertical emittance	ε_z	[π·m·rad]	
Momentum spread	σ_p		R.m.s. momentum spread
Calculated parameters			
Mean radius	*a*	cm	Mean beam radius is used for calculation of longitudinal form factor G_L, chapter 5 in ref. 1.
Longitudinal form factor	G_L		chapter 5 in ref. 1.
Space charge impedance			
Longitudinal	Z_L	Ohm	Is used for "Keil-Schnell" criterion calculation (formula 5.2 in ref. 1)
Transverse	Z_t	Ohm/m	Is used for "Schnell-Zotter" criterion calculation (formula 5.2 in ref. 1)
Peak current	I_{max}	A	Is calculated taking into account bunching factor, for coasting beam it is equal to mean value

Table 4.6. Tab sheet **Stability characteristics**

Image force correction factor			Is used for tune shift calculation [2], if this effect is not taken into account the image force correction factor is to be equal 1
Tune shift	ΔQ		Formula 5.1 in ref. 1
Factor of distribution function (for Keil-Schnell Fl = 1)	F_L		Is used for "Keil-Schnell" criterion calculation (formula 5.2 in ref. 1)
Longitudinal coupling impedance	Z_L	Ohm	This value is added to space charge longitudinal impedance
Microvawe instability			Formula 5.2 in ref. 1
Tune spread for first mode	ΔQ_n		Is used for "Schnell-Zotter" criterion calculation (formula 5.2 in ref. 1)
Factor of distribution function Ft	F_t		Is used for "Schnell-Zotter" criterion calculation (formula 5.2 in ref. 1), for standard criterion it is equal to 1.
Transverse coupling impedance	Z_t	Ohm/m	This value is added to space charge transverse impedance
Dipole instability			Formula 5.4 in ref. 1

Table 4.7. Tab sheet ***Bunch parameters***			
Number of bunches			Number of bunches in the bunched beam
Calculated parameters			
RMS bunch length	σ_s	cm	Is calculated in accordance with formula 5.8 in ref. 1 without taking into account the synchrotron tune depression
Maximum particle number	N_b^{max}		Formula 5.6 in ref. 1
Synchrotron tune	Q_s		Formula 5.5 in ref. 1
Bunching factor	B_f		

4.3. Parameters→Beam evolution

This sub item calls the form for output the beam parameters in the graphic format (Fig. 4.3). This form can be called also by the menu item **Show** in the **Beam Parameters** form.

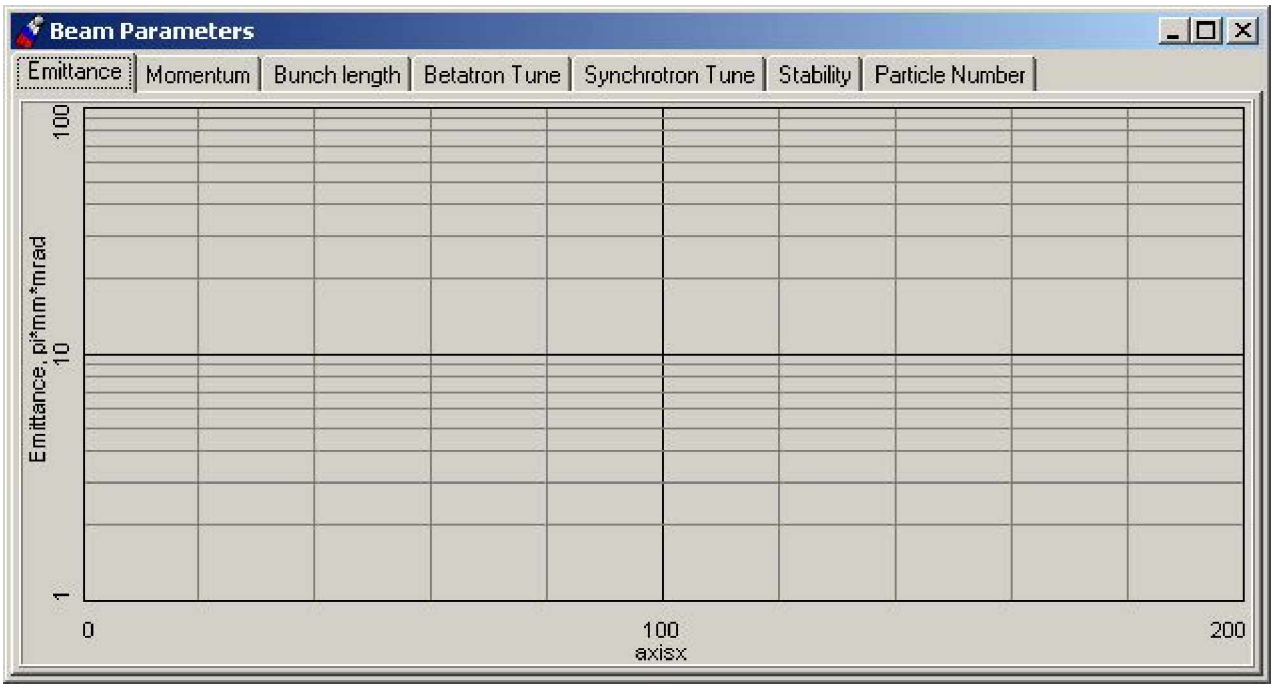

Fig. 4.3. The form for output the beam parameters in the graphic format.

The form includes 7 tab sheets:
Beam parameters→Emittance,
Beam parameters→Momentum,
Beam parameters→Bunch length,
Beam parameters→Betatron tune,
Beam parameters→Synchrotron tune,
Beam parameters→Stability,
Beam parameters→Particle number.

The tab sheets **Bunch length** and **Synchrotron tune** are visible only in the case when in the **Beam Parameters** form (Fig. 4.2) the option **Bunched** is chosen.

The 2D graphics are used for output the time dependencies of the general beam parameters. The **Bunch length** and **Synchrotron tune** are calculated taking into account the synchrotron tune depression due to the beam space charge (Formulae 5.5 and 5.8 in ref.1). The **Stability** presents the values calculated in accordance with the formulae 5.2, 5.3 in ref. 1.

To edit the plot parameters one need push the right button of the mouse when the cursor position is over the corresponding plot. The description of the graphic control interface is given in chapter 8.

Left mouse double click when the cursor position is over the plot region opens corresponded plot in the separate window.

4.4. Parameters→ Load Lattice

This sub item calls the form for input and visualisation of the ring lattice parameters required for intrabeam scattering calculation (Fig. 4.4). This form can be called also by the menu item **Load Lattice** in the **Ring parameters** form.

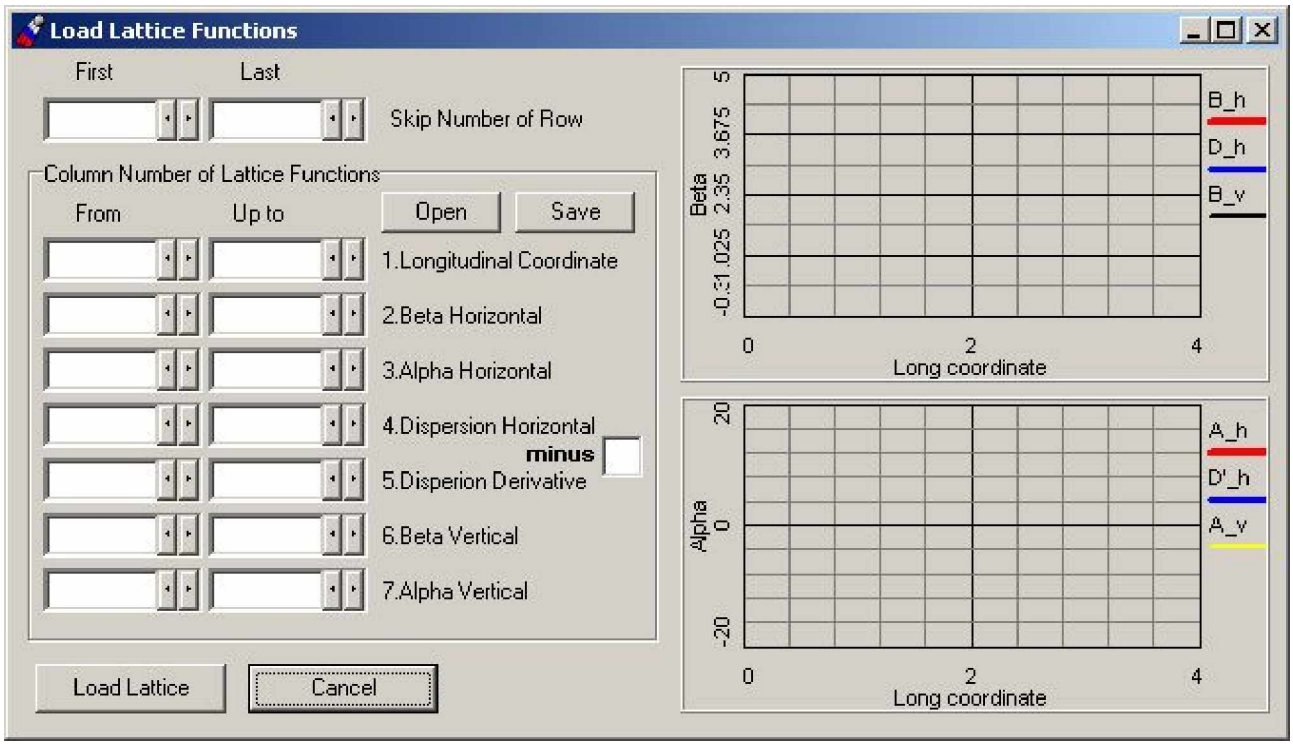

Fig. 4.4. The Load Lattice Form.

All the data from edit windows are saved in the ***.eta** file and then are filled after load of ***.eta** file.

The buttons **Open** and **Save** at the panel **Column Number of Lattice Functions** are related to the ***.llf** files. If the same format of ***.lts** file is used in the calculations the load of ***.llf** file is not necessary.

The file *.llf contains the **Skip Number of Row**, **Column Number of Lattice Functions** and **minus** parameters in the text format.

The file with lattice parameters ***.lts** has to contain in the text format the table of the longitudinal position of the point in the ring and lattice functions in this point. Position in the string of each element of the table has to be fixed (it is usually takes place for output file of FORTRAN programs). The file can also include the strings with comments below and after the table of lattice parameters. In this case this strings are skipped when file is loaded, and number of string to be skipped are inputted in the edit windows **First** (number of strings below the table) and **Last** (number of strings after the table) in the **Skip Number of Row** position.

The table in the **Load Lattice Functions** form **Column of Lattice Functions** contains specification of the ***.lts** file. **From** contains the number of initial position minus 1 of the corresponding lattice parameter. The column **Up to** – the number of last position minus 1.

The edit window **minus** at the panel **Column Number of Lattice Functions** is used only in the specific case of the lattice calculation with MAD program and usually this value is to be equal to 1. (The dispersion function is multiplied with this value).

In the case when there is incorrect symbol in the range of positions between **From** to **Up to, BOLIDE** system generates the **Warning window** Fig. 4.5.

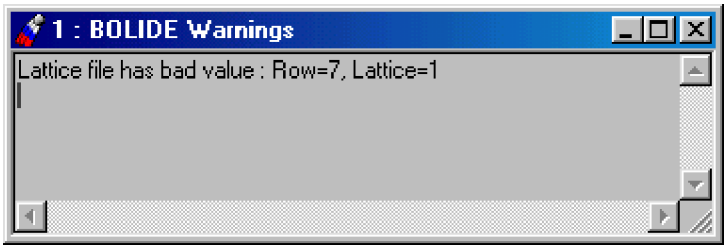

Fig. 4.5. Warning window.

The parameter **Row** indicates the string number with incorrect symbol, parameter **Lattice** indicates the parameter number in accordance with numbering at the **Column Number of Lattice Functions** panel. In the case of warning one need to correct the numbers in the edit windows **From** and (or) **Up to** in the corresponding string of the **Column Number of Lattice Functions** panel.

When the lattice parameters are loaded successfully the plots of corresponding lattice functions versus longitudinal co-ordinate in meters are outputted in the 2D plots in the right part of the form.

Using the button **Save** at the **Column Number of Lattice Functions** panel one can save current numbers in the edit windows of the form in a ***.llf** file.

5. Main menu → Effects:

5.1. Effects→ ECool

This sub item calls the form for input and analysis of electron cooling system parameters (Fig. 5.1).

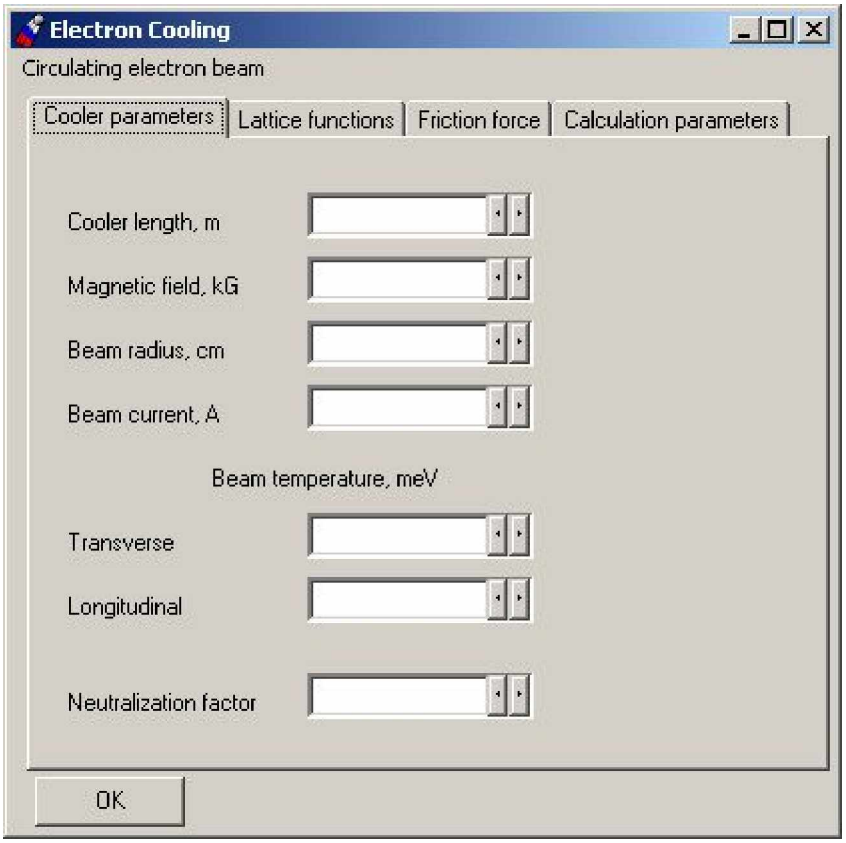

Fig. 5.1. The **Electron Cooling** form, tab sheet **Cooler parameters**.

Form contains four tab sheets:

Cooler parameters,
Lattice functions,
Friction force,
Calculation parameters

and menu item **Circulating electron beam.**

Main goal of the **BETACOOL** is calculation of the beam dynamics in the presence of electron cooling and this part of the program gives additional tools for analysis and optimisation of the electron cooling system. The calculations can be performed using different models of the cooling process. The components of the friction force used in the calculations can be presented as 3D graph. For electron cooling system with circulating electron beam the time dependence of the electron beam temperature during the circulation is presented as 2D graph.

5.1.1. Tab sheets **Cooler parameters** and **Lattice functions**

General cooler parameters from the tab sheet **Cooler parameters** (Table 5.1).

Table 5.1. ***Cooler parameters***

Coller length	L	m	
Magnetic field	B	kG	
Beam radius	a_e	cm	
Beam current	I	A	
Beam temperature, meV			
Transverse	$T_{\|}$	meV	
Longitudinal	$T_{\perp}$	meV	
Neutralization factor	η_n		

The ring lattice parameters in the cooling section from the tab sheet **Lattice functions** (Table 5.2).

Table 5.2. ***Lattice functions***

Horizontal			
Beta	β_x	m	Is used for calculation of the variation of the motion invariants after single pass the cooling section in accordance with formula 4.2.3 in ref. 1
Alpha	α_x		
Dispersion	D	m	
Dispersion derivative	D'		
Vertical			
Beta	β_z	m	Is used for calculation of the variation of the motion invariants after single pass the cooling section in accordance with formula 4.2.4 in ref. 1.
Alpha	α_z		

5.1.2. Tab sheet **Friction force**

The deviation of the particle angular spread when passed the cooling section is calculated only in the case, when particle distance from electron beam centre is less than electron beam radius, and is equal

$$\Delta\theta = \Delta \cdot \Phi(\theta^*),$$

$$\text{where } \Delta = K\frac{2r_p}{\beta^5\gamma^5}\frac{Z^2}{A}\frac{l}{a^2}\frac{eI}{m_e c^3} = 1.8\cdot 10^{-9} K\frac{Z^2}{A}\frac{I_{[A]}}{\beta^5\gamma^5}\frac{l_{[m]}}{a^2_{[cm]}}[mrad],$$

where $\Phi = \{\Phi_x, \Phi_z, \Phi_s\}$ is calculated by using one of the following formulae:

Flattened non magnetized
Derbenev-Skrinsky
Parkhomchuk

The formulae are not presented in ref 1, and here we introduce short description of them.

5.1.2.1. **Derbenev-Skrinsky** formulae

$$\overset{\circ}{\Phi}_{x,z}(\theta^*) = \begin{cases} (2L_F + k_{x,z}L_M)\dfrac{\theta^*_{x,z}}{\theta^3}, & \{I\} \\ 2(L_F + N_{col}L_A)\dfrac{\theta^*_{x,z}}{\theta_\perp^3} + k_{x,z}L_M\dfrac{\theta^*_{x,z}}{\theta^3}, & \{II\} \\ 2(L_F + N_{col}L_A)\dfrac{\theta^*_{x,z}}{\theta_\perp^3} + L_M\dfrac{\theta^*_{x,z}}{(\theta_{II}/\gamma)^3}, & \{III\} \end{cases} \tag{5.1}$$

$$\overset{\circ}{\Phi}_{s}(\theta^*) = \begin{cases} (2L_F + k_sL_M + 2)\dfrac{\theta^*_s}{\theta^3}, & \{I\} \\ 2\operatorname{sgn}\theta^*_s\cdot(L_F + N_{col}L_A)\dfrac{\gamma}{\theta_\perp^2} + (k_sL_M + 2)\dfrac{\theta^*_s}{\theta^3}, & \{II_a\} \\ 2(L_F + N_{col}L_A)\dfrac{\theta^*_s}{\theta_\perp^2\theta_{II}/\gamma} + L_M\dfrac{\theta^*_s}{(\theta_{II}/\gamma)^3}, & \{II_b + III\} \end{cases} \tag{5.2}$$

Domains *I*, *II* = II_a +II_b, and *III* are shown in Fig. 5.2.
Coulomb logarithms are defined by the formulae

$$L_M = \ln\frac{R}{2\langle\rho_\perp\rangle},\ L_A = \ln\frac{2\langle\rho_\perp\rangle}{\rho_F},\ L_F = \ln\frac{\rho_F}{\rho_{\min}}. \tag{5.3}$$

Note that if argument of a logarithm is less than 1, then the logarithm value is set to zero. The other parameters are

$$R = \min\left\{\sqrt{(V_x^2 + V_z^2 + V_s^2)\frac{m_e}{4\pi n_e e^2}},\quad \sqrt[3]{\frac{3Z}{n_e}}\right\} =$$

$$= \min\left\{0.06535a\theta\sqrt{\frac{\beta^3\gamma^3}{I}},\quad 0.00355\sqrt[3]{\frac{\beta\gamma a^2 Z}{I}}\right\} \text{ - the maximal impact parameter;} \tag{5.4}$$

$$\langle\rho_\perp\rangle = \frac{\beta\gamma\theta_\perp mc^2}{eB} = \frac{1.7\cdot10^{-3}\beta\gamma\theta_\perp}{B} \text{ - the Larmor radius of electron;} \tag{5.5}$$

$$\rho_F = \langle\rho_\perp\rangle\frac{|\theta + \theta_{II}/\gamma|}{\theta_\perp} \text{ - the intermediate impact parameter;} \tag{5.6}$$

$$\rho_{\min} = \frac{Ze^2}{m_e}\frac{1}{\beta^2\gamma^2(\theta + \theta_\perp)^2} =$$

$= 2.818 \cdot 10^{-7} \dfrac{Z}{\beta^2 \gamma^2 (\theta + \theta_\perp)^2}$ - the minimal impact parameter; (5.7)

$N_{col} = 1 + \left[\dfrac{\theta_e}{\pi \left| \theta + \theta_{II} / \gamma \right|} \right]$ - the number of multiple collisions; (5.8)

$k_{x,z} = 1 - 3 \left(\dfrac{\theta_s^*}{\gamma \theta} \right)^2$, $k_s = 2 + k_x$. (5.9)

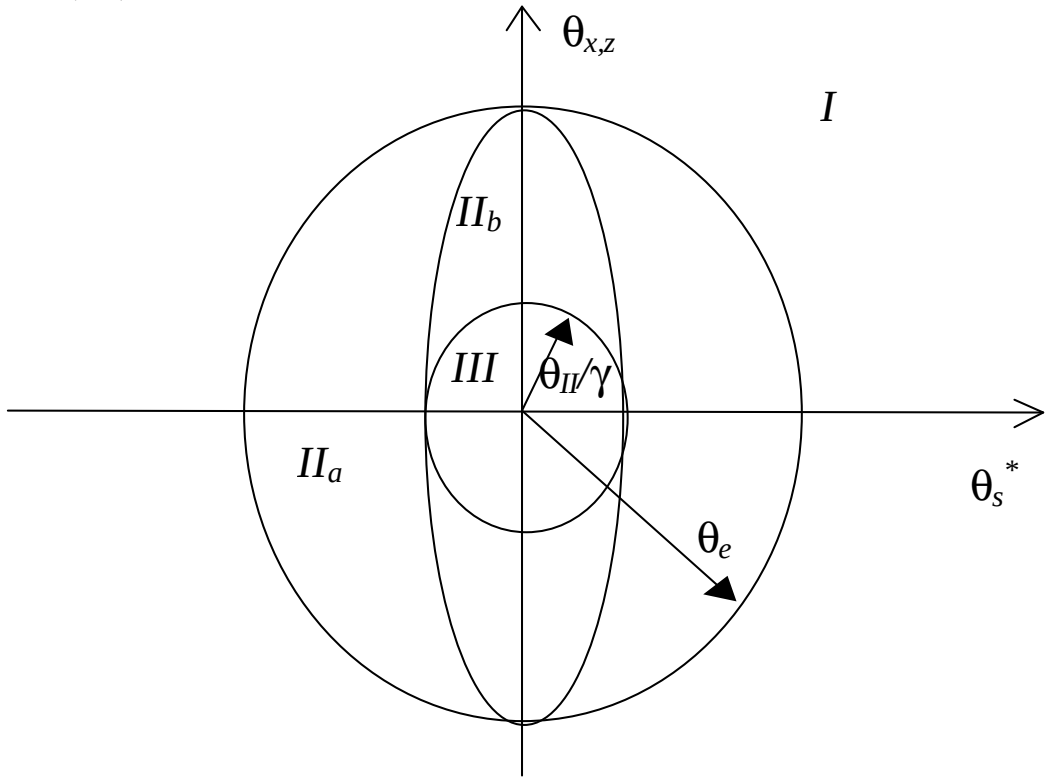

Figure 5.2: Domains in the velocity space in PRF for $\Phi(\theta^*)$.
$v_\perp$, v_{II} are electron velocity components in PRF.

5.1.2.2. **Flattened Non magnetized** friction force

$$\Phi_{x,z}(\theta^*) = \begin{cases} 2L_C \dfrac{\theta^*_{x,z}}{\theta^3}, & \{I\} \\ 2L_C \dfrac{\theta^*_{x,z}}{\theta_\perp^3}, & \{II\} \\ 0, & \{III\} \end{cases} \quad (5.10)$$

$$\Phi_s(\overset{\circ}{\theta}^*) = \begin{cases} 2L_F \dfrac{\theta_s^*}{\theta^3}, & \{I\} \\ 2\,\mathrm{sgn}\,\theta_s^* L_F \dfrac{\gamma}{\theta_\perp^2}, & \{II\} \\ 2L_C \dfrac{\theta_s^*}{\theta_\perp^2 \theta_{II}/\gamma}, & \{III\} \end{cases} \tag{5.11}$$

5.1.2.3. **Parkhomchuk** formulae

$$\overset{\circ}{\Phi}(\overset{\circ}{\theta}) = \frac{2}{\pi} L_P \frac{\theta}{\sqrt{\theta^2 + V_{effe}^2}^3} \tag{5.12}$$

$$L_P = \ln\left(\frac{R_{\max} + \langle \rho_\perp \rangle}{\rho_{\min} + \langle \rho_\perp \rangle}\right) \tag{5.13}$$

5.1.2.4. Electron beam space charge

For all the formulae angular and momentum spread of electrons are calculated taking into account self-field of the electron beam:

$$\theta_\perp = \frac{1}{\beta\gamma}\sqrt{\frac{T_\perp}{m_e c^2}} = \frac{1.4003}{\beta\gamma}\sqrt{10^{-3} T_{\perp[meV]}}[mrad], \tag{5.14}$$

$$\theta_{II} = \frac{1}{\beta}\sqrt{\frac{e^2 n_e^{1/3} + T_{II}}{m_e c^2}} = \frac{1.4}{\beta}\sqrt{5.814\cdot 10^{-5}\left(\frac{I_{[A]}}{\beta\gamma a_{[cm]}^2}\right)^{1/3} + 10^{-3} T_{II[meV]}}[mrad], \tag{5.15}$$

$$\delta\theta_{II} = (1-\eta_n(r^*))\frac{eI}{\beta^3\gamma m_e c^3}\left(\frac{r^*}{a}\right)^2 = (1-\eta_n(r^*))\frac{I_{[A]}}{17\beta^3\gamma}\left(\frac{r^*}{a}\right)^2 [mrad], \tag{5.16}$$

The difference between particle velocity and electron beam one is calculated taking into account the momentum shift of the electron beam

$$\theta_s^* = \theta_s - (\theta_{II}^* + \delta\theta_{II}) \tag{5.17}$$

To exclude the electron beam space charge from the calculation the value of **Neutralization factor** in the tab sheet **Cooler parameters** is to be equal 1.

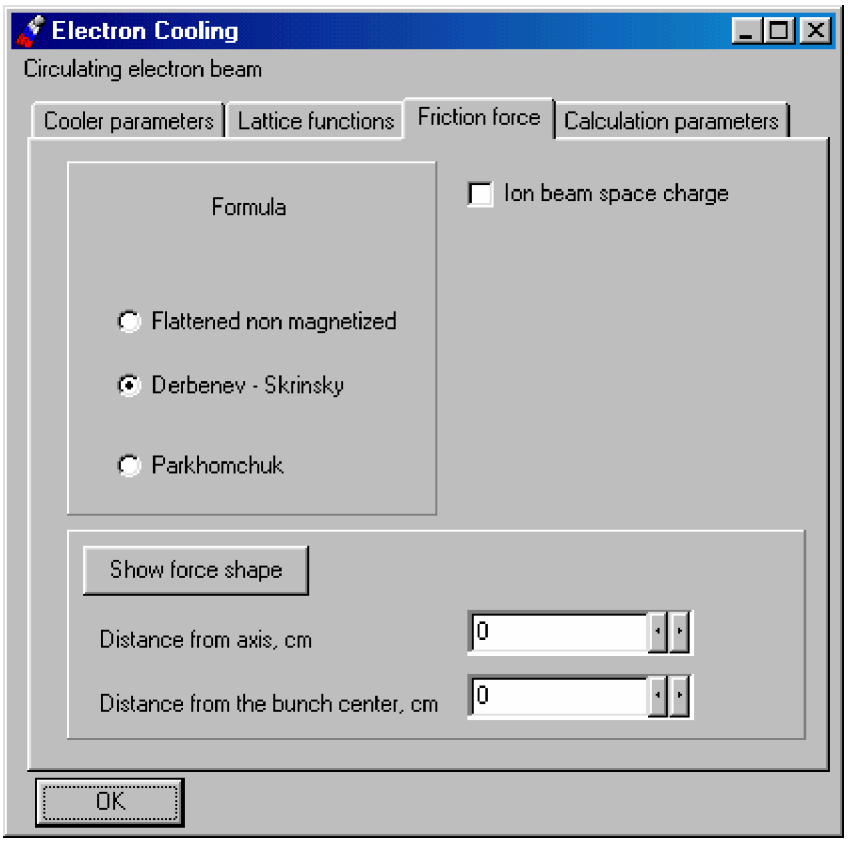

Fig. 5.2. The **Electron Cooling** form, tab sheet **Friction force**.

5.1.2.5. **Ion beam space charge**

The ion beam space charge is taken into account in accordance with the following model.

When the ion and electron beams merge in the cooling section, the kinetic energy of an electron changes according to its position inside the potential well of the ion beam space charge field. Let's suppose that we tune the particle initial energy so that the electron velocity is equal to the ion velocity when the electron comes to the center of the ion bunch. Then the momentum of the electrons varies across the beam in accordance with the following:

$$\left(\frac{\Delta p}{p}\right)_{s.c}^{e,i} = -\frac{2\lambda_i(s) r_e Z}{\beta^2 \gamma} F\left(\frac{r}{\sqrt{2}a_i}\right), \tag{5.18}$$

where $a_i = \sqrt{\frac{\varepsilon_x \beta_x + \varepsilon_z \beta_z}{2}}$ is the mean bunch radius, λ_i is ion linear density and *F(t)* is the function, which describes the ion beam potential distribution across the beam. When the beam density distribution across the beam is Gaussian, the function *F(t)* can be written as follows:

$$F(t) = \int_0^t \frac{1-\exp(-u^2)}{u} du, \; t = \frac{r}{\sqrt{2}a_i} \tag{5.19}$$

The effect (5.18) is calculated for two different longitudinal distribution of the ion beam density:

$$\lambda_i(s) = \begin{cases} \dfrac{N_b}{\sqrt{2\pi}\sigma_s} e^{\left(-\frac{s^2}{2\sigma_s^2}\right)}, & \textit{Gaussian bunch} \\ \dfrac{N}{C}, & \textit{coasting beam} \end{cases} \tag{5.20}$$

Another incoherent effect relates to the drift velocity of the electrons in the crossed longitudinal magnetic and bunch electric and magnetic fields. For Gaussian bunch the drift velocity can be calculated using the following formula:

$$\theta_d = \frac{eZ\lambda_i(s)}{\beta\gamma^2 B} F_2(r), \tag{5.21}$$

where B is the longitudinal magnetic field value and the bunch field radial dependence is given by the expression:

$$F_2(r) = 2\frac{1-\exp\left(-\dfrac{r^2}{2a_i^2}\right)}{r}. \tag{5.22}$$

The drift velocity can be included into calculation of the friction force as an addition the electron transverse velocity:

$$\theta_\perp = \sqrt{\theta_T^2 + \theta_d^2} \tag{5.23}$$

where θ_T is the electron angular spread corresponding to the thermo-velocity:

$$\theta_T = \frac{1}{\beta\gamma}\sqrt{\frac{T_\perp}{m_e c^2}}. \tag{5.24}$$

5.1.2.6. **Show force shape** button

For visualization of the deviation of the particle angular spread after passing the cooling section the form **Friction** is used (Fig. 5.3). Two tab sheets of the form contain 3D plots for output of transverse and longitudinal component of friction force in the unit “angular deviation of the ion after single crossing the cooling section”.

To output the friction force you need to specify co-ordinates of the ion (in which it crosses the cooling section) in the edit windows **Distance from axis** and **Distance from the bunch center** (both in cm) in the tab sheet **Friction force** and push the button **Show force shape.** The parameter **Distance from the bunch center** is required in the case of bunched ion beam when the parameter **Ion beam space charge** is checked.

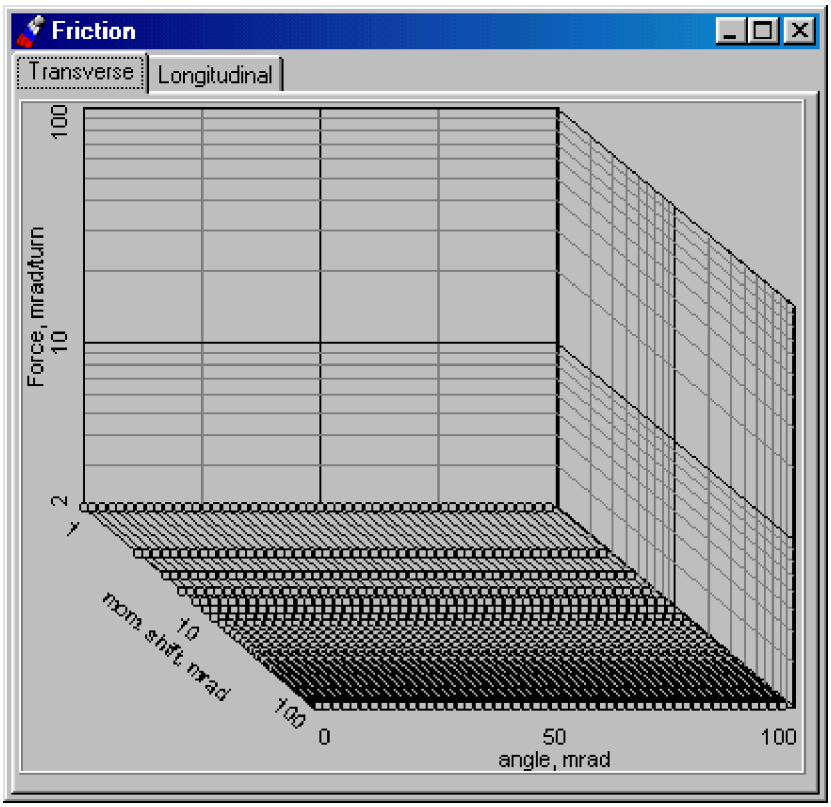

Fig. 5.3. The 3D plots of the friction force shape.

Note: The **Derbenev-Skrinsky** formula was used in the previous versions of the program. Other formulae were not well tested yet.

5.1.3. Tab sheet **Calculation parameters**

The parameters required for invariant deviation are inputted in the tab sheet **Calculation parameters** (Fig.5.4).

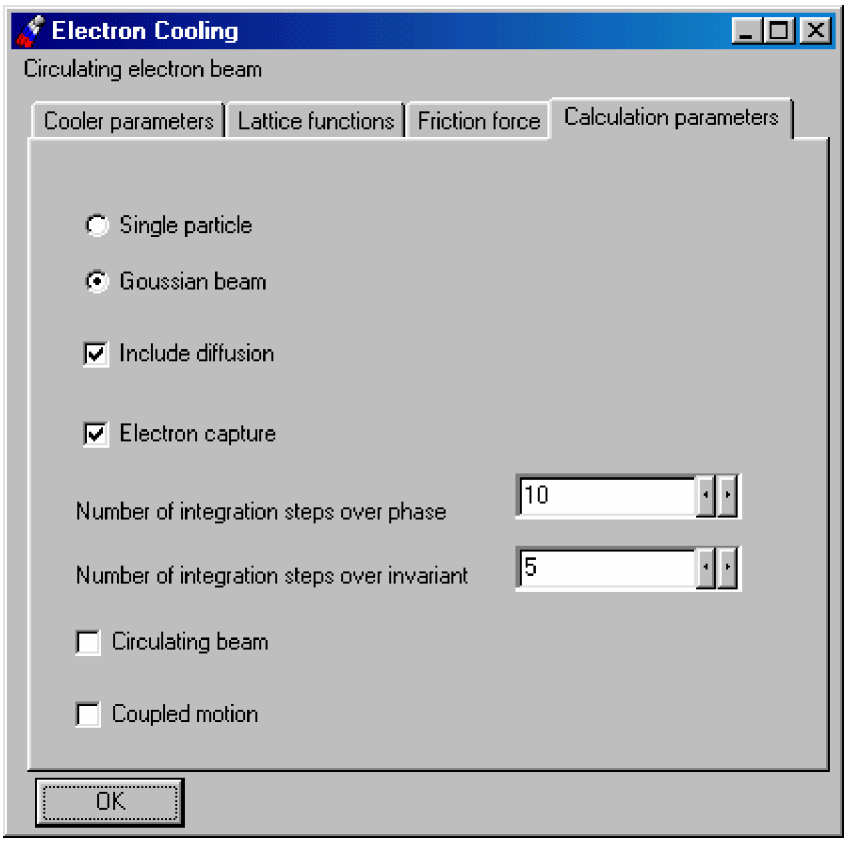

Fig. 5.4. The **Electron Cooling** form, tab sheet **Calculation parameters**.

The choice between

Single particle and
Gaussian beam

determines the regime of the friction force averaging.

The case **Single particle** corresponds to formula (4.2.6) for invariant deviation and formula (4.2.7) for cooling rate (ref. 1). In this case one need to input **Number of integration steps over phase** parameter, which is equal to number of divisions over betatron phase in the integral (4.2.6). In the case of bunched beam the same number of divisions is used for integration over the synchrotron phase. In the case of coasting beam deviation of longitudinal invariant is calculated through averaging the deviation at plus and minus r.m.s values.

The **Gaussian beam** corresponds to (4.2.8) and (4.2.9). In this case one need to specify **the Number of integration steps over invariant** parameter, which is equal to number of divisions over invariant in the integral (4.2.8).

When the parameter **Include diffusion** is checked the formulae (4.2.3) – (4.2.5) are calculated completely in the opposite case the terms proportional to square of ion angle deviation are excluded.

When the parameter **Circulating beam** is checked the cooling rates are calculated in accordance with chapter 4.2.2 of ref.1, and electron ring parameters are to be entered using menu item **Circulating electron beam** (see next chapter).

The parameter **Coupled motion** is not used in the calculations in this version of the program.

5.1.4. Menu item **Circulating electron beam**

In presented version of the program only the model corresponded to the model of magnetised electron beam with flattened velocity distribution is realised (chapter 4.2.2, ref. 1). Therefore the first two parameters in the form (Fig 5.5) –

Maxwelian plasma
Flattened distribution

are not used. Other parameters are listed in the Table 5.3.

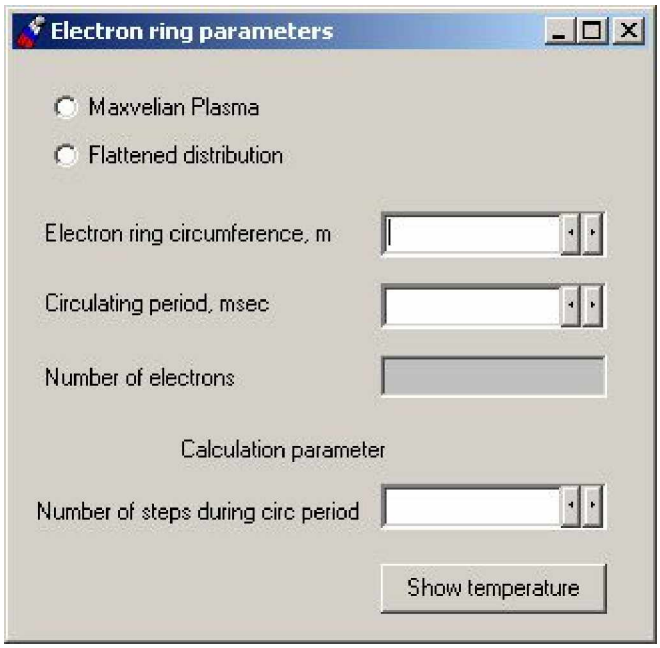

Fig. 5.5. The **Electron ring parameters** form.

Table 5.3. Electron ring parameters

Electron ring circumference	C	m	
Circulating period	T_{circ}	msec	
Number of electrons			output parameter $N_e = \frac{CI}{\beta c}$
Number of steps during circ. period	n		Is used in accordance with algorithm described in formulae (4.2.17) – (4.2.19) in ref. 1.

5.1.5. Effects→ ECool→ Circulating electron beam→ Show temperature button

With click on **Show temperature** button one can call the form **Electron temperature** (Fig.5.5) which presents the electron beam longitudinal and transverse temperature time dependencies during taken circulating period.

The calculation of the dependencies can take a long period of time, and they will be plotted only when the calculations finished.

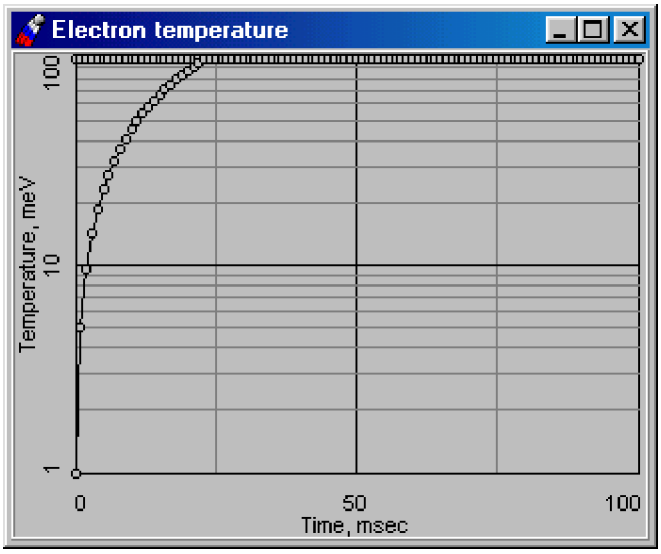

Fig. 5.5. The **Electron temperature** form.

5.2. Effects→ IBS

The form that dedicated to enter parameters required for Intra Beam Scattering rates calculation is presented in the Fig. 5.6.

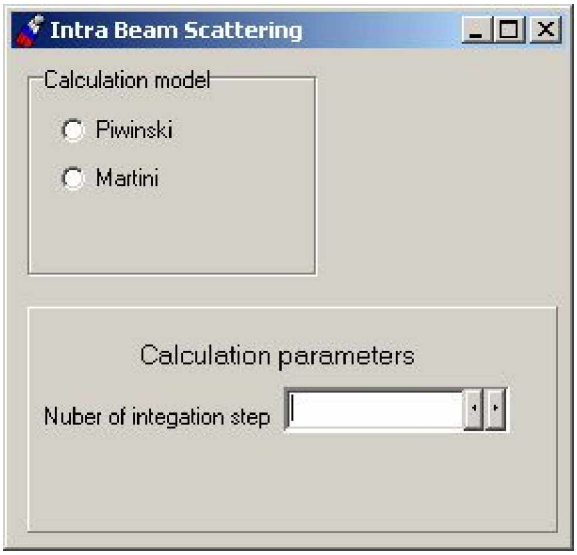

Fig 5.6. The Intra Beam Scattering form.

In the panel **Calculation model** you need to make a choice between two possibilities:

Piwinski - calculations are performed in accordance with chapter *2.2.1*, ref 1.
Martini - calculations are performed in accordance with chapter *2.2.2*, ref 1.

Number of integration step is calculation parameter, which specify the algorithm of numerical calculation of corresponding integrals.

5.3. Effects→ RestGas

The sub menu item **RestGas** calls the form **Scattering on gas** (Fig. 5.7.) where one can include inside the calculation following processes:

Single scattering (chapter **3.2.** in ref .1)
Nuclear scattering (chapter **3.1.** in ref .1)
Multiple scattering (chapter 2.3. in ref .1)
Electron capture.

For calculation of the single scattering process the ring acceptance is to be entered in the form **Ring parameters.**

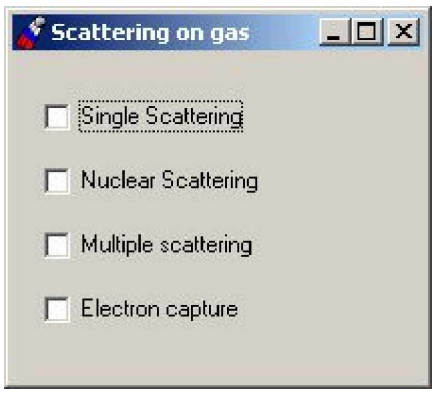

Fig. 5.7. The form **Scattering on gas.**

5.4. Effects→ Stochastic

For each degree of freedom of ion oscillation there is a corresponding tab sheet (Fig.5.8), where one need to enter

Lower frequency
Upper frequency

both in GHz.

Parameter **used** is to be checked in the case when corresponding chain of the stochastic cooling system is used in the calculations. The cooling rates are calculated in accordance with chapter 4.1.1, ref. 1.

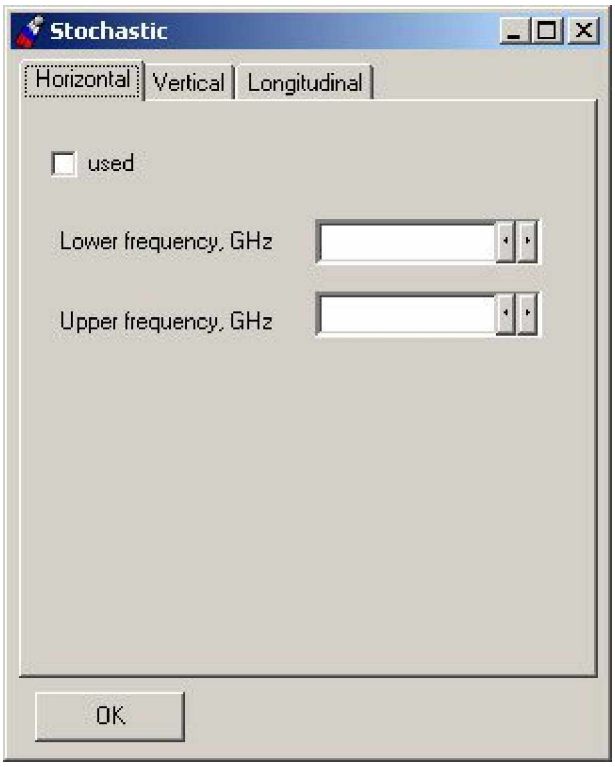

Fig. 5.8. The **Stochastic** form.

5.5. Effects→ Target

5.5.1. **Target** form

The **Target** form (Fig. 5.9) includes three tab sheets:

Target parameters
Lattice functions
Injection

and menu item **Target material.**

The tab sheet **Injection** is visible only when the parameter **Stripper foil** is checked. The menu item **Target material** calls the form **Target material** described in the next chapter.

The parameters of internal target are entered in the tab sheet **Target parameters (**Table 5.4) or calculated from the ion beam and parameters of the target from the **Target material** form.

Table 5.4. **Target parameters**			
Energy losses	E_{str}	eV	are used for calculations of formula (2.1.1) ref.1
Stripping angle	θ_{str}	rad	
Momentum spread	$\Delta p/p_{\text{target}}$		
Life time	τ_t	sec	is used for calculations of formula (2.1.4) ref.1
Target cross-section	S_t	cm^{-2}	is used for calculation of the probability of the target crossing by an individual particle in accordance with (2.1.3)

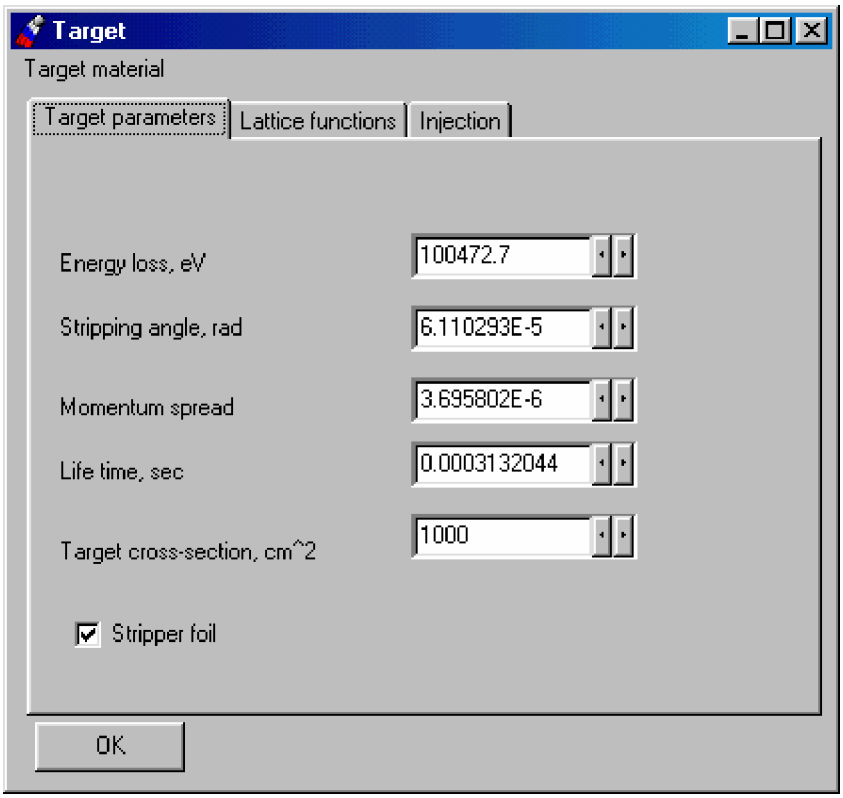

Fig. 5.9. The **Target** form.

The ion ring lattice functions in the target position are entered in the tab sheet **Lattice functions** (Table 5.5).

Table 5.5. ***Lattice functions***

Horizontal			
Beta	β_{hor}	m	are used for calculations of formula (2.1.1) ref.1
Alpha	α_{hor}		
Dispersion	D	m	
Dispersion derivative	D’		
Vertical			
Beta	β_{vert}	m	
Alpha	α_{vert}		

When the internal target is used for multiple charge exchange injection the parameter **Stripper foil** is to be checked and parameters of the injection system are to be entered in the tab sheet **Injection** (Table 5.6.).

Table 5.6. ***Injection***

Repetition period	T_{target}	sec	are used for calculations of formula (2.1.2) ref.1
Number of crossings	n_{target}		

5.5.2**. Target material** form

The target parameters used for invariant variation calculation can be calculated using characteristics of the target material, density and ion beam parameters using the menu item **Target material** of the **Target** form. The target parameters are entered in the **Target material and geometry** form (Fig. 5.10). They are listed in the Table 5.7. The calculations are performed in accordance with chapter *2.1.3, ref. 1.*

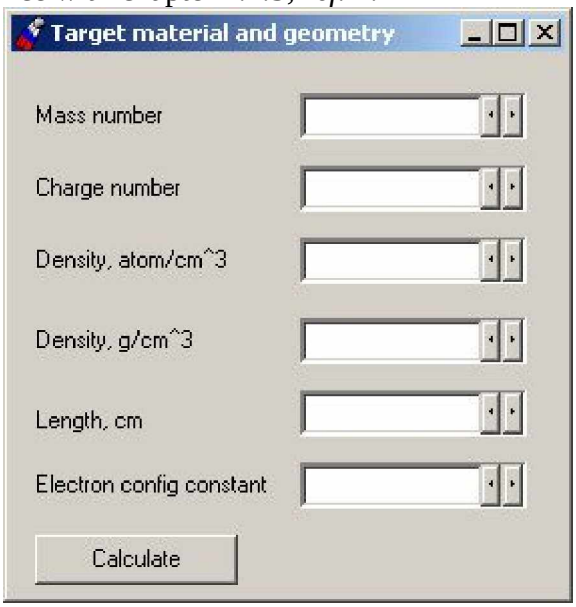

Fig. 5.10. The **Target material and geometry** form.

Table 5.7. ***Target material and geometry***

Mass number	A_T		
Charge number	Z_T		
Density	N	atom/cm^3	input parameter
Density	ρ	g/cm^3	is output parameter calculated from N
Length	x	cm	
Electron cooling constant	u_{in}		output parameter

Effects→ Target → Target material→ "Calculate" button

The calculation of the parameters $E_{str,}$ θ_{str}, $\Delta p/p_{\text{target}}$, τ_t, is performed only when one pushes the button **Calculate** in the **Target material and geometry** form.

Note. If the beam energy or ion kind was changed one need to push the button **Calculate** to recalculate the target parameters $E_{str,}$ θ_{str}, $\Delta p/p_{\text{target}}$, τ_t,.

5.6. Effects→ Injection

The beam parameters variation due to repeated injection is calculated in accordance with the following algorithm:

In the case, when new portion of N_0 ions at emittance ε_{i0} are injected into the ring and injection repetition period is equal to $T_{inj,}$ the characteristic times of emittance variation are given by the expression:

$$\frac{1}{\tau_{i,inj}} = -\frac{1}{\varepsilon_i}\frac{(\varepsilon_i - \varepsilon_{i0})N_0}{(N + N_0)T_{inj}}, \tag{5.25}$$

where N is the particle number in the circulating beam.

Beam life time at injection has a positive sign, which corresponds to increase the particle number:

$$\frac{1}{\tau_{life,inj}} = \frac{N_0}{NT_{inj}} \tag{5.26}$$

Required parameters are entered using the **Injection** form (Fig. 5.11) and listed in the Table 5.8.

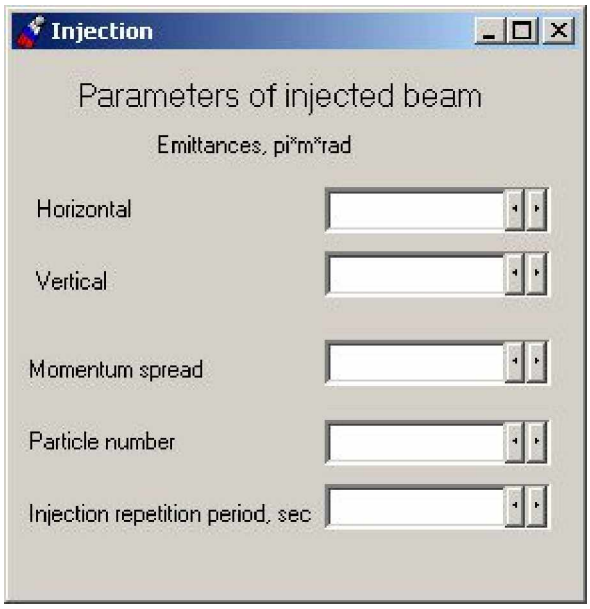

Fig. 5.11. The **Injection** form.

Table 5.8. ***Emittances, π·m·rad***

Horizontal	ε_0		
Vertical	ε_0		
Momentum spread	$\Delta p/p$		
Particle number	N_0		
Injection repetition period	T_{inj}	sec	

5.7. Effects→ External heating

The linear or diffusion increases of the invariants of motion are calculated in accordance with the chapter 2.5 of ref. 1.

The diffusion coefficients P_{trans} are imputted in the $(pi*m*rad)^2$ and P_{long} in rad^4.

In the External heating form (Fig. 5.11) one can enter speed of the emittance growth and diffusion coefficients independently for each degree of freedom. The linear increase is included into calculation when the parameter

Linear increase

is checked.

The diffusional increase is included when the parameter

Diffusion

is checked.

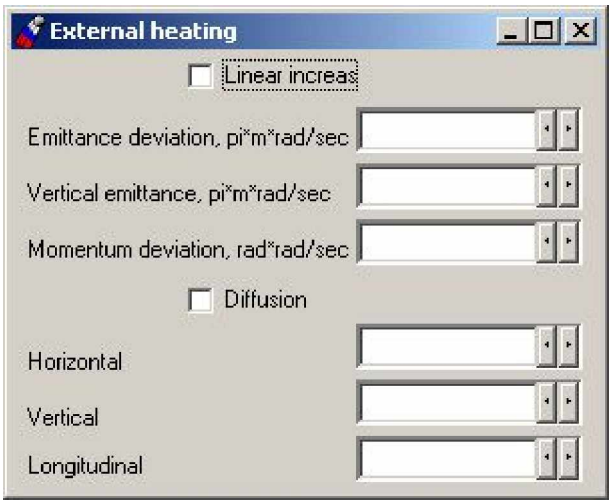

Fig. 5.11. The **External heating** form.

6. Main menu → Task:

6.1. Task→ Rates

At the panel **Active Effects** (Fig. 6.1) one need to check the effects, which are included in the calculations, from the list.

When pushed the button OK the sum of the corresponding rates is displayed into edit windows. The edit windows are used only for output. If some parameters of process were entered incorrectly **BOLIDE** system generates the **Warning window** analogous to that one in the Fig. 4.5. In this case one need to correct parameters in the corresponding form called by sub menu items of the menu item **Effects**. Calculations of the beam parameter evolution can be started using the button **Run** in the **Dynamics** form (next chapter) after correct loading of the process parameters.

The 2D plot in the right side of the form is used for output the rates during dynamics simulation. After push the bottom **Run** in the **Dynamics** form (next chapter) the absolute values of the rates are plotted versus time in seconds.

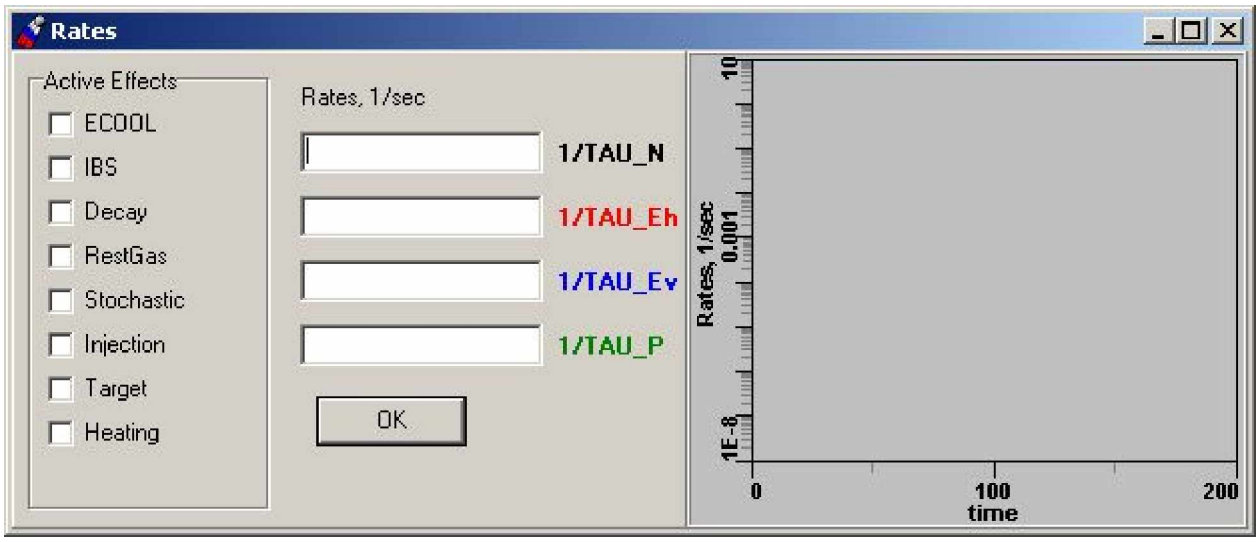

Fig. 6.1. The **Rates** form.

6.2. Task→ Dynamics

This form includes

the **Process control** panel in the right part (more detail about this object of **BOLIDE** see in the chapter 8),

edit window **Step, sec** for input initial step over time for numerical integration of the system (1.1), ref. 1 using Euler method,

edit window **Scale,** which is used for set the horizontal axis in the plots in the forms Rates (chapter 6.1) and Beam parameter evolution (chapter 4.3): the minimum of the axis is equal to 0, the maximum is equal to **Scale*Step, sec** (this parameter is not used in the calculations and plot parameters can be corrected if necessary, using Graphics control tools (chapter 8),

check box **Beam scrapers,** if this parameter is checked the particle losses due to acceptance limitation in accordance with chapter 1.2, ref. 1.

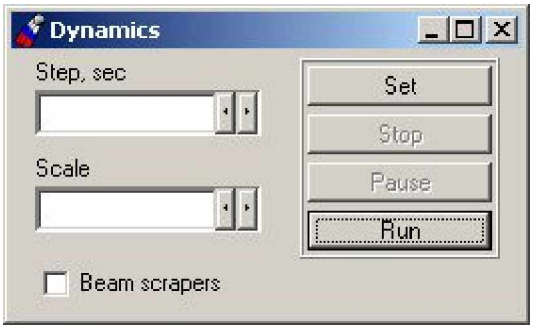

Fig. 6.2. The **Dynamics** form.

In order to start the calculations one need to push the button **Run** in the **Process control** panel. When the calculations are started in the button **Set** of the panel the time of calculations is indicated. The button **Pause** stops the calculations with keeping all the current data. If you push the **Run** button after **Pause** the calculations will be prolonged from the stop point. Button **Stop** stops the calculations and sets all the parameters to their initial values.

Note. If calculations were stopped the values of characteristic rates will not be recalculated. To have a correct initial values of the rates at the first step of integration it is better to push the button **OK** in the **Rates** form before push the button **Run**.

For stable work of the numerical algorithm the step of numerical integration has to be small enough in comparison with the characteristic times of the beam parameters evolution. In the case, when initial step has very big value the program automatically divides it by 2, and makes this procedure fixed number of times. If after that the step is big yet the window about numerical mistake (Fig. 6.3) and **BOLIDE** Warning window Fig. 6.4. will appear.

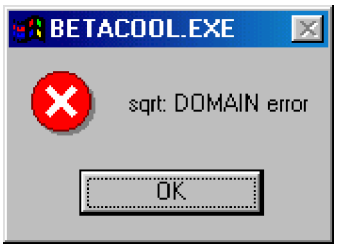

Fig. 6.3. Mistake window.

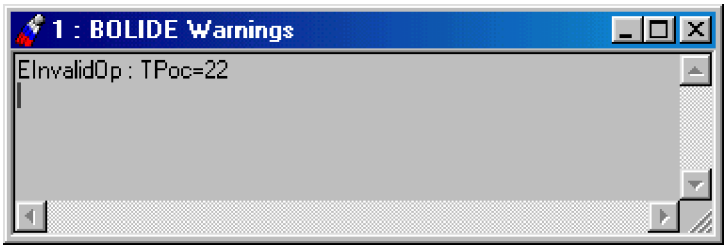

Fig. 6.4. **BOLIDE** Warning window.

In this case you need to

-push the button **OK** in the **Mistake** window,
-push the button Stop in the Dynamics form,
-correct the **Step** value,
-push the button OK in the **Rates** form,
- push the button Run to start the calculations again.

For some values of the **Step** such situation can take place, when mistake is absent, but representation into graphics is also absent. It means, that step value after the automatic decrease has very small value. In this case you need to stop the program, then to decrease initial **Step** value and to start the program once again.

7. Main Menu→ Tools

The submenu item Calculator calls the **Form1** form (Fig. 7.1). The steps of the program are indicated in the panel in the left bottom corner of the form, all other functions are similar to the standard Windows calculator.

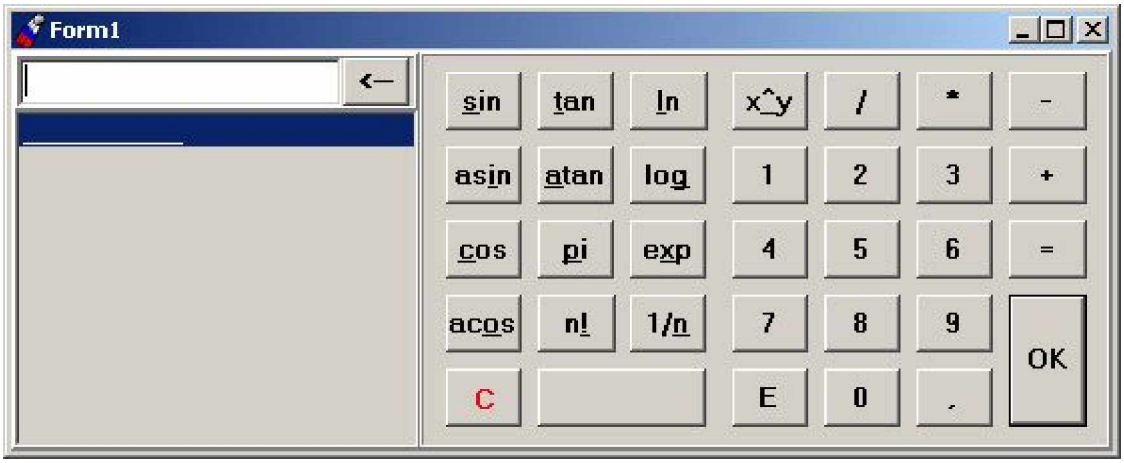

Fig. 7.1. Programming calculator

The sub menu item **Periodic table** calls the form **Mendeleev's Periodic Table of Elements** (Fig. 7.2).

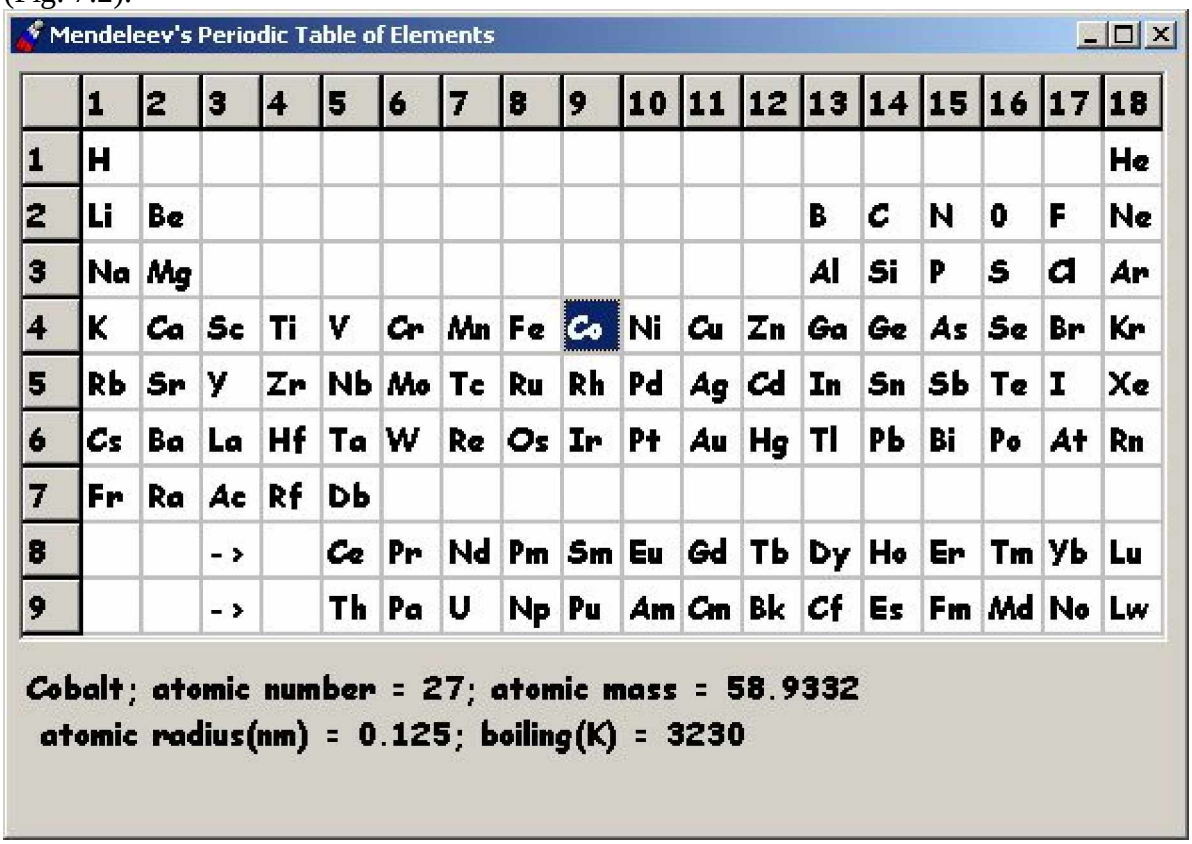
Mendeleev's Periodic Table of Elements
1 2 3 4 5 6 7 8 9 10 11 12 13 14 15 16 17 18
1 H He
2 Li Be B C N O F Ne
3 Na Mg Al Si P S Cl Ar
4 K Ca Sc Ti V Cr Mn Fe Co Ni Cu Zn Ga Ge As Se Br Kr
5 Rb Sr Y Zr Nb Mo Tc Ru Rh Pd Ag Cd In Sn Sb Te I Xe
6 Cs Ba La Hf Ta W Re Os Ir Pt Au Hg Tl Pb Bi Po At Rn
7 Fr Ra Ac Rf Db
8 - > Ce Pr Nd Pm Sm Eu Gd Tb Dy Ho Er Tm Yb Lu
9 - > Th Pa U Np Pu Am Cm Bk Cf Es Fm Md No Lw
Cobalt; atomic number = 27; atomic mass = 58.9332
atomic radius(nm) = 0.125; boiling(K) = 3230

Fig. 7.2. Periodic table.

The sub menu item **Constants** calls the **Physical Constants** form (Fig. 7.3). Units of first 7 constants can be chosen from the corresponding lists. The numbers from edit windows can be copied to the system buffer using **Ctrl-Insert** combination.

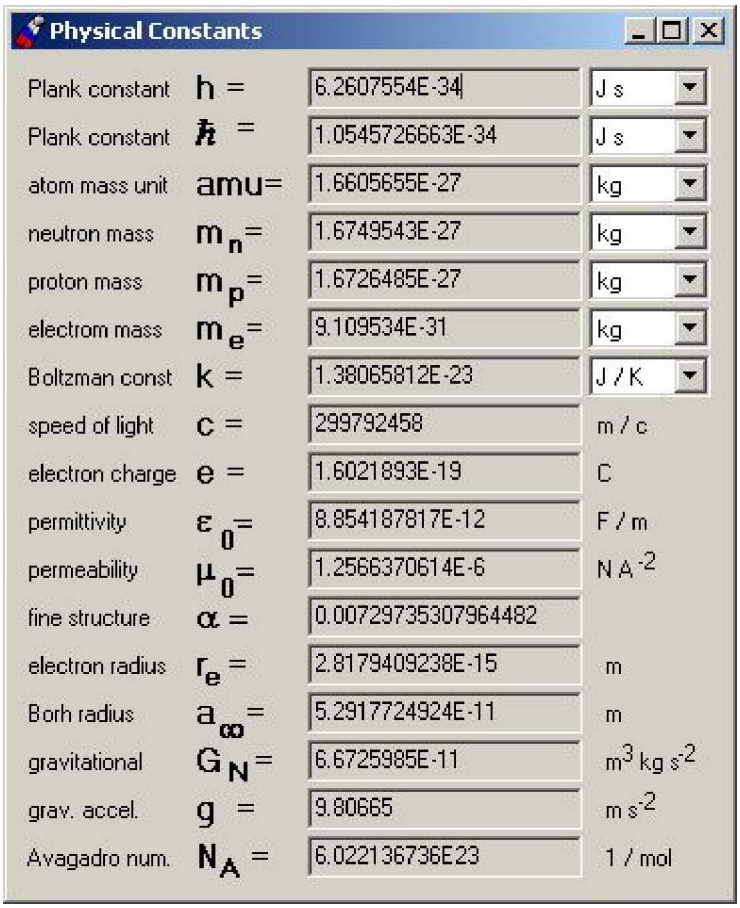
Physical Constants
Plank constant h = 6.2607554E-34 J s
Plank constant ħ = 1.0545726663E-34 J s
atom mass unit amu= 1.6605655E-27 kg
neutron mass m n= 1.6749543E-27 kg
proton mass m p= 1.6726485E-27 kg
electrom mass m e= 9.109534E-31 kg
Boltzman const k = 1.38065812E-23 J / K
speed of light c = 299792458 m / c
electron charge e = 1.6021893E-19 C
permittivity ε 0= 8.854187817E-12 F / m
permeability μ 0= 1.2566370614E-6 N A-2
fine structure α = 0.00729735307964482
electron radius r e = 2.8179409238E-15 m
Borh radius a ∞= 5.2917724924E-11 m
gravitational G N= 6.6725985E-11 m3 kg s-2
grav. accel. g = 9.80665 m s-2
Avagadro num. N A = 6.022136736E23 1 / mol

Fig. 7.3. The **Physical Constants** form.

Example of the game is presented in the Fig 7.4.

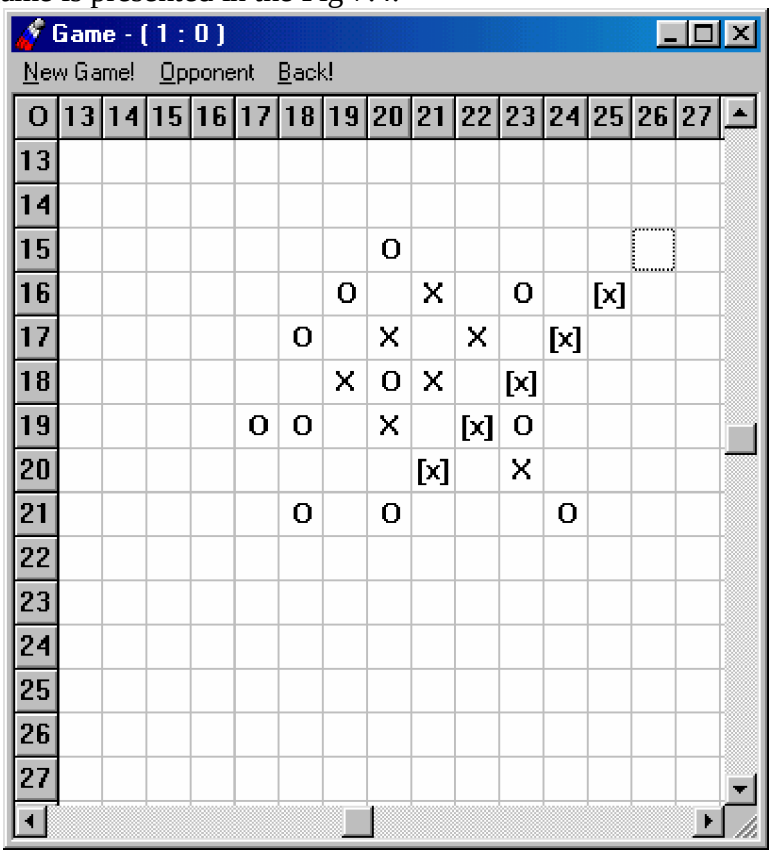

Fig. 7.4. The **Game** form.

8. Graphics and process parameters

To control the 2D and 3D plot parameters one need to click right mouse when the cursor is over the corresponding object. To control the procedure parameters one need to push the button **Set** in the procedure panel. In the **BETACOOL** only one procedure is used – in the **Dynamics** form.

8.1. 2D graph

The form for controlling the 2D plot parameters includes 5 tab sheets:

Axis
Grids
Other
Curves
Values

which are presented in the Fig 8.1, 8.3 – 8.6.

In the upper string of the form the Graph number and name of the current curve are indicated.

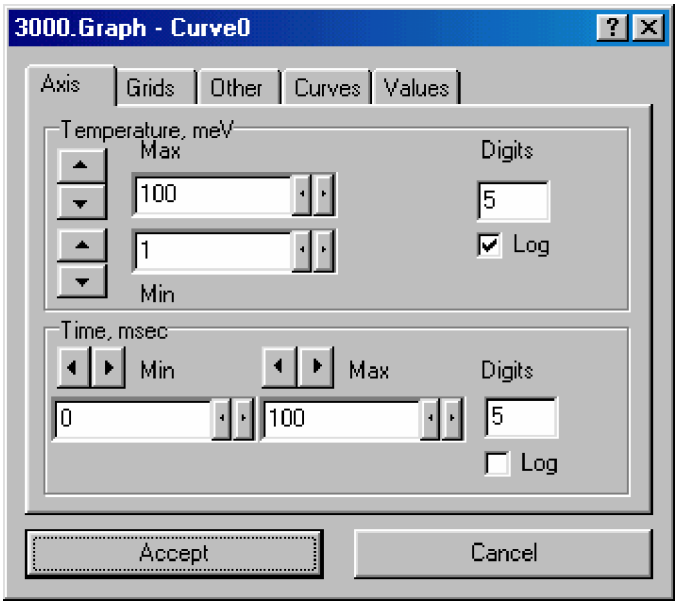

Fig 8.1. The **Axis** tab sheet**.**

The **Axis** tab sheet is used for modifying the scales and type (linear or logarithmic) of x and y axis.

In the case, when the **Max**imum or **Min**imum value is determined incorrectly **BOLIDE** system generates Warning window (Fig. 8.2).

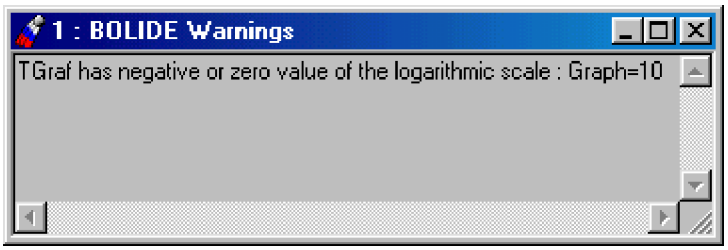

Fig. 8.2. The **BOLIDE** Warning window.

The warning includes short description of the mistake and number of the Graph. To prolonge the work after the Warning message one need to correct the mistake and push the button **Accept**.

Note. Depending on Windows version the control of the plot can be loosed after mistake in the plot parameters. In this case one need to input correct values of the plot parameters push the button **Accept,** save current file in necessary, exit **BETACOOL** and start it again.

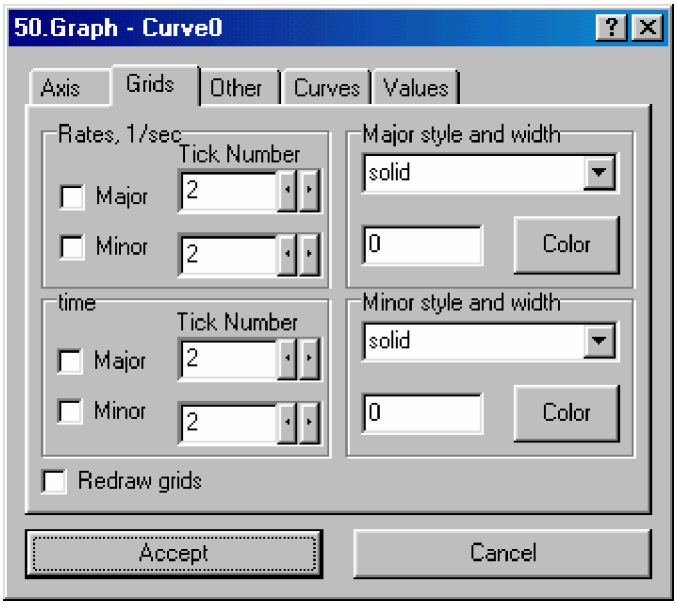

Fig. 8.3. The **Grids** tab sheet.

Number of divisions and sub divisions, style and color of the grid lines in the plot can be entered using the **Grids** tab sheet (Fig. 8.3).

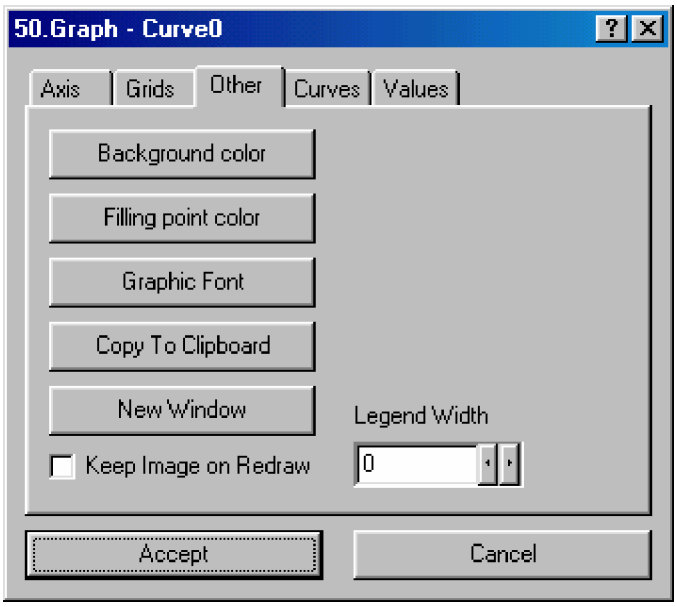

Fig. 8.4. The **Other** tab sheet.

The plot background colour, font of the axis and legend, legend width can be modified using tab sheet **Others** (Fig. 8.3).

Note. The button **Copy To Clipboard** does not work in the presented version of the program, and to copy the plot to the clipboard can be performed only using **Alt+PrintScreen** buttons combination.

The button **New Window** opens new separate window for the same plot. The separate window for each plot can be opened by double click of the mouse left button when the cursor is inside the plot region. Example of such a separate window is presented in the Fig. 8.5. All the points of the curves are displayed in both windows and the separate window for plot can be edited like usual 2D plot.

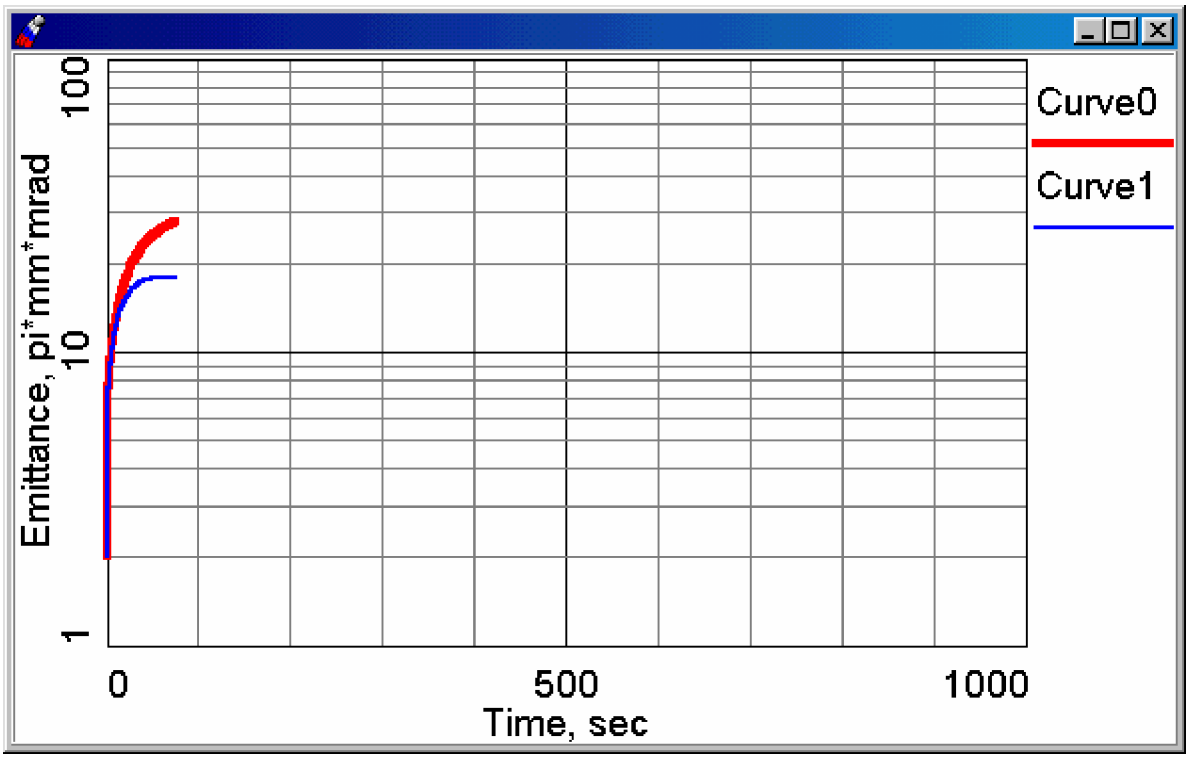

Fig. 8.5. Separate window for 2D plot.

The number in the edit window **Legend Width** determines the width of the legend field which is placed in the left side of the plot window (Fig. 8.5). If this parameter is equal to zero the legend is not displayed.

If parameter **Keep Image on Redraw** is checked the curves calculated in previous run are not redrawn after push the button **Run** in the **Dynamics** form.

The tab sheet **Curves** (Fig. 8.6) contains the list of the curves displayed in the plot. The example of the curve checked in the list is displayed in the left upper corner of the tab sheet. The curve is visible in the plot only in the case when parameter **Visible** is checked. This tab sheet is used for editing of the line and point stile, width and colour.
Note. The line style can be edited only in the case when the line width is 0.

Each curve of the plot can be saved in the text format using the button **Save**. The button calls **Save as** dialog window. The BOLIDE automatically generates the extension for the file, and this file contains two column: first one - the independent variable values, second – function. The curve in the numerical format is also displayed in the tab sheet **Values** (Fig 8.7) which structure coincides with the structure of ***.cur** file. Each curve of the plot can be used for displaying numerical data from the file – for this aim the button Load is intended.

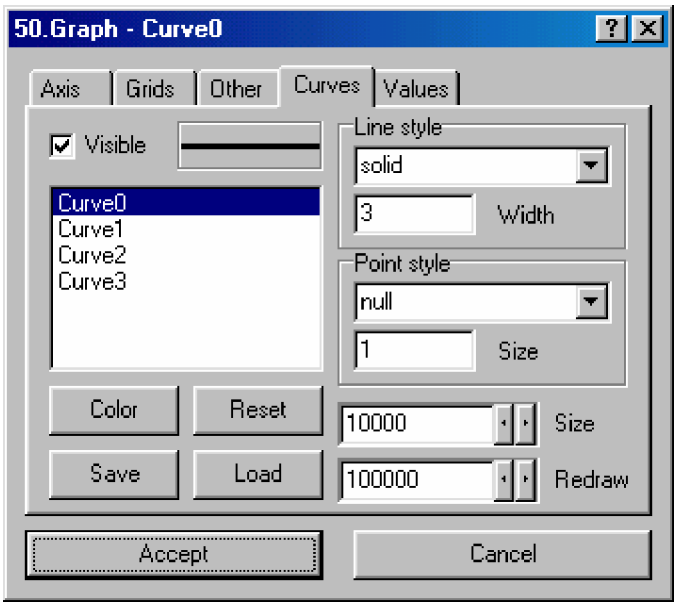

Fig. 8.6. The **Curves** tab sheet.

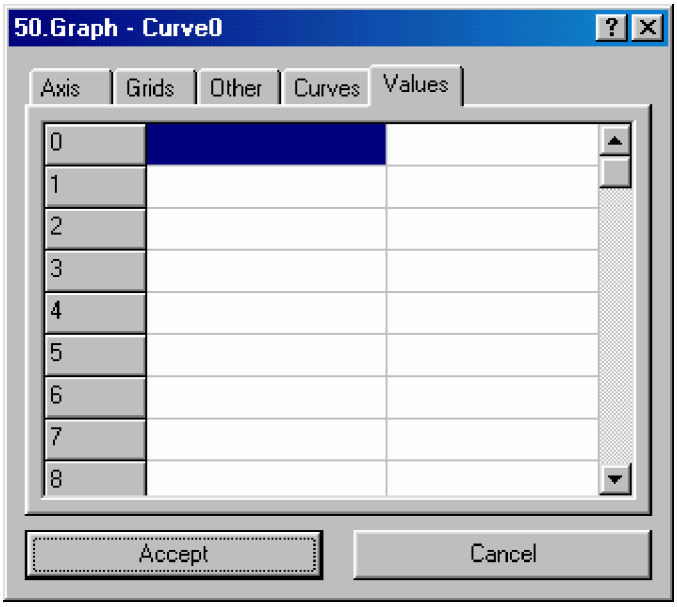

Fig. 8.7. The **Values** tab sheet.

8.2. 3D graph

The form for control of 3D graph parameters (Fig. 8.8 – 8.10) has similar structure as for 2D graph.

The tab sheet **Others** (Fig. 8.8) includes additional panel in the right upper corner for rotation of the axis, and parameter 3D View – if it is not checked the projection of the curve is displayed in the graph.

The 3D surface also can be saved or loaded from file (the file extension is *.sur). The file structure is similar to the numerical presentation of the surface in the tab sheet **Values** (Fig.

8.9). It is the table of the numbers: the first column contains x-variable values, first string contains y-variable values, all other - the function values in the corresponding points.

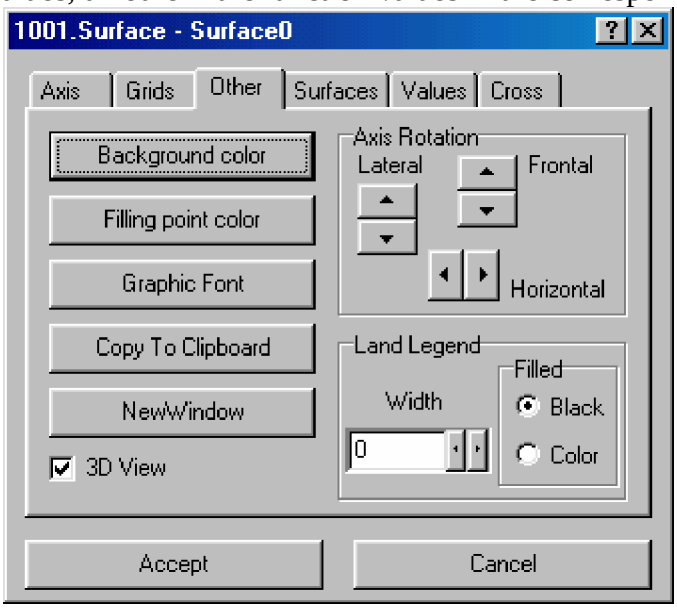

Fig. 8.8. 3D graph, tab sheet **Others**.

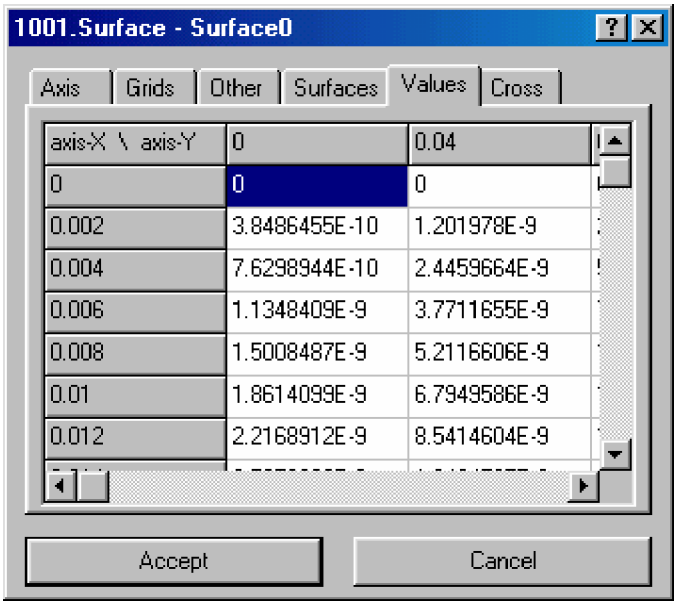

Fig. 8.9. 3D graph, tab sheet **Values**.

Additional tab sheet **Cross** (Fig. 8.10) is used for displaying the cross-sections of the 3D surface. The panel **Cross on** permits to determine the variable along which the cross-section is made. Using the edit window **Line number** one can introduce the variable value in which the cross-section is made. When the parameter **Integral** is checked the plot in the tab sheet shows the sum of all the points with the same co-ordinate of the surface. The 2D plot in the tab sheet is usual 2D graph and its parameters can be controlled as described in the previous chapter. For instance, the cross-section can be displayed in the separate window (Fig. 8.11), saved or loaded like 2D curve.

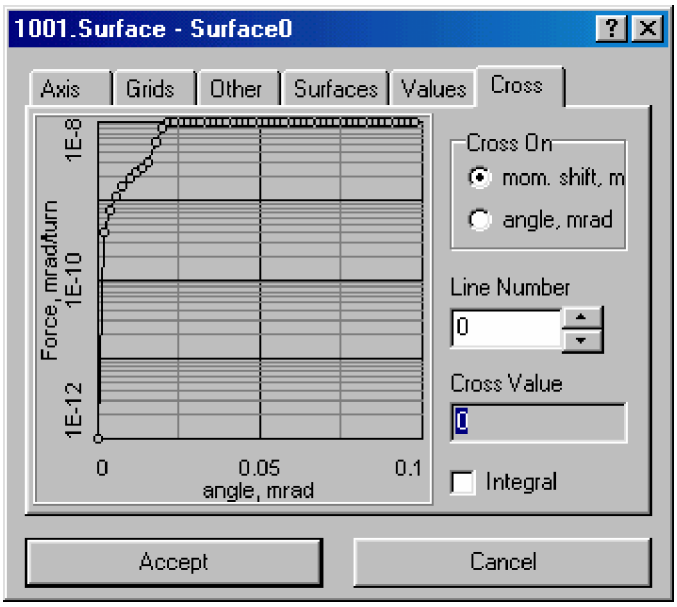

Fig. 8.10. The tab sheet **Cross**.

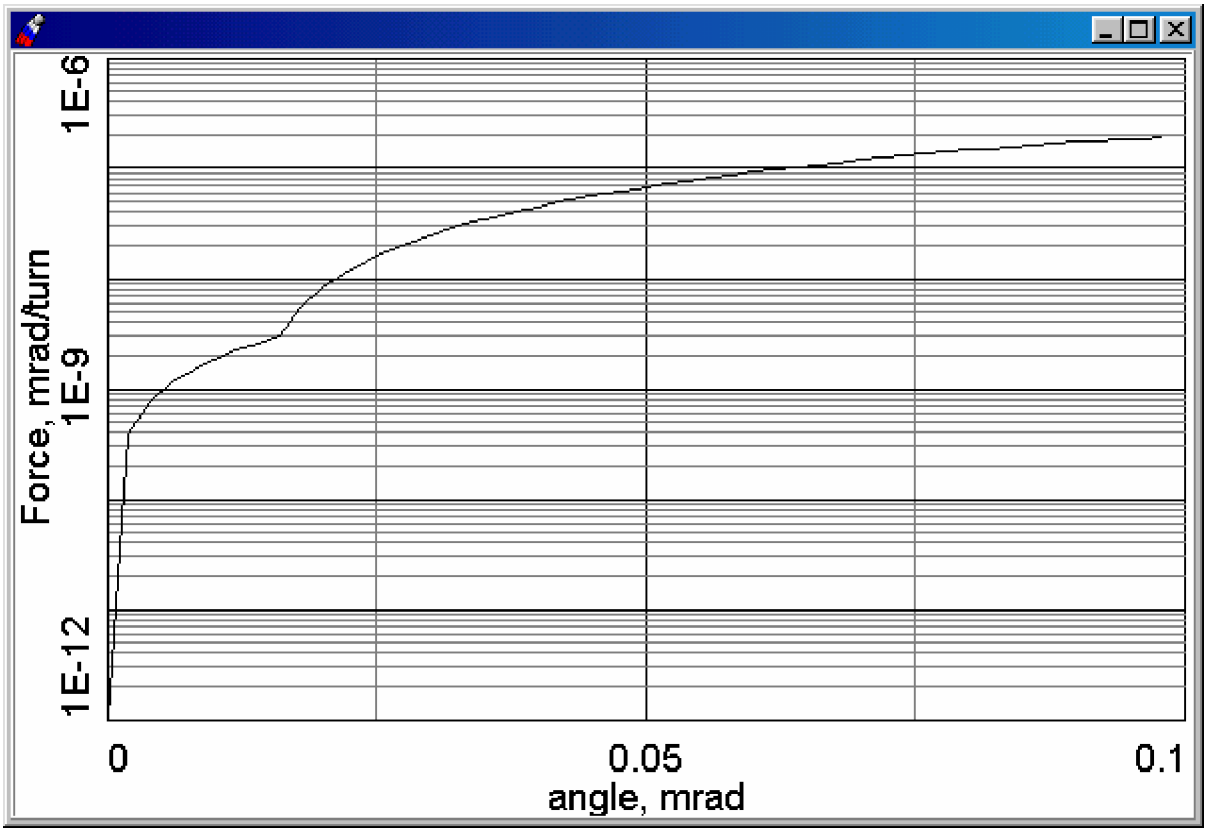

Fig. 8.11. New window for cross-section plot.

8.3. Process control

The upper button in the process panel of the **Dynamics** form (chapter) calls the **Process control** window. The process control service was elaborated in the frame of **BOLIDE** system for programs using several separate processes during calculations. In the presented version of **BETACOOL** only one process is used and optimisation of the process parameters is not

necessary. The button **Kill** can be used to stop the calculations in the case of cycling the program, when it is not stopped by the button **Stop** in the Dynamics form.

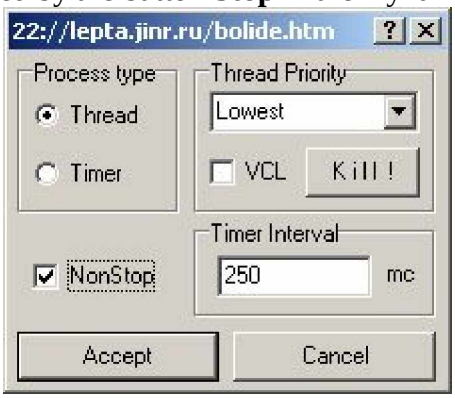

Fig. 8.12. The **Process control** window.

More detail description of the graphs and process control will be done in the manual for **BOLIDE** system.

Reference

1. I.N.Meshkov, Yu.V.Korotaev, A.L.Petrov, A.O.Sidorin, A.V.Smirnov, H.J.Stein, E.M.Syresin, G.V.Trubnikov, S.V.Yakovenko, Electron cooling application for luminosity preservation in an experiment with internal targets at COSY. Interim report, Dubna, 2001.

2. http://nuweb.jinr.ru/~lepta